

NOTE TO USERS

This reproduction is the best copy available.

UMI[®]

University of Alberta

**Toward Helical Twist Sense Bias in Conjugated *iso*-Polydiacetylene
and Synthesis and Characterization of
7,7,8,8-Tetraethynyl-*p*-quinodimethane (TEQ) derivatives**

by

CLEMENT OSEI AKOTO



A thesis submitted to the Faculty of Graduate Studies and Research in partial
fulfillment of the requirements for the degree of Master of Science

Department of Chemistry

Edmonton, Alberta

Spring, 2004



Library and
Archives Canada

Bibliothèque et
Archives Canada

Published Heritage
Branch

Direction du
Patrimoine de l'édition

395 Wellington Street
Ottawa ON K1A 0N4
Canada

395, rue Wellington
Ottawa ON K1A 0N4
Canada

Your file *Votre référence*
ISBN: 0-612-96533-3
Our file *Notre référence*
ISBN: 0-612-96533-3

The author has granted a non-exclusive license allowing the Library and Archives Canada to reproduce, loan, distribute or sell copies of this thesis in microform, paper or electronic formats.

L'auteur a accordé une licence non exclusive permettant à la Bibliothèque et Archives Canada de reproduire, prêter, distribuer ou vendre des copies de cette thèse sous la forme de microfiche/film, de reproduction sur papier ou sur format électronique.

The author retains ownership of the copyright in this thesis. Neither the thesis nor substantial extracts from it may be printed or otherwise reproduced without the author's permission.

L'auteur conserve la propriété du droit d'auteur qui protège cette thèse. Ni la thèse ni des extraits substantiels de celle-ci ne doivent être imprimés ou autrement reproduits sans son autorisation.

In compliance with the Canadian Privacy Act some supporting forms may have been removed from this thesis.

Conformément à la loi canadienne sur la protection de la vie privée, quelques formulaires secondaires ont été enlevés de cette thèse.

While these forms may be included in the document page count, their removal does not represent any loss of content from the thesis.

Bien que ces formulaires aient inclus dans la pagination, il n'y aura aucun contenu manquant.

Canada

Abstract

Due to interest in their unique π -electron delocalization and their potential as nonlinear optical materials, a series of triethylsilyl (TES) and *tert*-butyldimethylsilyl (TBDMS) end-capped *iso*-polydiacetylenes (*iso*-PDAs) has been synthesized. The *iso*-PDA series has been assembled using a sequence of deprotection/Pd-catalyzed cross-coupling protocols. The π -electron delocalization and electronic communication across the oligomeric backbones has been investigated via UV-vis spectroscopy. In order to explore the conformational preference (folding) of the *iso*-PDA oligomers in solution state, a chiral auxiliary has been synthesized with the aim of incorporating it into the oligomer chain, in an attempt to bias the "twist sense" of the helix based on the 'Sergeants-and-Soldiers' principle. The synthesis and characterization of a series of 7,7,8,8-tetraethynyl-*p*-quinodimethane (TEQ) derivatives have also been reported in this thesis. The TEQ derivatives were constructed primarily using Pd-catalyzed cross-coupling protocols. The structural properties of all the compounds have been characterized by IR, ^1H and ^{13}C NMR spectroscopies, as well as high-resolution MS spectrometry and in certain cases optical rotation, melting point and elemental analysis.

Acknowledgements

My profound gratitude goes to God Almighty for His love, care, protection, strength and faithfulness throughout my life and my stay at the University of Alberta campus.

Grateful acknowledgement is made to my supervisor, Dr. Rik R. Tykwinski for his valued comments and criticisms during my graduate program, and his assistance in the preparation of this thesis.

My deepest appreciation goes to all the staff in Special Services including IR, NMR, Microanalysis, X-ray, storeroom, machine shop, MS especially Angie Morales-Izquierdo and general office especially Ilona Baker for her openness, generosity, non-discriminatory and care. May God richly bless you and your family, Ilona.

I am greatly indebted to all my research group members, especially Dr. Yuming Zhao for starting materials, encouragement and advice and Katie Campbell for proof reading this thesis. I am also thankful for my good friend Dan Spantulescu for his support, care, openness and concern. Dan, may God bless you.

I would like to thank all my church members for their love, care and support especially Pastor Nicholas Ameyaw and family and Brother Francis Nsiah and family.

This acknowledgement would not be complete without appreciating to a very large extent the love, care, prayers and assistance offered to me by my mother Miss Grace Yeboah, my sister Indira Ghandi Osei Akoto and my brothers Samuel, Harry and Andy.

Finally, I wish to thank my inspirer, late uncle Mr. Michael Asamoah Yeboah for his advice, encouragement and support throughout my life.

To God be the Glory. Amen.

Table of Contents

	Page
Chapter 1 Introduction	1
1.1 Helicity and its Significance to Oligomers and Polymers	1
1.2 Folded Oligomers and Polymers in Solution	5
1.3 Chiral Oligomers and Polymers for Asymmetric Catalysis	7
1.3.1 <i>Synthetic Polypeptide Catalyst</i>	8
1.3.2 <i>Chiral Polymer Catalysts Containing Amide, Urea, and Ester Functionality</i>	9
1.3.3 <i>Polymers of Rigid and Sterically Regular Chiral Chains</i>	10
1.4 Chiral π -Conjugated Oligomers and their Potential	
Optical Applications	12
1.5 Nonlinear Optical Properties of Conjugated Oligomers	14
1.6 Cross-conjugated Compounds and their Significance	16
1.7 Thesis Goals	21
1.8 Results and Discussion	23
1.8.1 <i>Synthesis of Perphenylated iso-Polydiacetylene) (iso-PDA) Oligomers</i>	23
1.8.2 <i>Physical Characteristics</i>	27
1.8.3 <i>Electronic Absorption Properties</i>	28
1.8.4 <i>Synthesis of the Chiral Auxiliary</i>	31
1.8.5 <i>Negishi Cross-Coupling of Chiral Auxiliary</i>	34
1.8.6 <i>Suzuki Cross-Coupling of Chiral Auxiliary</i>	37
1.9 Conclusions	41
1.10 References and Notes	43

Chapter 2 Synthesis and Characterization of	
7,7,8,8-Tetraethynyl-<i>p</i>-quinodimethane (TEQ) Derivatives	48
2.1 Introduction	48
2.2 Results and Discussion	54
2.2.1 <i>Synthesis of Tetrakis(trimethylsilyl) Protected</i> <i>Derivative of 7,7,8,8-Tetraethynyl-<i>p</i>-quinodimethane)</i> (TEQ)	54
2.2.2 <i>Toward the Synthesis of Bis(trimethylsilyl) and</i> <i>Bis(triisopropyl-, tert-butyl dimethylsilyl- and</i> <i>triethylsilyl) Protected Derivatives of</i> 7,7,8,8-Tetraethynyl- <i>p</i> -quinodimethane) (TEQ)	58
2.3 Conclusions	84
2.4 References and Notes	85
Chapter 3 Experimental Section	88
Appendix	125

List of Tables

	Page
Table 1. Crystallographic Experimental Details	126
Table 2. Atomic Coordinates and Equivalent Isotropic Displacement Parameters	128
Table 3. Selected Interatomic Distances (Å)	129
Table 4. Selected Interatomic Angles (deg)	130
Table 5. Torsional Angles (deg)	131
Table 6. Least-Squares Planes	132

List of Figures

	Page
Fig. 1.1 Proposed assembly of perphenylated <i>iso</i> -PDA oligomers	22
Fig. 1.2 Electronic absorption spectra (ϵ [L mol ⁻¹ cm ⁻¹]) in CHCl ₃ comparing the effects of oligomer length between TBDMS-encapped perphenylated <i>iso</i> -PDA oligomers: 34, 36, 40 and 41	30
Fig. 2.1 ORTEP drawing (20% probability level) of 66a	63
Fig. A.1 Perspective view of Triflate 66a	125
Fig. A.2 ¹ H and ¹³ C NMR spectra of compound 30	133
Fig. A.3 ¹ H and ¹³ C NMR spectra of compound 32	134
Fig. A.4 ¹ H and ¹³ C NMR spectra of compound 34	135
Fig. A.5 ¹ H and ¹³ C NMR spectra of compound 36	136
Fig. A.6 ¹ H and ¹³ C NMR spectra of compound 40	137
Fig. A.7 ¹ H and ¹³ C NMR spectra of compound 41	138
Fig. A.8 ¹ H and ¹³ C NMR spectra of compound 46a	139
Fig. A.9 ¹ H and ¹³ C NMR spectra of compound 65	140
Fig. A.10 ¹ H and ¹³ C NMR spectra of compound 70	141
Fig. A.11 ¹ H and ¹³ C NMR spectra of compound 71	142
Fig. A.12 ¹ H and ¹³ C NMR spectra of compound 66	143
Fig. A.13 ¹ H and ¹³ C NMR spectra of compound <i>trans</i> - 66	144
Fig. A.14 ¹ H and ¹³ C NMR spectra of compound 72	145
Fig. A.15 ¹ H and ¹³ C NMR spectra of compound <i>trans</i> - 72	146
Fig. A.16 ¹ H and ¹³ C NMR spectra of compound 73	147
Fig. A.17 ¹ H and ¹³ C NMR spectra of compound <i>cis</i> - 73	148
Fig. A.18 ¹ H and ¹³ C NMR spectra of compound 67	149

Fig. A.19 ^1H and ^{13}C NMR spectra of compound 74	150
Fig. A.20 ^1H and ^{13}C NMR spectra of compound 75	151
Fig. A.21 ^1H and ^{13}C NMR spectra of compound 68	152
Fig. A.22 ^1H and ^{13}C NMR spectra of compound 76	153
Fig. A.23 ^1H and ^{13}C NMR spectra of compound 77	154
Fig. A.24 ^1H NMR and MS spectra of compound 80	155
Fig. A.25 ^1H and ^{13}C NMR spectra of compound 81	156
Fig. A.26 ^1H NMR and MS spectra of compound 82	157

List of Schemes

	Page
Scheme 1.1 A representative selection of cross-conjugated molecules	16
Scheme 1.2 Reagents and conditions for formation of 31 and 32	24
Scheme 1.3 Formation of monomer	24
Scheme 1.4 Reagents and conditions for formation of 35 and 36	25
Scheme 1.5 Tetrameric homocoupled by-products	26
Scheme 1.6 Reagents and conditions for formation of 41	27
Scheme 1.7 Pattern of the conjugated segments of the <i>iso</i> -PDA oligomers	29
Scheme 1.8 Reagents and conditions for formation of 45	32
Scheme 1.9 Formation of 46a-c	33
Scheme 1.10 Formation of chiral auxiliary 46a	33
Scheme 1.11 Reagents and conditions for formation of 48b	35
Scheme 1.12 Reagents and conditions for formation of 49b	36
Scheme 1.13 Reagents and conditions for formation of 52	38
Scheme 1.14 Reagents and conditions for formation of 53a-c	39
Scheme 1.15 Reagents and conditions for formation of 50a-b	41
Scheme 2.1 A selection of important cross-conjugated systems	49
Scheme 2.2 Formation of TCNQ anion-radical in resonance hybrid	51
Scheme 2.3 Formation of dibromoalkene 60	55
Scheme 2.4 Formation of geminal eneyne 61	56
Scheme 2.5 Formation of dihydro-TEQ derivative 58a	57
Scheme 2.6 Ineffective oxidation of 58a	57
Scheme 2.7 Formation of ketone 65 (mixture of <i>trans</i> - 65 , <i>cis</i> - 65)	60
Scheme 2.8 Formation of triflate 66 (mixture of <i>trans</i> - 66 , <i>cis</i> - 66)	61
Scheme 2.9 Formation of geminal eneyne, 67 (mixture of <i>trans</i> - 67 , <i>cis</i> - 67)	65

Scheme 2.10 Attempted oxidation of dihydro-TEQ derivative 68 (<i>cis-trans</i>)	67
Scheme 2.11 Ineffective oxidation of 68 (<i>cis-trans</i>)	68
Scheme 2.12 Formation of ketones 70 and 71 (<i>cis-trans</i>)	70
Scheme 2.13 Formation of triflates 72 and 73 (<i>cis-trans</i>)	71
Scheme 2.14 Formation of geminal eneyne 74 and 75 (<i>cis-trans</i>)	73
Scheme 2.15 Attempted oxidation of dihydro-TEQ derivatives 76 and 77 (<i>cis-trans</i>)	76
Scheme 2.16 Ineffective oxidation of 76 and 77 (<i>cis-trans</i>)	77
Scheme 2.17 Formation of di-donor dihydro-TEQ derivative 80 (<i>cis-trans</i>)	79
Scheme 2.18 Formation of diaceptor dihydro-TEQ derivative 81	82
Scheme 2.19 Formation of tetra-donor dihydro-TEQ derivative 82	84

List of Symbols, Nomenclature and Abbreviations

Å	Angstrom
A	Acceptor
Ac	Acetate
Aq	Aqueous
Ar	Argon
APT	Attached Proton Test
AM1	Austin Model 1
Bu	Butyl
β	Microscopic First Hyperpolarizability
δ	Chemical Shift
c	Concentration
C–C	Carbon–Carbon
^{13}C	Carbon–13
ca.	Approximately
cm	Centimeter
CsF	Cesium Fluoride
d	Doublet
dd	Doublet of Doublets
D	Donor
D/A	Donor or Acceptor
D–A	Donor and Acceptor
DBU	1,8–Diazabicyclo[5.4.0]undec–7–ene
DMF	Dimethylformamide
DHP	3,4–Dihydro–2H–pyran

DNA	Deoxyribonucleic Acid
DDQ	2,3-Dichloro-5,6-dicyano- <i>p</i> -benzoquinone
DOKE	Differential Optical Kerr Effect
\vec{E}	Electric Field
ee	Enantiomeric Excess
Et	Ethyl
e.g.	For Example
<i>et al.</i>	And Others
eV	Electron Volt
esu	Electrostatic Unit
EI-MS	Electron Impact Mass Spectrometry
ESI	Electrospray Ionization
ECL	Effective Conjugation Length
ϵ	Molar Extinction Coefficient
ϵ_0	Dielectric Constant
g	Gram(s)
gem	Geminal
h	Hour(s)
^1H	Proton (Hydrogen)
HOMO	Highest Occupied Molecular Orbital
HRMS	High Resolution Mass Spectrometry
Hz	Hertz
Δ	Heat
<i>i</i>	Iso
i.e.	That is

IR	Infrared
J	Coupling Constant
KOH	Potassium Hydroxide
L	Litre(s)
LAH	Lithium Aluminium Hydride
LED	Light Emitting Diode(s)
α	Microscopic Linear Polarizability
λ	Lowest Energy Wavelength of Maximum Absorption
LUMO	Lowest Unoccupied Molecular Orbital
m	Meta
m	Multiplet
M	Molar
M^+	Molecular ion
Me	Methyl
mg	Milligram(s)
min	Minute(s)
mL	Milliliter(s)
mmol	Millimole(s)
mol	Mole(s)
Mp	Melting Point
MS	Mass Spectrometry
m/z	Mass-to-Charge Ratio
γ	Microscopic Second Hyperpolarizability
\mathbf{P}	Macroscopic Polarization of a Medium
nm	Nanometer(s)

N ₂	Nitrogen
NLO	Nonlinear Optical (Optics)
NMR	Nuclear Magnetic Resonance
χ	Macroscopic Nonlinear Optical Susceptibility Coefficient
<i>o</i>	Ortho
OLED	Organic Light-Emitting Device(s)
ORTEP	Oak Ridge Thermal Ellipsoid Plot
O ₂	Oxygen
$[\alpha]_D$	Optical Rotation
<i>p</i>	Para
Ph	Phenyl
ppm	Parts Per Million
PNA	<i>para</i> -Nitroaniline
%	Percentage
PDA	Polydiacetylene
PPE	Poly(phenylene)
PPP	Pariser-Parr-Pople
PPV	Poly(phenylene vinylene)
Pr	Propyl
q	Quartet
ROMP	Ring Opening Metathesis Polymerization
rt	Room Temperature
s	Singlet
S	Electric Conductance
SEC	Size Exclusion Chromatography
SCF	Self-Consistent Field

S_N2	Second-Order Nucleophilic Substitution Reaction
t	Triplet
<i>t</i>	Tertiary
TBAF	Tetrabutylammonium fluoride
TCNE	Tetracyanoethylene
TCNQ	Tetracyanoquinodimethane
TEE	Tetraethynylethene
TEQ	Tetraethynylquinodimethane
THF	Tetrahydrofuran
THP	Tetrahydropyran
TBDMS	<i>tert</i> -Butyldimethylsilyl
TLC	Thin Layer Chromatography
TES	Triethylsilyl
Tf	Triflate
TIPS	Triisopropylsilyl
TMS	Trimethylsilyl
TMSA	Trimethylsilylacetylene
TsCl	<i>para</i> -Toluenesulfonyl Chloride
UV	Ultraviolet
UV-Vis	Ultraviolet-Visible
vs	Versus

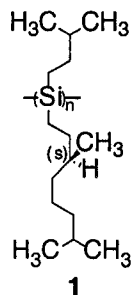
Chapter 1 Introduction

1.1 Helicity and its Significance to Oligomers and Polymers

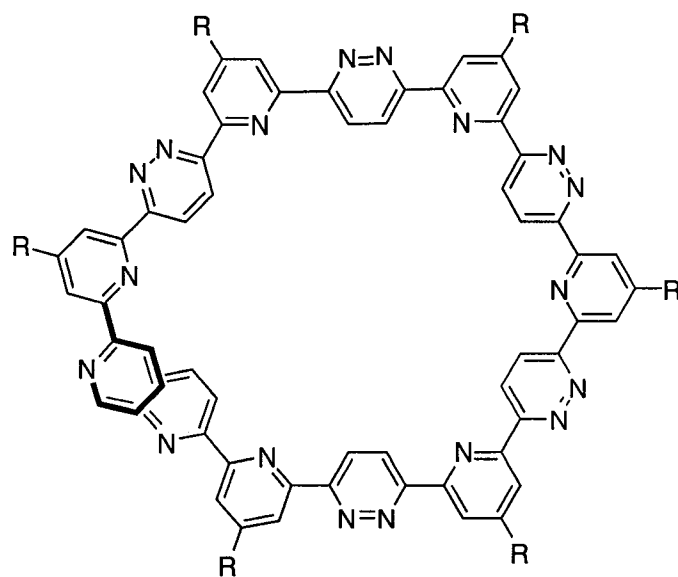
From the advances that have been made more than three decades ago in supramolecular chemistry and the knowledge that has come from the study of biological self-assembly, it is no wonder why there is great enthusiasm for synthetic supramolecular oligomers and polymers. For more than 15 years there has been growing activity to develop macromolecules whose monomeric units are held together by non-covalent forces, thus, supramolecular oligomers or polymers.^{1,2} Molecular biology has shown that large molecules provide fertile ground for seeding sophisticated supramolecular design. A typical example is that sequence specific peptide chains can store the information necessary to direct the complex assembly of multi-molecular components.³

Biology teaches the importance of helical constructs in macromolecular recognition. For example, helical structures play critical roles in DNA–protein and protein–protein binding, as well as regulating various biological events such as genetic information.⁴⁻⁶ As a result of this, there is growing interest in the design of synthetic chain molecules that acquire well-defined conformations in solution, analogous to the folded state of proteins or nucleic acids.⁷⁻¹⁰ Thus, the design of oligomers and polymers with well-defined secondary structures is an active area of research aimed at creating synthetic systems that can mimic biologically polymers in their ability to derive function from structure.^{8,10-11} Perhaps the most common secondary structural motif identified in these synthetic systems is the helix, a structure that can exist in either a right- or left-handed twist sense.¹²⁻¹³ Several strategies have been used to bias the twist sense of helical conformations of chain molecules, including the use of chiral monomers,¹⁴⁻¹⁶ additives,^{14,17-18} and initiators.¹⁹

In order to explore thermo-driven helix-helix transition process in a flexible rod helical polysilylenes **1**, Fujiki and co-workers have prepared an optically active helical polymer comprising of a flexible rodlike silicon main chain and enantiopure alkyl side chains, poly{(*S*)-3,7-dimethyloctyl-3-methylbutylsilylene}.²⁰ This polymer undergoes a thermo-driven helix-helix transition at -20 °C in isoctane.²⁰

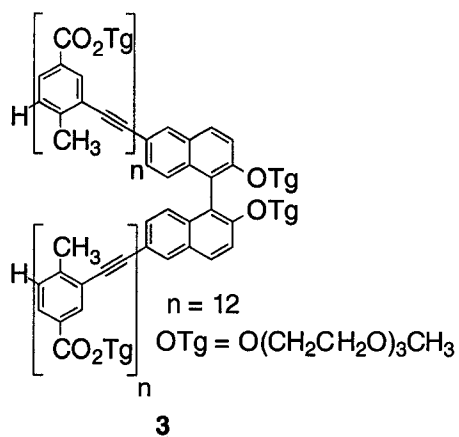


Lehn and co-workers have recently reported the helical self-organisation and hierarchical self assembly of an oligoheterocyclic pyridine-pyridazine strand **2** into extended supramolecular fibers.²¹ They point out that spontaneous folding into a helical secondary structure is based on a general self-organization process enforced by the conformational information encoded within the primary structure of the molecular strand itself.²¹

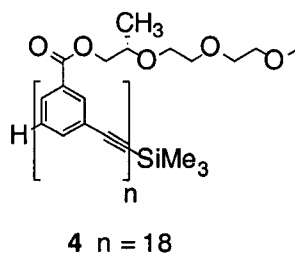


2 R = S-*n*Pr

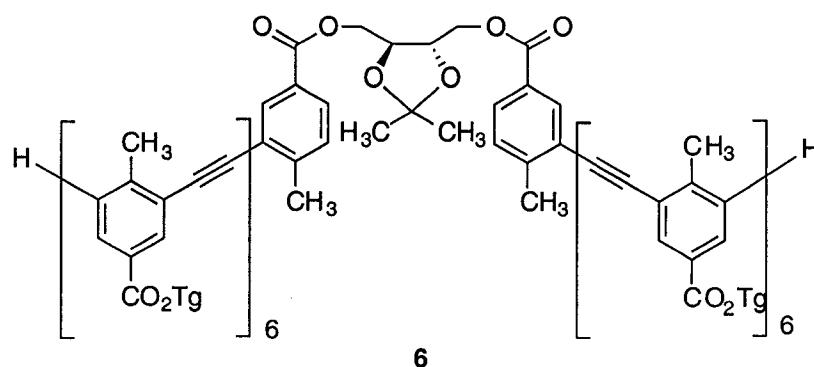
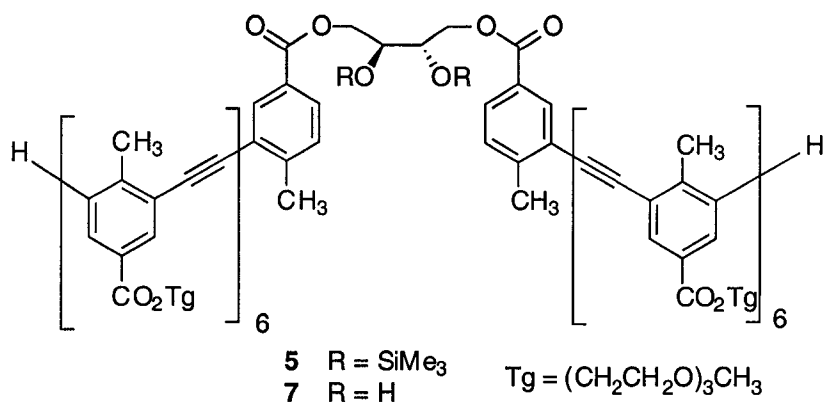
Moore and co-workers have presented the use of an optically active binaphthol derivative **3**. This derivative when inserted into the oligomer chain, impart a bias in the twist sense of the helical structure, which was shown by solvent-dependent changes in the circular dichroism spectra.²²



An elegant way to synthesize helically folded oligomers **4**, whose twist sense bias was induced by chiral side chains, has also been reported by Moore and co-workers. They demonstrate that a small, chiral perturbation to the side chain causes a bias to the twist sense without disrupting the conformational stability.²³ This is in contrast to the system **3**, where the kinked binaphthol monomer significantly decreased the stability of the folded conformation.²²



In a comprehensive study, Moore and Gin have synthesized and studied the oligo(phenylene ethynylene)s **5–7** whose helical twist sense bias is induced by an optically active flexible tether. Interestingly, the use of trimethylsilyl ether protecting groups on the (+)-tartaric acid derived tether **5** results in the formation of helices with a large twist sense bias. In contrast, an isopropylidene ketal protecting group **6** or no protecting group **7**, is not only ineffective at helical discrimination but may even inhibit helix formation.²⁴

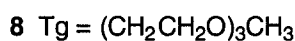
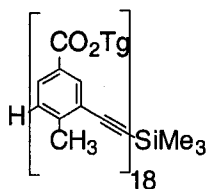


1.2 Folded Oligomers and Polymers in Solution

Strategically functionalized oligomers and polymers provide an opportunity for an intramolecular aspect of supramolecular chemistry, affording folded macromolecules in solution. While ordered conformations in solution are very common among biopolymers, it has only been in the last decade or so that significant results have been achieved with synthetic oligomers or polymers.⁶⁻⁸ The question one may ask is why are oligomers or polymers important for this type of supramolecular chemistry? Clearly the local concentration of interacting segments within an oligomer or polymer chain can be much higher than the bulk concentration. As a result, segments in an oligomeric or polymeric linear chain will experience a lot of intramolecular interactions in dilute solution. These interactions may be weak individually, but collectively they can become

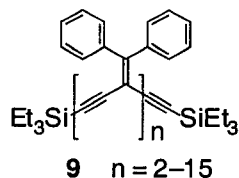
very significant. The conformational transitions of oligomers or polymers can therefore exhibit high cooperativity because the intramolecular interactions are coupled through constraints imposed by the backbone's covalent connectivity. Cooperativity can provide an enormous tool for supramolecular organization, and it is a design principle ideally suited to oligomers and polymers.²⁵

Moore and co-workers have successfully shown that phenylene ethynylene oligomers **8**, can be driven to fold into helical conformations by solvophobic forces alone. Based on molecular modeling studies, they hypothesized that an essential element in the design is the molecular contact area per degree of conformational freedom. According to this idea, they state that the best monomer units would have a large, solvent-accessible surface area and be relatively rigid. Because van der Waals and solvophobic interactions are weak forces, they should be ideal for building up a folded structure that can undergo a cooperative conformational transition. Moore concluded by reporting that the stability of the folded conformation of **8** has been found to be dependent on chain length, solvent quality, and temperature.¹⁰



Tykwinski and Zhao²⁶ have successfully synthesized perphenylated *iso*-polydiacetylene (*iso*-PDA) oligomers **9**, whose folding/unfolding process cannot be easily controlled by solvation effect, i.e., hydrophobically-driven folding. They pointed out that a molecular mechanics study on the conformational properties of perphenylated

iso-polydiacetylene oligomers **9** suggests that the oligomers start folding from the stage of heptamer ($n \geq 7$). They concluded that the conformational preference was suggested by the UV-vis and fluorescence spectroscopic analysis, and differential optical Kerr effect (DOKE) experimental results.²⁶



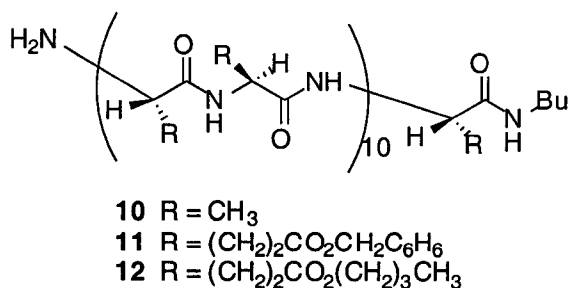
1.3 Chiral Oligomers and Polymers for Asymmetric Catalysis

Asymmetric catalysis is one of the most important methods to prepare optically active organic molecules.²⁷ With the increasing demand for optically pure drugs, the need for recoverable and reusable chiral catalysts is also growing because of the expense of optically active reagents. The application of polymeric chiral catalysts in asymmetric catalysis has a number of advantages, such as facile recovery of the normally quite expensive chiral catalysts, simplified product purification, and the potential to carry out flow reactor or flow membrane reactor synthesis.

Three general classes of synthetic main chain chiral polymers have been applied in asymmetric catalysis, including: (1) helical polymers from polypeptides; (2) polymers with flexible chiral chains such as polyesters and polyamides; and (3) polymers of rigid and sterically regular chiral chains represented by chiral conjugated polybinaphthyls.

1.3.1 Synthetic Polypeptide Catalyst

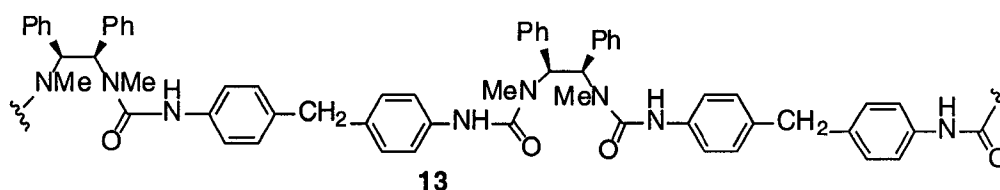
Synthetic polypeptides have been used as catalysts to carry out a number of organic reactions such as Michael additions, oxidations, and reductions. It was not until 1980, however, that the first highly enantioselective asymmetric reaction using synthetic polypeptides was discovered by Juliá et al.²⁸ In their study, different polypeptides such as poly[(*S*)-alanine] (**10**), poly[5-benzyl-(*S*)-glutamate] (**11**), and poly[5-butyl-(*S*)-glutamate] (**12**) were synthesized. They pointed out that **10** was the better catalyst in terms of chemical yields and enantioselectivity among the three polypeptides. They also showed that the enantioselectivity of the reported epoxidation was dependent on the molecular weight of the polypeptides. Thus, when the degree of polymerization of the peptides was increased from 10 to 30 units, the enantioselectivity in epoxidation of chalcone to the chiral epoxy ketone was increased from 85% to 93% ee. They concluded by doing intensive studies on the influence of polypeptide conformation on the stereoselectivity of the epoxidation. They found that polymers with a high content of α -helical conformation, e.g. **10**, had the maximum enantioselectivity.^{28,29} The increase in β -structure at the expense of the α -helical conformation, led to significantly reduced stereoselectivity.



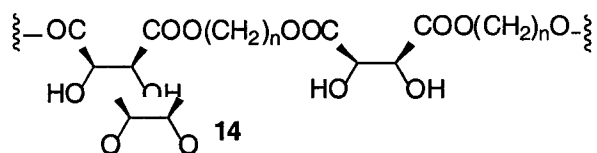
Bentley et al. recently improved upon Juliá's epoxidation reaction.³⁰ By using urea–hydrogen preoxide complex as the oxidant, 1,8–diazabicyclo[5.4.0]undec–7–ene (DBU) as the base and the Itsuno's immobilized poly[(*S*)–leucine] as the catalyst, the epoxidation of chalcone gave 100% conversion and >99% ee.

1.3.2 Chiral Polymer Catalysts Containing Amide, Urea and Ester Functionality

Lemaire and co-workers have reported the use of a chiral polyamide and a chiral polyurea for asymmetric catalysis.³¹ They showed that the chiral polyurea **13**, could be used for the catalytic transfer hydrogenation of acetophenone to enantiomeric alcohol in 60% ee.



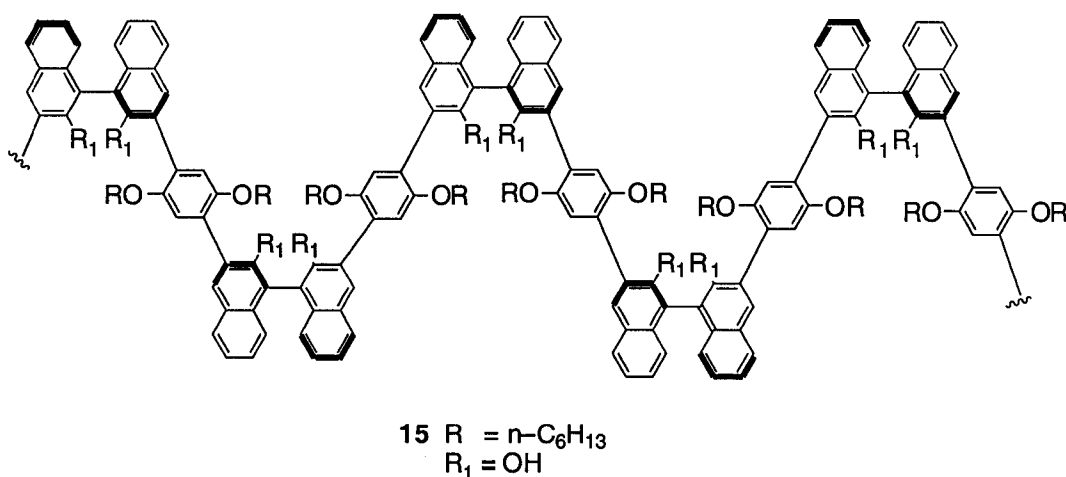
Canali and co-workers have successfully synthesized chiral polymers containing tartrate esters in the main chain for the Sharpless epoxidation of allylic alcohols.³² They pointed out that chiral polymer **14** catalyzed the conversion of an allylic alcohol to an epoxide in 79% ee.



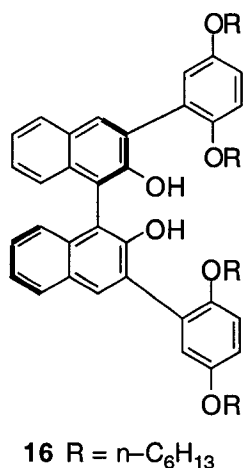
1.3.3 Polymers of Rigid and Sterically Regular Chiral Chains

The traditional approach toward preparing a polymeric chiral catalyst involves the development of a highly enantioselective monomeric catalyst and then the attachment of this monomeric catalyst to a flexible and sterically irregular polymer backbone. Although a few enantioselective polymer catalysts have been obtained in this way, a significant drop in enantioselectivity is often observed when a monomeric chiral catalyst is attached to a polymer support due to the changes in the microenvironment of the catalytic sites.³³

Recently, Pu and co-workers have been working on the synthesis of binaphthyl-based chiral conjugated polymers for materials application as well as for catalysis.³⁴⁻³⁸ They have discovered that the chiral polymer **15** has induced an excellent enantioselectivity in the reaction of benzaldehyde with diethylzinc to produce 1-phenylpropanol in 92% ee with no side products observed. They have shown that whilst high enantioselectivity was observed for the reaction of *para*-substituted benzaldehydes and cinnamaldehyde, the enantioselectivity for the *ortho*-substituted benzaldehydes was low.³⁹



The same group has successfully prepared **16** as a monomeric model of chiral polymer **15**. They elegantly reported that compound **16** was the best enantioselective catalyst yet for the reaction of aldehydes with diethylzinc and a broad range of aldehydes, including *para*-, *ortho*- or *meta*-substituted aromatic aldehydes, linear or branched aliphatic aldehydes, and aryl or alkyl substituted α,β -unsaturated aldehydes, can be alkylated in excellent enantioselectivity.⁴⁰ They hypothesized that the dramatic difference in enantioselectivity between the model compound **16** and the polymer **15** may be related to their different steric environments. They pointed out that in a coiled helical structure, all the binaphthyl units are cisoid, and in a completely extended zigzag structure, all the binaphthyl units are transoid. They concluded that the cisoid and transoid transitions cause interference between an adjacent catalytic sites in polymer **15**. This interference does not exist in the monomer **16**. Thus, there was a reduction in enantioselectivity observed for the reaction of diethylzinc with aldehydes using polymer **15** versus monomer **16**.⁴¹



Seebach and co-workers have recently reported the synthesis of cross-linked polystyrenes containing chiral $\alpha,\alpha,\alpha',\alpha'$ -tetraphenyl-1,3-dioxolane-4,5-dimethanol functionality. This polymer catalyzed the reaction of diethylzinc with heptyl aldehyde in 92% ee (75% yield) and with cyclohexanecarboxaldehyde in 86% ee (57% yield) in the presence of 1.2 equiv. of $\text{Ti}(\text{OCHMe}_2)_4$.⁴²

1.4 Chiral π -Conjugated Oligomers and their Potential Optical Applications

Many oligomers and a few polymers with intrinsically chiral π -conjugated systems are known. The traditional approach to π -conjugated polymers and small donor/acceptor molecules directed at interesting material properties, however, is based on attaching chiral non- π -conjugated pendants to the approximately planar π -conjugated system of polymers and small donor/acceptor molecules.⁴³ An alternate approach might rely on introducing chiral π -conjugated group, such as chiral binaphthyls, as part of the polymer chain or network.

Organic conductors, superconductors, and magnets are based on electroactive π -conjugated oligomers and polymers. For planar π -conjugated systems, the material properties are typically limited by weak intermolecular interactions in three-dimensional assemblies.⁴⁴

The π -conjugated electron system in oligomers qualify them as chromophores with a broad range of optical properties and as electrophores with the ability to accept or donate charge. Many physical properties important to materials science are related to the

initiation, transport, annihilation, or storage of charge. Basically, there are two main factors for studying oligomers of conjugated polymers:

(1) Oligomers can be model systems for understanding the fundamental electronic properties of the corresponding polymer, because oligomers can be designed and synthesized with a well-defined molecular length. They have been used most frequently as model systems for extrapolating physical properties of the corresponding ideal polymer of infinite length. Conversely, conjugated polymers show a distribution of lengths along which π -conjugation is effective. The actual conjugated segments of polymeric chains, however, are perturbed by defects, which may be of a conformational nature (e.g., bending or twisting of the chain so that it is no longer planar) or of a chemical nature, such as a saturated sp^3 -hybridized carbon atom located somewhere along the chain. Oligomeric systems on the other hand are well-defined monodisperse molecules, with a greatly diminished existence of defects within the molecular chains, when compared to polymers. They may serve as better candidates in terms of ordering of the molecules and with subsequent well-defined optical properties. This makes them significant for both theoretical and experimental investigations into a number of issues, which cannot be easily addressed in polymeric systems.⁴⁵

(2) Oligomers have proved in some cases to exhibit characteristics superior to those currently found in many conjugated polymers. A typical example is oligothiophenes which have been shown to possess high field-effect mobilities for thin film transistors due to very effective intermolecular charge transport.⁴⁶ In addition, short oligomers have been employed to achieve blue electroluminescence devices (e.g., blue emitting LEDs) due to their more confined band gaps that lead to blue emission.

1.5 Nonlinear Optical Properties of Conjugated Oligomers

Perhaps one of the most intriguing aspects of π -conjugated oligomers is their ability to interact with light in a nonabsorptive manner giving rise to nonlinear optical (NLO) properties.⁴⁷ The magnitude of the effect is governed by the polarizability of the molecule or oligomer. A question that one may ask is what factors affect polarizability. An organic chemist may say that the bonding electrons in, for example, polyacetylene are more polarizable than those in butane. Likewise, the inorganic chemist, may say that semiconductors are more polarizable than insulators. These simple observations suggest that the extent of electron delocalization is related to polarizability. In organic molecules, the extent of delocalization is affected by the atomic hybridization, the degree of coupling, and number of orbitals (and electrons) in the electronic system of interest. It is also evident that molecules/materials with strong, low-energy, absorption bands tend to be highly polarizable.

To date, applications using the nonlinear optical properties of materials have relied almost exclusively on inorganic crystals such as potassium niobate (KNbO₃) and lithium niobate (LiNbO₃). However, these inorganic materials are often very expensive and difficult to process.⁴⁸ As an alternative, organic materials, which offer many advantages over their inorganic candidates, have been explored. These advantages include faster nonlinear response times, lower costs, and comparable or greater off-resonance susceptibilities. Also important is the possibility of tuning the photophysical properties of a material to enhance a particular NLO effect simply by altering its chemical structure, as well as ease of synthetic adjustment and processing that allow the incorporation of functional groups for solubility.^{47,49}

Conjugated organic compounds have great potential as new third-order NLO materials as a result of their highly polarizable π -electron systems. The synthesis of

materials for device applications has a diverse set of requirements. The question one may ask is what does the device do and what factors will affect its performance? The answer to this question provides the requirements necessary for practical application and device fabrication, including optical transparency, one- and two-photon optical stability, thermal stability, orientational stability, high nonlinear susceptibilities (in other words the magnitude of the desired optical nonlinearity), a rapid nonlinear response, and finally processability.⁵⁰

Theoretically, nonlinear optics is concerned with the interaction of one or more electromagnetic radiation fields with matter to produce a new field that differs in phase, frequency, polarization or direction from the initial field(s) (i.e., the path of incident light).⁴⁷ The alternating electric field of light \vec{E} , imparts a polarization on the charged particles in the material. In an optically nonlinear material, the resulting polarization \vec{P} is described as a power series expansion of the form:

$$\vec{P} = \epsilon_0 \left(\chi^{(1)} \vec{E} + \chi^{(2)} \vec{E} \vec{E} + \chi^{(3)} \vec{E} \vec{E} \vec{E} + \dots \right)$$

where ϵ_0 is the dielectric constant and the $\chi^{(n)}$ are electric susceptibilities of the n-th order. In materials composed of molecules, the contributions of the induced molecular dipoles are similar:

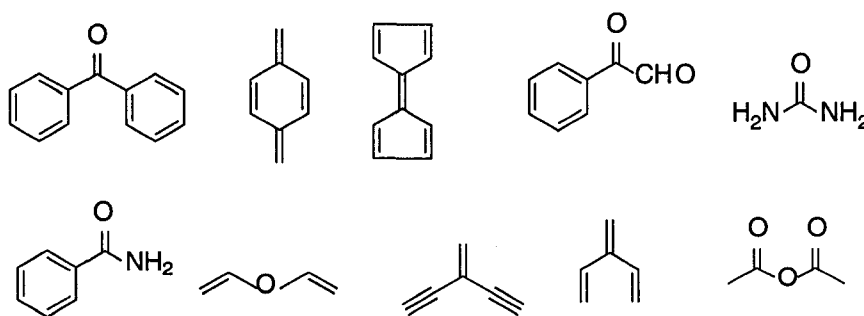
$$\vec{P} = \alpha \vec{E} + \frac{1}{2} \beta \vec{E} \vec{E} + \frac{1}{3} \gamma \vec{E} \vec{E} \vec{E} + \dots$$

where α being first polarizability or linear polarizability, β and γ are second and third-order polarizabilities. The quantities β and γ are also known as the molecular first and second hyperpolarizability, respectively. In bulk samples, the polarization per unit

volume is considered, leading to the susceptibility χ and nonlinear susceptibilities $\chi^{(2)}$ and $\chi^{(3)}$. A contribution from $\chi^{(2)}$ can come from only noncentrosymmetric media, whereas $\chi^{(3)}$ can arise from any medium regardless of symmetry. The organic compounds urea and *p*-nitroaniline (PNA), are commonly used as references, having β values of 2.3×10^{-30} esu⁵¹ and 34.5×10^{-30} esu,⁵² respectively.

1.6 Cross-conjugated Compounds and Their Significance

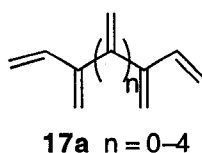
Cross-conjugation in organic compounds represents an alternative mode of π -electron communication.⁵³⁻⁵⁵ Cross-conjugated oligomers have potential for applications in electronic (e.g., organic conducting and semiconducting) and optical (third-order NLO) materials. Cross-conjugation has been defined as the situation in which two unsaturated fragments are not conjugated to each other, but are both conjugated to a third unsaturated moiety.⁵⁴ Each unsaturated center possesses $2n$ π -electrons, where n is an integer. The lone pair of electrons of a singly bonded nitrogen or oxygen atom is considered an unsaturated center, and compounds from a representative selection of cross-conjugated molecules are listed in Scheme 1.1.



Scheme 1.1 A representative selection of cross-conjugated molecules.

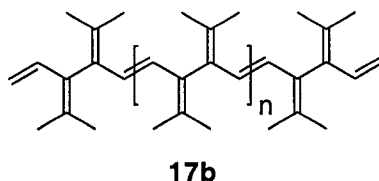
One interesting advantage of cross-conjugated materials is that they may be transparent to light in the visible region of the spectrum. Linearly conjugated materials are often light absorbing in this range, which can limit their optical application at these wavelengths. The synthetic tools for the construction of cross-conjugated compounds are not yet as well developed as for other areas of organic chemistry. As a result there is wide potential for the study of cross-conjugated compounds.

The first members of cross-conjugated oligomeric series are the [*n*]dendralenes, the simplest acyclic cross-conjugated hydrocarbons.^{56a} Sherburn *et al.* synthesized a series of dendralenes **17a**.^{56b} They reported that the UV-vis spectra of **17a** shows a single absorption maximum at $\lambda_{max} = 219.8\text{--}232.2$ nm (0.4% CDCl₃ in ethanol), confirming the nonplanar, nonconjugated arrangement of *s-trans*-1,3-butadiene and ethylene units in these molecules.

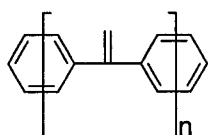


Grubbs and co-workers have reported the synthesis of a cross-conjugated polymer **17b** containing a [3]dendralene repeating unit, using ring-opening olefin-metathesis polymerization (ROMP).⁵⁷ They pointed out that the polymer possesses an average molecular weight between 12,000 and 51,000 with polydispersity being as low as 2.1. They claim that despite the lack of delocalization due to its cross-conjugation nature, surprisingly, polymer **17b** is quite easily oxidized and allows high carrier concentrations. They further pointed out that, modest conductivity (from $10^{-3}\text{--}10^{-4}$ S cm⁻¹) as well as paramagnetism could be achieved upon doping. They concluded by reporting that the UV-vis spectrum of **17b** displays a maximum absorption $\lambda_{max} = 278$

nm, manifesting the fact that its π -system is segregated into triene segments, and a nonplanar backbone conformation was assumed owing to the presence of large steric interactions.

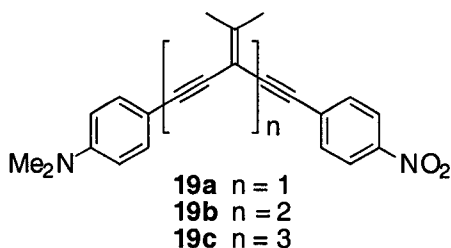


New insight into the behavior of cross-conjugated oligomers has been presented by van der Mass and co-workers.⁵⁸ Their studies on oligo(*p*-phenylenevinylidene)s **18a-d** using electronic spectra and electrochemical data as well as AM1 and PPP/SCF calculations have revealed that the cross-conjugated compounds basically behave as linearly π -conjugated systems in the sense that molecular orbitals are delocalized over the entire structure and systematically change in energy. The electronic interaction between the repeating units is, however, not very strong, which has the consequence that the spatial extension of the molecular orbitals does not lead to a red shift of the HOMO-LUMO electronic transition. This is related to the feature that the modest narrowing of the HOMO-LUMO gap with the chain length is accompanied by a relatively large reduction of electron repulsion. Their finding implies that care should be taken in the use of electronic spectra for the evaluation of conjugation phenomena.



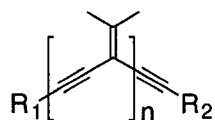
18a-d $n = 1-4$

In order to probe the influence by donor-acceptor (D-A) substitution on cross-conjugated enyne frameworks, Tykwinski and Ciulei have elegantly reported the synthesis and characterization of a series of D-A substituted *iso*-PDA oligomers, **19a-c**.⁵⁹ They have shown that the UV-vis spectra of **19a-c** display similar absorption characteristics, however, with the notable exception that there is no lower energy absorption for the longer derivatives ($n = 2$ and 3). They concluded from UV-vis spectroscopy that only monomer **19a** exhibits an observable influence from the incorporation of D-A groups.



Tykwinski and co-workers have successfully synthesized a series of *iso*-PDAs **20-26**.^{55,60-62} An investigation into the electronic properties has showed that an increase in the molar absorptivity and red-shift in λ_{max} as the number of enyne monomer units increased for the series **22a-g**.^{55,62} Thus π -electron communication is present along the cross-conjugated framework. Pendant functionality change from isopropylidene to adamantylidene had only a small effect on the molar absorptivity and overall shape of the UV-vis spectra. The lower energy cut-offs for the adamantylidene trimer **23b** and pentamer **23c** are red-shifted by about 10 nm versus those of analogous isopropylidene derivatives **22c** and **22e**. A totally different result was obtained from the analysis of the UV-vis spectra of **25** and **26**.⁶¹⁻⁶² The longer conjugated path in **26** (*vs*

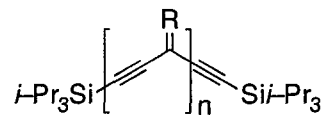
25) did not produce a bathochromic shift. Thus, a minimal contribution from cross-conjugation has been observed from the spectra of these compounds.



20a-e $\text{R}_1, \text{R}_2 = \text{SiMe}_3; n = 1, 3, 4, 5, 7$

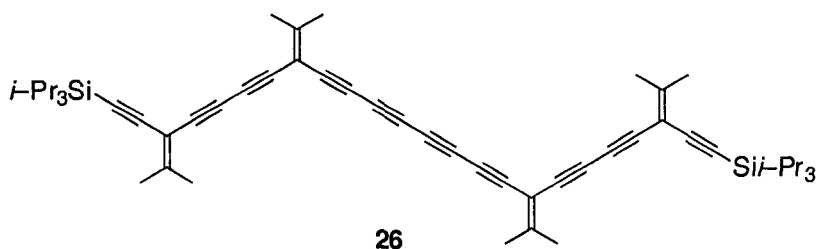
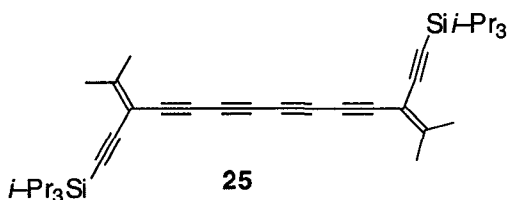
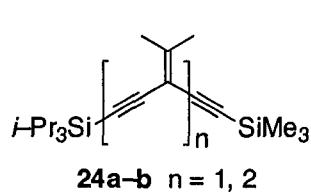
21a-b $\text{R}_1 = \text{SiMe}_3; \text{R}_2 = \text{Si}i\text{-Pr}_3; n = 1, 2$

22a-g $\text{R}_1, \text{R}_2 = \text{Si}i\text{-Pr}_3; n = 1, 2, 3, 4, 5, 7, 9$

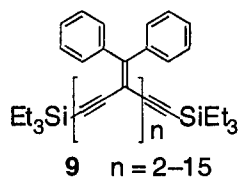


23a-c $n = 1, 3, 5$

$\text{R} = \text{adamantylidene}$



Tykwinski and Zhao²⁶ have elegantly synthesized perphenylated *iso*-polydiacetylene oligomers **9**, with triethylsilyl (TES) endcapping groups as described in Section 1.2 of this chapter. They reported that molecular mechanics studies on the conformational properties of these molecules suggest that they fold into a helical conformation that also supports the results obtain from the nonlinear optical studies.



1.7 Thesis Goals

Cross-conjugated compounds have been of interest due to their unique mode of π -electron delocalization as well as their potential for applications in electronic (e.g., organic conducting and semiconducting) and optical (third-order NLO) materials which possesses electronic transparency.

Previous studies on cross-conjugated *iso*-PDAs with cyclohexylidene substituent and triisopropylsilyl (TIPS) endcapping groups have shown reduced stability due to the allylic protons on cyclohexane.⁶² The *iso*-PDA with adamantylidene substituent and TIPS endcapping groups showed dramatic reduced solubility with increasing chain length.⁶²

A series of perphenylated *iso*-PDA oligomers, with diphenylvinylidene substitution and TES endcapping groups were first assembled by Zhao.^{26a} The reasons for the incorporation of the diphenylvinylidene groups into the oligomer backbone was: (a) the diphenyl groups were expected to improve solubility, (b) the lack of an allylic proton would eliminate the possible decomposition under air; thereby improving the stability,⁶² and (c) the diphenyl groups would also contribute to the π -conjugation enhancing the properties for potential applications such as nonlinear optics and electroluminescence.

In order to elaborate on the third-order NLO studies done by Slepko^{26b} *et al.* *iso*-PDAs with the TES endcapping groups and to more fully understand the structure-property relationships, our investigation targeted cross-conjugated *iso*-PDAs with *tert*-butyldimethylsilyl (TBDMS) endcapping groups. These oligomers were assembled through Sonogashira cross-coupling reaction shown in Fig. 1.1. Besides increasing stability and solubility, the TBDMS endcapping groups were cost-effective. That is, whilst 10 g of triisopropylsilyl chloride (TIPS-Cl) cost \$250.00, 10 g of *tert*-butyldimethylsilyl chloride (TBDMS-Cl) cost \$30.00, almost a ten-fold savings.

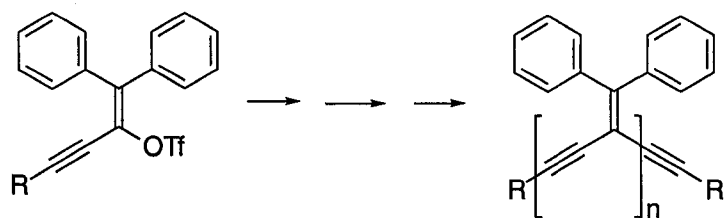


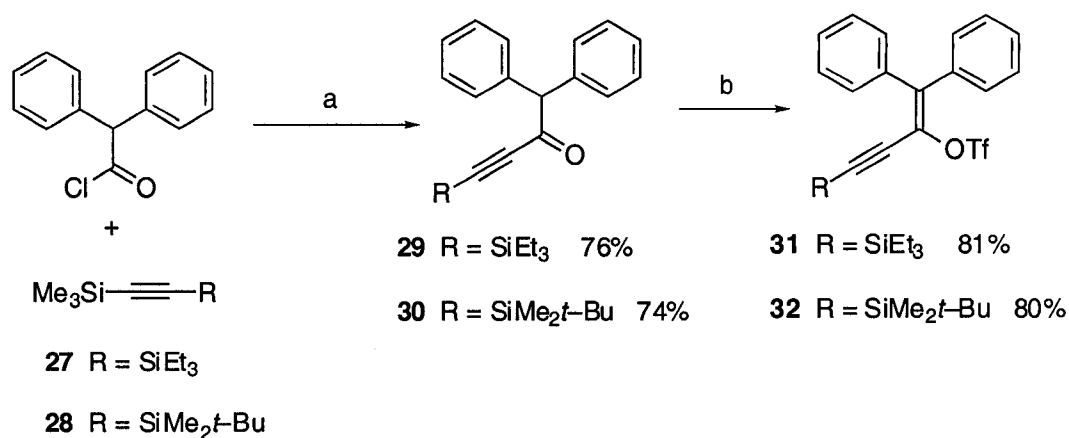
Fig. 1.1 Proposed assembly of perphenylated *iso*-PDA oligomers

As mentioned in the introduction, studies have been done in our group toward showing that the perphenylated *iso*-PDA oligomers fold in solution. Molecular mechanics studies on the conformational properties of these molecules suggest that the perphenylated *iso*-PDA oligomers fold into a helical conformation. In order to confirm the above observation, a chiral auxiliary has been synthesized with the aim of incorporating it into the oligomer chain, in an attempt to bias the "twist sense" of the helix, based on the 'Sergeants-and-Soldiers' principle.^{26c} That is to say that by the attachment of pendant, chiral 'Sergeant' to an achiral system of 'Soldiers', the Sergeants might control the chirality of the entire system. The synthesis of the chiral auxiliary has been outlined in the results and discussion below.

1.8 Results and Discussion

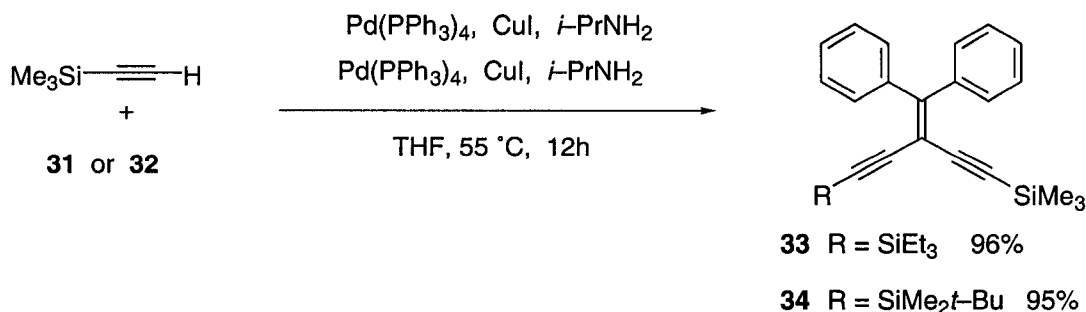
1.8.1 *Synthesis of Perphenylated iso-Polydiacetylene (iso-PDA) Oligomers*

The synthetic building blocks vinyl triflates **31** and **32**, can be made through modification of the procedure described by Stang, as shown in Scheme 1.2.⁶³⁻⁶⁴ It has been reported that using bistrimethylsilylacetylene as the starting material in the Friedel-Crafts type acylation of silyl-protected acetylenes,⁶⁵ could result in a mixture of bis-acylated and mono-acylated products.^{26a} In addition, desilylation of the newly formed ketone under the reaction conditions was also observed. These side-reactions made the isolation difficult. Changing one of the protecting groups in bistrimethylsilylacetylene with a more robust silyl group, such as TES **27** and TBDMS **28** groups, actually limited the formation of the side-products as well as the purification problem, especially with the TBDMS groups. The ketone **29**, with the TES group, showed limited stability over time even when stored under an inert gas environment and at low temperature (-20 °C), whereas **30** (with the TBDMS group) showed little decomposition at room temperature over a period of months. In this sense, there is the need to immediately transform **29** into vinyl triflate **31**. Triflation of **29** and **30** took place in the presence of excess triflic anhydride and 2,6-di(*tert*-butyl)-4-methylpyridine in CH₂Cl₂ at room temperature. Even though this reaction took more than 3 days to complete, excellent yields were obtained, 81% for **31** and 80% for **32**.

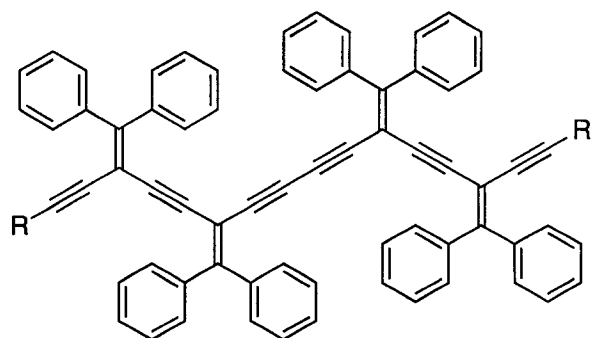


Scheme 1.2 Reagents and conditions: (a) AlCl₃, CH₂Cl₂, 0 °C. (b) triflic anhydride, 2,6-di(*tert*-butyl)-4-methylpyridine, CH₂Cl₂, rt.

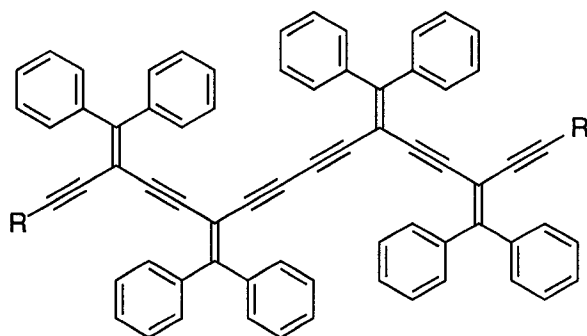
The synthesis of the diphenylvinylidene substituted enediyne **33** and **34** was achieved using Sonogashira Pd-catalyzed cross-coupling conditions.⁶⁶ Triflate **31** and **32** were cross-coupled with trimethylsilylacetylene (TMSA) using PdCl₂(PPh₃)₂ as catalyst, CuI as co-catalyst, and *i*-Pr₂NH base in THF for 12 h under reflux (in this case 55–60 °C). Using Pd(PPh₃)₄ as catalyst under an Ar or N₂ atmosphere, gave similar results as PdCl₂(PPh₃)₂. More homocoupled by-product (bistrimethylsilylbutadiyne), however, was formed when PdCl₂(PPh₃)₂ was used. After purification through a silica gel column, enediyne monomers **33** and **34** were isolated in pure form as colorless solids with defined melting points of 61–62 °C and 100–102 °C, respectively.



Scheme 1.3 Formation of monomer



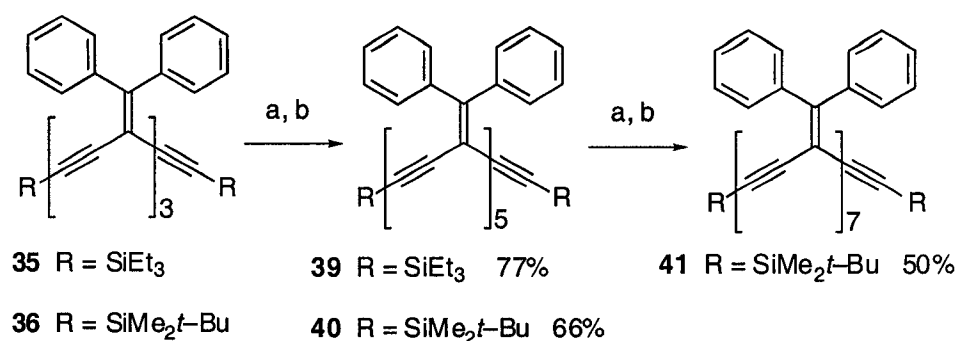
37 R = SiEt₃



38 R = SiMe₂t-Bu

Scheme 1.5 Tetrameric homocoupled by-products

Desilylation of trimers **35** and **36** with TBAF, followed by cross-coupling with triflates **31** and **32**, using the optimized cross-coupling conditions afforded pentamers **39** and **40** as yellow solids in 77% and 66% yields, respectively after purification via column chromatography (Scheme 1.6). Likewise, heptamer **41** was formed from pentamer **40** as a yellow solid in 50% yield after purification via size-exclusion chromatography (SEC). To date, all the perphenylated *iso*-PDA oligomers show decent stability and solubility for NMR spectroscopic analysis.



Scheme 1.6 Reagents and conditions: (a) TBAF, wet THF, rt. (b) **31** or **32**, Pd(PPh₃)₄, CuI, *i*-Pr₂NH, THF, 55–60 °C, 12 h.

1.8.2 Physical Characteristics

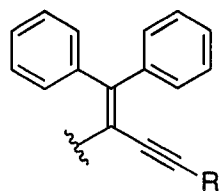
The structures of the perphenylated *iso*-PDA oligomers were judged by their spectroscopic data. In the ¹H NMR spectra of the diphenylvinylidene series, the resonances of the aromatic protons are observed in the range of 7.1–7.5 ppm for both the TES- and TBDMS-encapped oligomers. In the ¹³C NMR spectra of the diphenylvinylidene series, the resonances of the phenyl groups are observed in the range of δ 127–130 for the tertiary carbons and δ 139–140 for the quaternary carbons. The vinylidene carbons outside of the main chain (Ph₂C=C) are quite deshielded, resonating at δ 154–157 for both the TES- and TBDMS-encapped molecules. For monomer **34**, this carbon is discernible at δ 157.6, at δ 156.6 and 154.8 for trimer **36**, at δ 157.0, 155.0 and 154.9 for pentamer **40**, and at δ 156.9, 155.4, 155.1 and 150.0 for heptamer **41**. The in-chain vinylidene carbons (Ph₂C=C) fall into the chemical shift range of the acetylenic carbons, from δ 90–104 for both the TES- and TBDMS-encapped series. The reason why the vinylidene carbons outside of the main chain (Ph₂C=C) are quite

deshielded whilst the in-chain vinylidene carbons ($\text{Ph}_2\text{C}=\text{C}$) are quite shielded is because for olefins, it is known that phenyl substituents increase the chemical shift of the adjacent carbon atom and decrease the chemical shift of the other carbon in the vinyl moiety, whereas acetylene substituents have an opposite effect.⁶⁷ In addition, the synergetic effect of the two ethynyl bonds and the two geminal phenyl groups polarizes the vinylidene bond resulting in the deshielding of the vinylidene carbons outside of the main chain ($\text{Ph}_2\text{C}=\text{C}$).

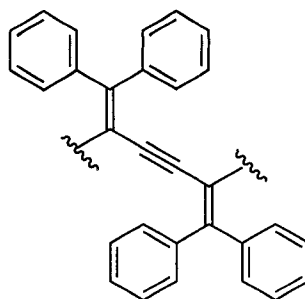
All the perphenylated *iso*-PDA oligomers, with both the TES- and TBDMS-encapped groups, show improved thermal stability compared to their cyclohexylvinylidene counterparts which decomposes under air.⁶² The monomeric **33**, trimeric **35** and pentameric **39** members of the TES-encapped series show well-defined melting points at 61–62, 60–60, and 85–86 °C, respectively. The monomeric **34**, trimeric **36**, pentameric **40** and heptameric **41** members of the TBDMS-encapped series also show well-defined melting points at 100–102, 169–171 (decomp),⁶⁸ 119–121 and 116–118 °C, respectively. In addition, all of the perphenylated *iso*-PDA oligomers (with either the TES- and TBDMS-encapping groups) show good kinetic stability. Thus, they are stable to air and can be stored for extended periods of time at ambient temperature without any sign of decomposition by either TLC or NMR spectroscopic analysis.

1.8.3 Electronic Absorption Properties

The most interesting feature of the perphenylated *iso*-PDA oligomers is their unique cross-conjugated π -electronic framework. The UV-vis absorption in CHCl_3 of the TBDMS-encapped oligomers ranging from monomer to heptamer are shown in Fig. 1.2.



34 phenyl-ene-yne



35-41 phenyl-ene-yne-ene-phenyl

Scheme 1.7 Pattern of the conjugated segments of the *iso*-PDA oligomers

The important feature of the electronic absorption behavior of the perphenylated *iso*-PDA oligomers is a steadily increasing molar absorptivity as the number of enyne monomer units is increased. In the spectrum of trimer **36**, one distinct, low-energy absorption is due to the π - π^* transition from HOMO to LUMO. In the cisoid orientation (C_{2v}), the HOMO to LUMO ($A_1 \rightarrow B_1$) and HOMO to LUMO+1 ($A_1 \rightarrow A_1$) transitions are both symmetry-allowed. However, in the centro symmetric transoid orientation (C_{2h}), only the HOMO to LUMO ($A_g \rightarrow B_u$) transition is symmetry-allowed, whereas the HOMO to LUMO+1 ($A_g \rightarrow A_g$) transition is symmetry forbidden.^{26a} The low-energy absorption peak at 369 nm is ascribed to the HOMO to LUMO transition in the transoid orientation, whereas the higher-energy absorption peaks seen at 257 and 324 nm likely correspond to HOMO to LUMO+1 and HOMO to LUMO transitions, respectively of the cisoid orientation. In the spectrum of pentamer **40**, the higher-energy absorption peak at 324 nm has merged into the low-energy intensified peak at 377 nm. The heptamer also

shows a very broad and featureless peak with a maximum absorption energy of $\lambda_{\max} = 378$ nm. This can also be attributed to the $\pi-\pi^*$ transition from HOMO to LUMO.

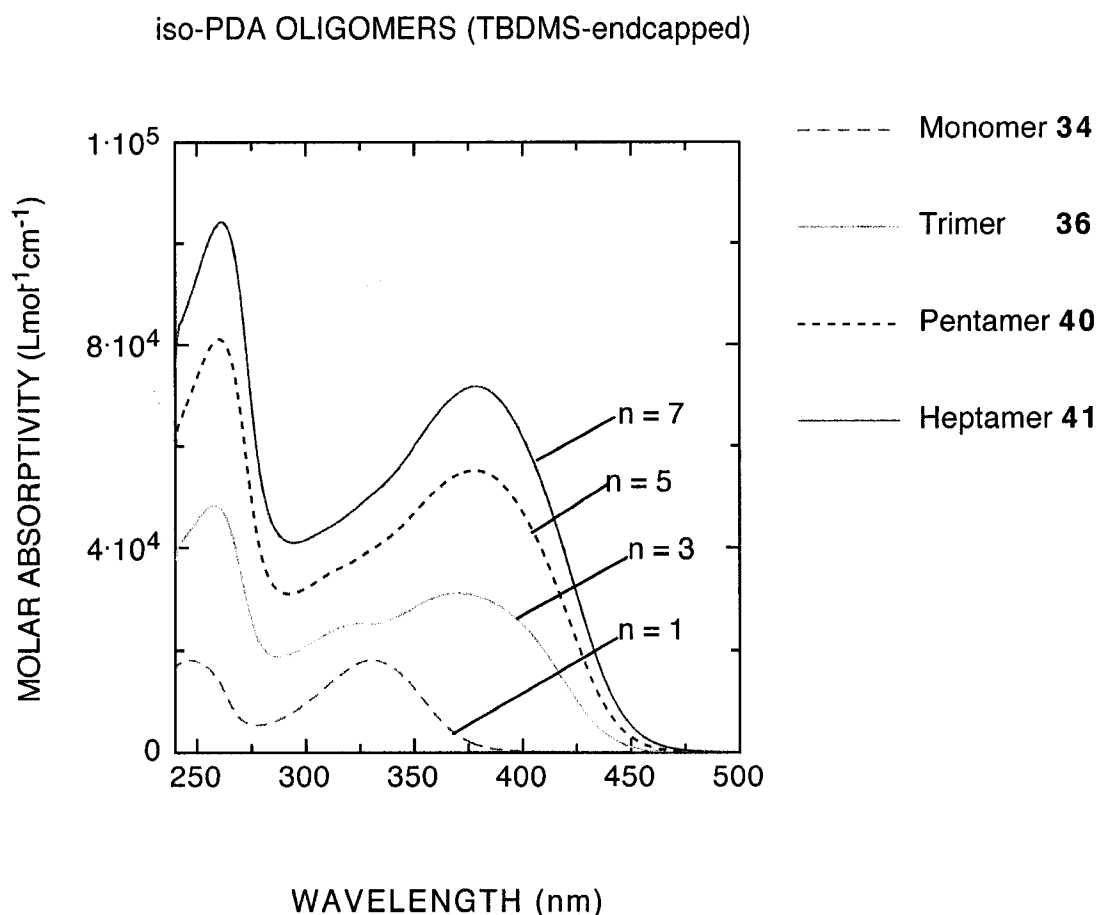


Fig. 1.2: Electronic absorption spectra ($\epsilon[\text{L mol}^{-1} \text{cm}^{-1}]$) in CHCl_3 , comparing the effects of oligomer length between TBDMS-encapped perphenylated *iso*-PDA oligomers: **34**, **36**, **40** and **41**.

In comparison, the TBDMS-encapped *iso*-PDA oligomers show similar absorption characteristics to the TES analogues. The TES-encapped *iso*-PDA oligomers, trimeric

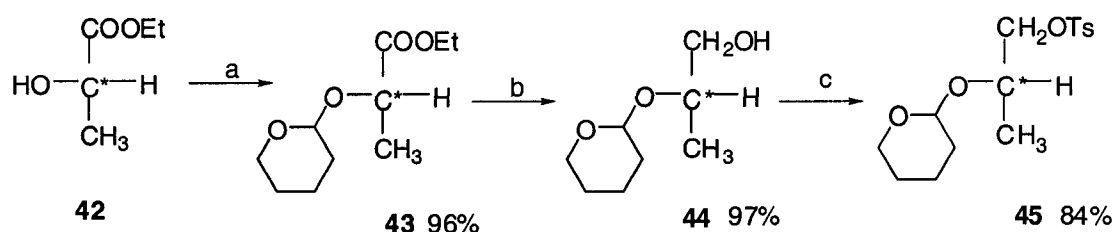
35, has λ_{max} (ϵ) 324 (26200), 373 (31100), pentameric **39**, 377 (49300) and heptameric 378 (76800), respectively.^{26a} In the same way as described above, with the TBDMS-encapped *iso*-PDA oligomers, trimeric **36**, has λ_{max} (ϵ) 324 (25300), 369 (31200), pentameric **40**, 377 (55200) and heptameric **41**, 378 (71700), respectively. These results show that as the conjugation length increases from monomer through to heptamer, one observes a slight red shift in λ_{max} , as well as increase in molar absorptivity. The π -electron delocalization along the phenyl-ene-yne-ene-phenyl conjugated segments of trimer to heptamer might be predicted to be reduced as a result of the non-planar conformations due to rotation, nonetheless a slight lowering in the energy of the longest wavelength cutoff is still observed as the chain length increases from monomer **34** to heptamer **41**.

1.8.4 Synthesis of the Chiral Auxiliary

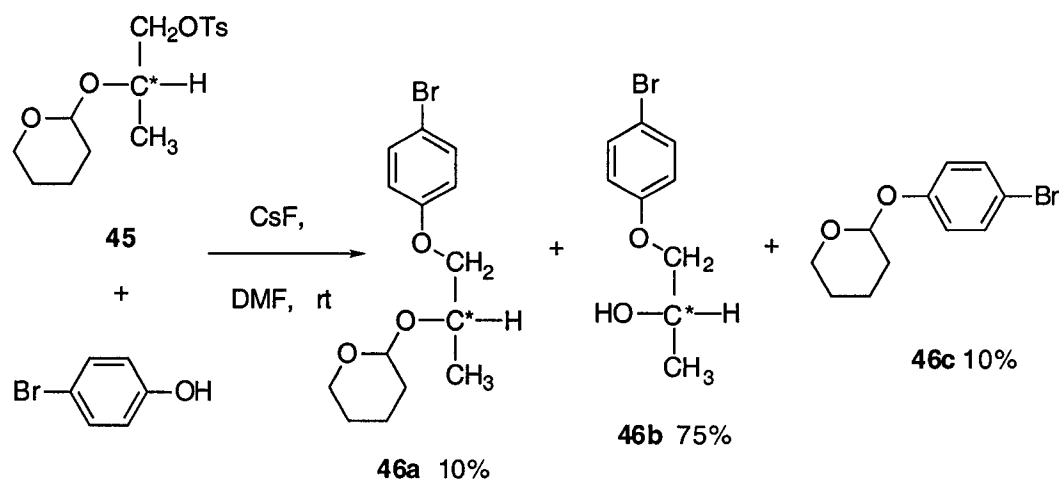
As mentioned in the introduction, extensive studies have been done in our group toward showing that perphenylated *iso*-PDA oligomers fold in solution. Molecular mechanics studies on the conformational properties of these molecules suggest that the perphenylated *iso*-PDA oligomers fold into a helical conformation. In order to confirm the above observation, a chiral auxiliary has been synthesized with the aim of incorporating it into the oligomer chain, in an attempt to bias the "twist sense" of the helix, based on the 'Sergeants-and-Soldiers' principle.^{26c} The outline of the synthesis of the chiral auxiliary is shown in Scheme 1.8.

The chiral starting material in our synthesis was ethyl (*S*)-(+)-lactate **42**, which was readily protected with 3,4-dihydro-2H-pyran (DHP) to give **43**, the tetrahydropyran-2-yl ether of ethyl (*S*)-(+)-lactate. Reduction of **43** in the presence of

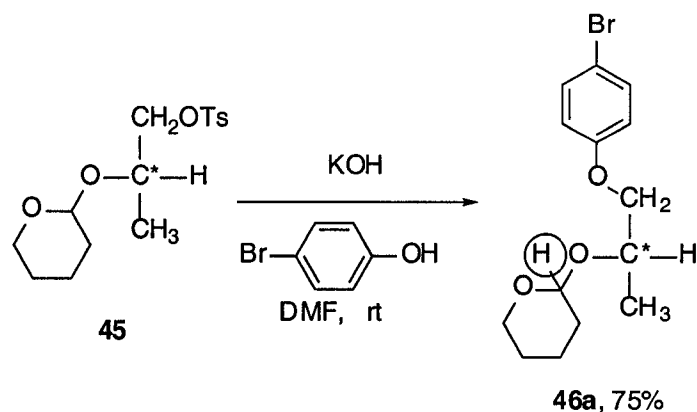
lithium aluminium hydride (LAH) was readily achieved through a modification of the procedure described by Kitching⁶⁹ to form (2*S*)-2-((tetrahydropyran-2'-yl)oxy)-1-propanol **44**. Conversion of alcohol **44** into the tosylate **45** was carried out through a modification of the method described by Chielliani.⁷⁰ The etherification reaction of tosylate **45** with 4-bromophenol in the presence of CsF⁷¹ resulted in a mixture of products **46a-c** as shown in Scheme 1.9. The formation of **46b** was believed to result from the formation of hydrofluoric acid, which is the product of deprotonation of phenol by CsF, followed by deprotecting/removing the tetrahydropyranyl (THP) group. Compound **46c** then resulted from the reaction of the phenoxide on the deprotected THP. Because this methodology failed to give satisfactory results, our attention was then turned to a procedure described by Wawrzenczyk⁷² more than two decades ago. Through a modification of this procedure, tosylate **45** was successfully converted to **46a** as approximately 5:1 mixture of diastereomers in the presence of 4-bromophenol and potassium hydroxide (KOH) in 75% yield as outlined in Scheme 1.10.



Scheme 1.8 Reagents and conditions: (a) DHP, HCl (conc.); (b) LiAlH₄, Et₂O; (c) TsCl, pyridine.



Scheme 1.9 Formation of **46a–c**



Scheme 1.10 Formation of chiral auxiliary **46a**

Confirmation of the structure of **46a** is based on analysis of the spectroscopic data. In the ^1H NMR spectrum, the two aromatic protons ortho to bromine atom are deshielded and show up at δ 7.32 (d, $^3J_{\text{H,H}} = 8.8$ Hz). The two protons, ortho to the alkoxy group, are shielded and their signal appears at δ 6.74 (d, $^3J_{\text{H,H}} = 8.8$ Hz). The remaining signals are also consistent with the structure, in particular the deshielded circled acetal proton at δ 4.80. The ^{13}C NMR spectrum also support this assignment. The resonances of the

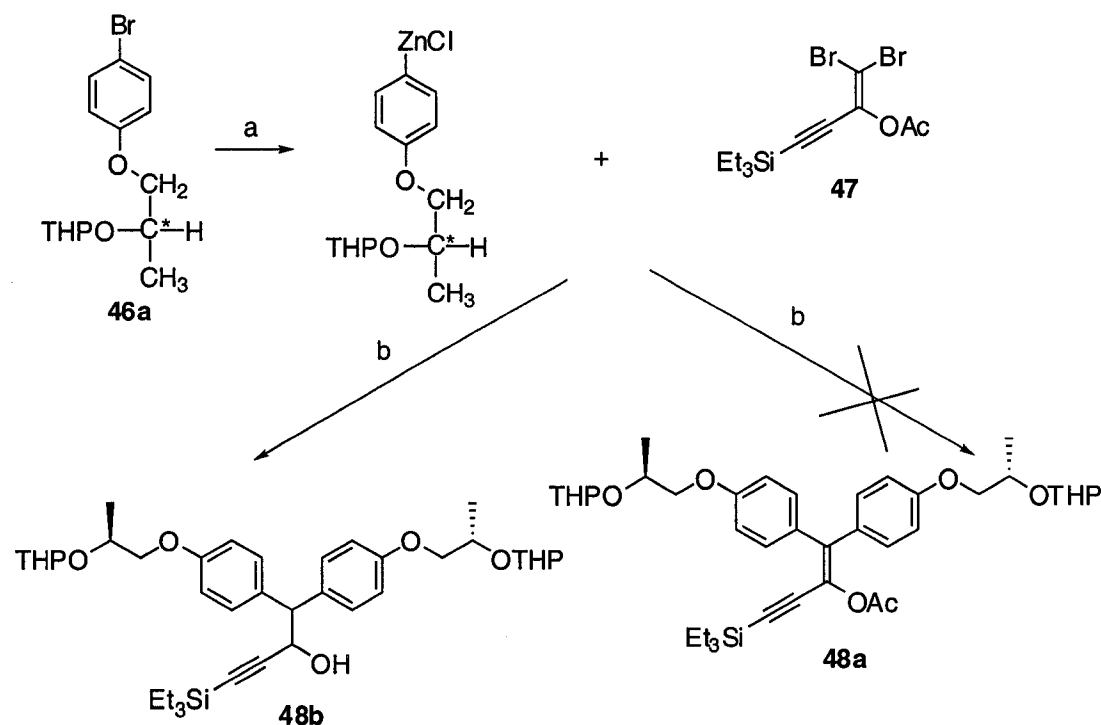
ipso aromatic carbons are observed at 158.1 ppm and 132.2 ppm for the C–O and C–Br, respectively. The shielded carbon atoms on the aromatic ring appear upfield at δ 116.4 and 112.8. The acetal carbon is observed at δ 98.9. The IR spectrum shows absorptions for the aromatic ring double bonds at 1590 cm^{-1} and for the sp^2 C–H stretches in the aromatic group at 3052 cm^{-1} . The mass spectrum shows a molecular ion peak at m/z 314 corresponding to the molecular mass of **46a**. Elemental analysis calculated for $\text{C}_{14}\text{H}_{19}\text{O}_3\text{Br}$ (**46a**): C, 53.53; H, 6.10. Found: C, 53.46; H, 6.20. The optical rotation measurement of **46a** was $[\alpha]_{\text{D}}^{22} = -30^\circ \text{ mL g}^{-1} \text{ dm}^{-1}$ ($c = 0.5$, CHCl_3). The spectral data for **42–45** were all consistent with the literature.^{69,70}

1.8.5 Negishi Cross–Coupling of Chiral Auxiliary

Rankin and Tykwinski⁷³ have reported studies on the formation of vinyl triflates, which are a major building block for functionalized macrocycles and expanded radialenes. Based on this, we decided to transform our chiral auxiliary **46a**, into a vinyl triflate using Negishi⁷⁴ Pd(0)–mediated cross–coupling reaction and subsequently incorporate it with the *iso*–PDA oligomers. Chiral auxiliary **46a**, was reacted with *n*–BuLi to effect lithium–halogen exchange. Lithiation was followed by transmetalation with zinc(II) chloride and then the Pd(0)–mediated Negishi cross–coupling reaction with vinyl acetate dibromide **47** prepared by Rankin.⁷³ However, this reaction failed to yield the required target, the vinyl acetate **48a**, but may have rather formed the hydrolyzed product alcohol **48b**, as outlined in Scheme 1.11.

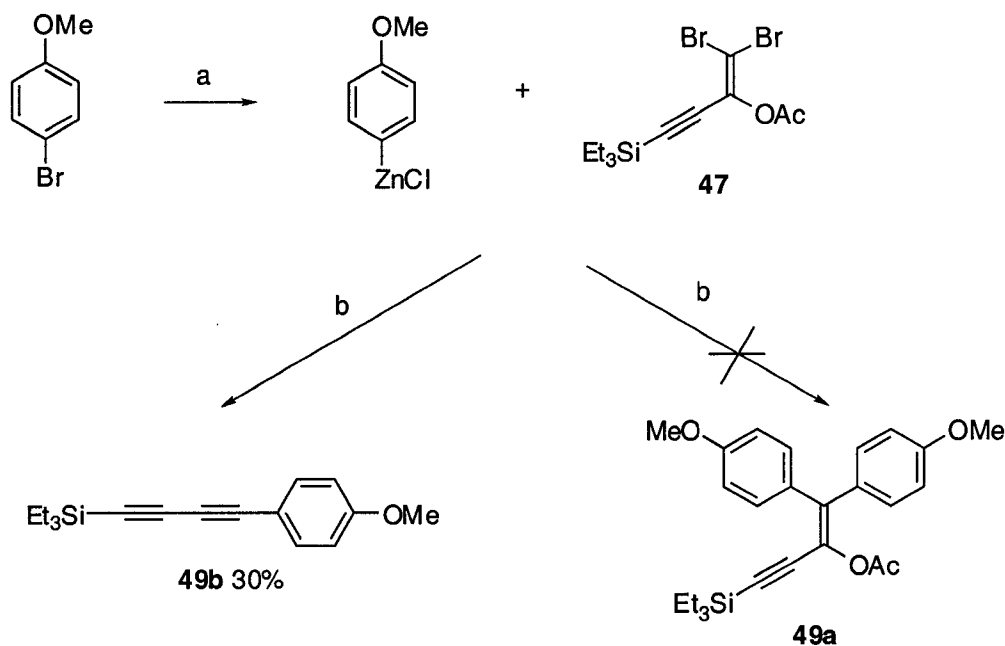
The formation of the alcohol **48b** was suggested through evidence such as IR spectrum: the ester functionality at 1765 cm^{-1} had disappeared and a broad and medium

peak at 3400 cm^{-1} was observed, suggesting the presence of alcohol. The ^1H NMR spectrum also showed the absence of the acetate (CH_3) peak at δ 2.0.



Scheme 1.11 Reagents and conditions: (a) BuLi, ZnCl₂, THF, -78 °C; (b) Pd(PPh₃)₄, THF, Δ.

This prompted us to try the same reaction with commercially available *para*-bromoanisole. To our surprise, we obtained diyne **49b**, instead of **49a**, as shown in Scheme 1.12. Presumably, the electron-donating substituent on the aryl halide retarded the Negishi cross-coupling reaction or the resulting organozinc species was unstable to the reaction conditions, resulting in the metal halogen exchange and ultimately elimination into the diyne product.



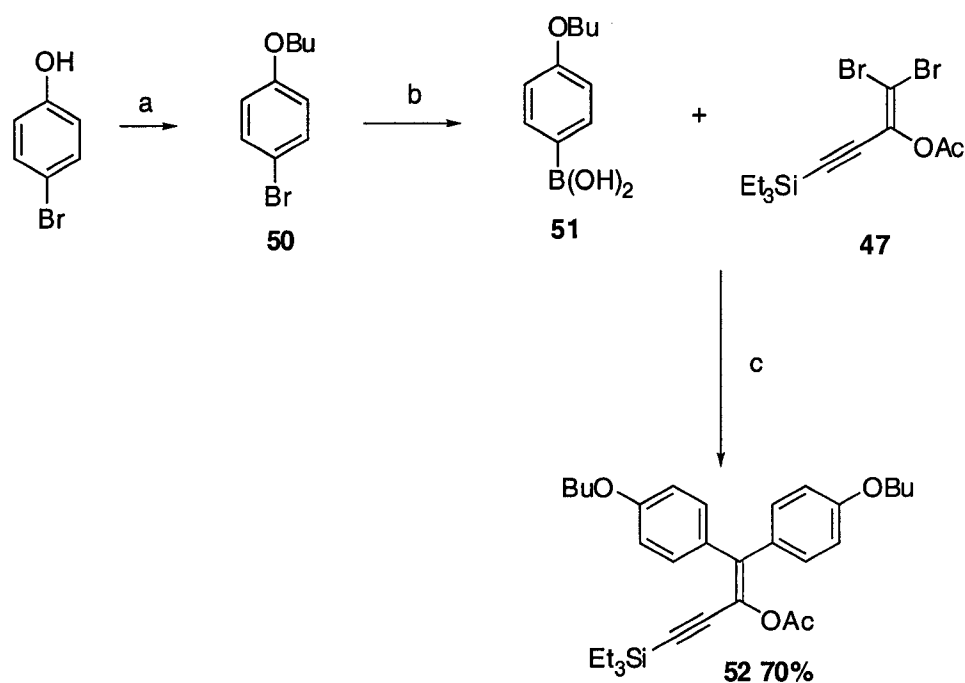
Scheme 1.12 Reagents and conditions: (a) BuLi, ZnCl₂, THF, -78 °C; (b) Pd(PPh₃)₄, THF, Δ.

Confirmation of the diyne structure **49b** is based on analysis of the spectroscopic data. In the ¹H NMR spectrum, the two aromatic protons ortho to the diyne group are deshielded and show up at δ 7.44 (d, ³J_{H,H} = 8.7 Hz). The two protons ortho to the methoxy group are shielded and their signal appears at δ 6.84 (d, ³J_{H,H} = 8.7 Hz). The methoxy protons resonate at δ 3.8. The TES protons show a triplet at δ 1.04 (³J_{H,H} = 8.1 Hz) and a quartet at δ 0.66 (³J_{H,H} = 8.1 Hz). The ¹³C NMR (APT) spectrum also supports this assignment. The resonances of the phenyl group are observed at 161 ppm and 113 ppm for the quaternary carbons C–O and C–C≡, respectively, whereas the tertiary carbons appear at 135 ppm and 114 ppm. The resonances for all four acetylene

carbons were discernible at δ 90, 88, 77, and 73. The methoxy carbon was observed at δ 55. The resonances for the TES group were seen at 18 ppm and 15 ppm for the methyl and methylene carbons, respectively. The IR spectrum shows the presence of all the respective functional groups. A strong peak at 2201 cm^{-1} and a medium peak at 2100 cm^{-1} correspond to C \equiv C stretches whereas the strong peaks at 1603 cm^{-1} , 1509 cm^{-1} and a medium peak at 1567 cm^{-1} all correspond to the stretching of the aromatic C=C bonds. The mass spectrum shows a molecular ion peak at m/z 270 corresponding to the molecular mass of **49a**.

1.8.6 Suzuki Cross-Coupling of Chiral Auxiliary

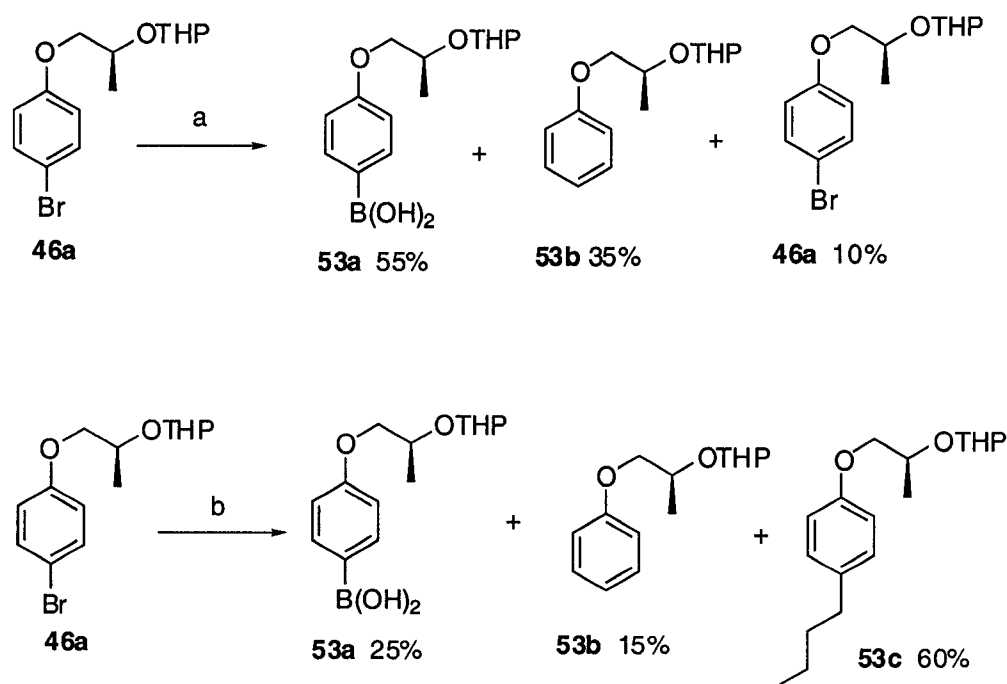
Our attention was then drawn to work done previously by my colleague Rankin,⁷³ and we evaluated the effectiveness of Suzuki cross-coupling reaction on vinyl acetates. On this note, etherification of commercially available butyl bromide with 4-bromophenol in the presence of KOH gave 4-bromobutoxybenzene **50** in 95% yield. 4-Bromobutoxybenzene **50** was then reacted with butyllithium (*n*-BuLi) to effect lithium-halogen exchange and trimethylborate was then added. Following a basic workup⁷⁵ that consisted of extracting the boronic acid into aqueous NaOH, acidifying and back-extracting into Et₂O, the butoxy substituted boronic acid **51** was isolated and recrystallized to give pure **51** in 70% yield. This compound was confirmed by IR, ¹H NMR and ¹³C NMR spectroscopy as well as its electron impact mass spectrum. The purified boronic acid **51** was readily converted into the vinyl acetate **52** via a Pd(0)-mediated Suzuki cross-coupling reaction with vinyl acetate **47** as shown in Scheme 1.13. All the spectral characteristics of vinyl acetate **52** were consistent with those reported by Rankin.⁷³



Scheme 1.13 Reagents and conditions: (a) BuBr, KOH, EtOH; (b) *n*-BuLi, B(OMe)₃, THF, -78 °C; (c) Pd(PPh₃)₄, K₂CO₃, PhMe, 110 °C.

We anticipated that a similar Suzuki reaction could be accomplished on the chiral auxiliary **46a**. To synthesize the boronic acid of **46a**, we reacted **46a** with *n*-BuLi in THF at -78 °C to effect the lithium-halogen exchange, and trimethylborate was then added. A basic workup was then performed consisting of extracting the boronic acid into aqueous NaOH, acidifying, and then back-extracting into Et₂O. In this case, we could not acidify to pH = 1, but rather pH = 6–6.5 because the tetrahydropyran (THP) protecting group on **46a** was acid labile. This resulted in approximately 55% of the boronic acid with the chiral auxiliary **53a**, 10% of the starting material **46a** and 35% of a by-product **53b**. This was verified by mass spectrometry data as well as ¹H and ¹³C NMR spectroscopic analysis. The presence of the starting material in the product mixture prompted us to modify the reaction conditions. On this note, **46a** was reacted

with 1.2 equiv. of *n*-BuLi in THF, followed by slow warming of the mixture from -78 to 0 °C to effect lithium-halogen exchange and trimethylborate was then added at -78 °C. Following a basic workup that consisted of extracting the boronic acid into aqueous NaOH, acidifying to pH = 6–6.5, and back-extracting into Et₂O resulted in approximately 25% of the boronic acid with the chiral auxiliary **53a**, 60% of butylated by-product **53c** and 15% of by-product **53b** as outlined in Scheme 1.14. The proposed structures of these by-products were supported by mass spectrometric data, as well as ¹H and ¹³C NMR spectroscopic analysis.



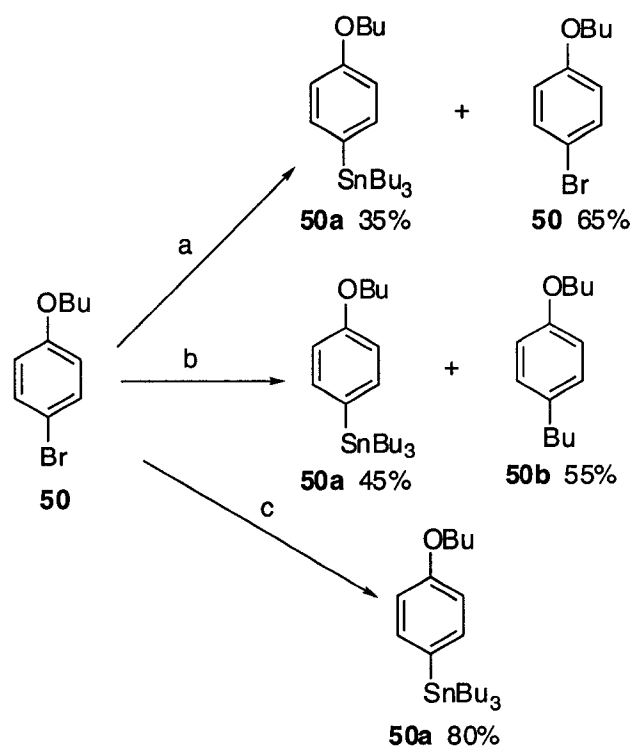
Scheme 1.14 Reagents and conditions: (a) *n*-BuLi, B(OMe)₃, THF, -78 °C; (b) *n*-BuLi, B(OMe)₃, THF, -78 ° – 0 °C.

Formation of the butylated derivative of the chiral auxiliary **53c** can be attributed to the following possibility. If the lithium-halogen exchange were occurring, then the

resulting intermediate should be stable enough to react with the generated butyl bromide in an S_N2 fashion. The formation of the by-product **53b** might have resulted from exposure of the lithiated species **46a** with adventitious H₂O or possibly during the workup.

Evaluation of the boronic acid formation from chiral auxiliary **46a** has revealed that although these precursors do have the potential to form boronic acids in a manner analogous to the simple pendant butoxy groups, the reaction is not as facile.

We then decided to evaluate the effectiveness of the stannane reagents in cross-coupling reactions with **47**.⁷³ To synthesize the aryl stannane, previously prepared 4-bromobutoxybenzene **50** was treated with *n*-BuLi in Et₂O at -78 °C to effect lithium-halogen exchange, then reacted with tributyltinchloride. After workup, approximately 35% of the stannane product **50a** as well as 65% of the starting material **50** were obtained. The product ratio was suggested by integration of the ¹H NMR spectrum. Modification of the reaction conditions as described above was done by changing the solvent to THF and warming the reaction mixture slowly from -78 to 0 °C. This resulted in approximately 45% of the stannane product **50a** as well as 55% of butylated by-product, **50b**. This ratio was also assigned by the ¹H NMR spectroscopic analysis. The formation of the butylated by-product **50b** can be assigned to the reasons described above (i.e., the reaction of the aryl lithium with BuBr). Further modification by reacting the *n*-BuLi in THF at -78 °C without slowly warming the reaction mixture to 0 °C resulted in approximately 80% of the pure stannane product **50a** as judged by ¹H NMR spectroscopy.



Scheme 1.15 Reagents and conditions: (a) *n*-BuLi, Bu₃SnCl, Et₂O, -78 °C; (b) *n*-BuLi, Bu₃SnCl, THF, -78 °– 0 °C; (c) *n*-BuLi, Bu₃SnCl, THF, -78 °C.

To date, attempts to couple **50a** to **47** have not yet been attempted due to lack of time.

1.9 Conclusions

In this chapter, the role that conjugated oligomers play in understanding of the chemistry of conjugated polymers, especially for optical and electronic properties has been introduced. Some of the practical applications of conjugated oligomers in electronic and optical devices, as well as recent reports on oligomers have also been outlined. Besides linearly conjugated oligomers, cross-conjugated oligomers, which have

received a lot of attention due to their unique π -delocalization and resultant unique properties, have been also discussed. Our group has elaborated on the general framework of these cross-conjugated oligomers, the focus of which is on the third-order nonlinear optical (NLO) applications. A brief introduction on the NLO properties and their measurement techniques has thus been outlined.

In the second part of this chapter, an efficient synthesis of a modified cross-conjugated *iso*-PDA oligomeric series, namely perphenylated *iso*-PDAs, with TES- and TBDMS-encapping groups is described. These oligomers can be synthesized and isolated in reasonable to excellent yields as stable and soluble solids. Electronic absorption measurements have been conducted to explore the π -electron delocalization and communication characteristics. The predominant feature of the electronic absorption behavior of these perphenylated *iso*-PDA oligomers is a steadily increasing molar absorptivity as the number of enyne monomer units is increased. In addition, the electronic absorption spectra of the TBDMS-encapped *iso*-PDAs show similar characteristics with the TES-analogues.

Finally, we have described the synthesis and characterization of the chiral auxiliary for *iso*-PDAs with the intent of converting it into a vinyl triflate that could subsequently be incorporated into the framework of the *iso*-PDA oligomers. Negishi cross-coupling protocol has proved ineffective on both model compound and chiral auxiliary. Suzuki cross-coupling protocol works successfully for the model compound. Although boronic acid formation on the chiral auxiliary has been possible, the reaction is not optimized: (a) conditions and reaction needs to be varied, and (b) the THP protective group could be changed to benzyl or TIPS group which is not as acid labile, but if only racimization can be avoided. Formation of the Stannane analogous reagent also needs further optimization, and the subsequent Stille coupling should be explored.

1.10 References and Notes:

- (1) Moore, J. S. *Curr. Opin. Solid State Mater. Sci.* **1996**, *1*, 777-788.
- (2) Zimmerman, N.; Moore, J. S.; Zimmerman, S. C. *Chem. Ind.* **1998**, 604-610.
- (3) Pabo, C. O.; Sauer, R. T. *Ann. Rev. Biochem.* **1984**, *53*, 293-321.
- (4) Travers, A. A. *Ann. Rev. Biochem.* **1989**, *58*, 427-452.
- (5) Pavletich, N. P.; Pabo, C. O. *Science* **1991**, *252*, 809-817.
- (6) Cho, Y. J.; Gorina, S.; Jeffrey, P. D.; Pavletich, N. P. *Science* **1994**, *265*, 346-355.
- (7) Lokey, R. S.; Iverson, B. L. *Nature* **1995**, *375*, 303-305.
- (8) Gellman, S. H. *Acc. Chem. Res.* **1998**, *31*, 173-180.
- (9) Seebach, D.; Matthews, J. L. *Chem. Commun.* **1997**, 2015-2022.
- (10) Nelson, J. C.; Saven, J. G.; Moore, J. S.; Wolynes, P. G. *Science* **1997**, *277*, 1793-1796.
- (11) Holmes, D. L.; Smith, E. M.; Nowick, J. S. *J. Am. Chem. Soc.* **1997**, *119*, 7665-7669.
- (12) Bassani, D. M.; Lehn, J. M.; Baum, G.; Fenske, D. *Angew. Chem., Int. Ed. Engl.* **1997**, *36*, 1845-1847.
- (13) Blake, A. J.; Cooke, P. A.; Doyle, K. J.; Gair, S.; Simpkins, N. S. *Tetrahedron Lett.* **1998**, *39*, 9093-9096.
- (14) Yashima, E.; Maeda, Y.; Okamoto, Y. *J. Am. Chem. Soc.* **1998**, *120*, 8895-8896.
- (15) Schlitzer, D. S.; Novak, B. M. *J. Am. Chem. Soc.* **1998**, *120*, 2196-2197.
- (16) Takata, T.; Furusho, Y.; Murakawa, K.; Endo, T.; Matsuoka, H.; Hirasa, T.; Matsuo, J.; Sisido, M. *J. Am. Chem. Soc.* **1998**, *120*, 4530-4531.
- (17) Yashima, E.; Maeda, K.; Okamoto, Y. *Nature* **1999**, *399*, 449-451.

- (18) Akagi, K.; Piao, G.; Kaneko, S.; Sakamaki, K.; Shirakawa, H.; Kyotani, M. *Science* **1998**, *282*, 1683-1686.
- (19) Wittung, P.; Eriksson, M.; Lyng, R.; Nielsen, P. E.; Norden, B. *J. Am. Chem. Soc.* **1995**, *117*, 10167-10173.
- (20) Fujiki, M. *J. Am. Chem. Soc.* **2000**, *122*, 3336-3343.
- (21) Cuccia, L. A.; Ruiz, E.; Lehn, J. M.; Homo, J. C.; Schmutz, M. *Chem. Eur. J.* **2002**, *8*, 3448-3457.
- (22) Gin, M. S.; Yokozawa, T.; Prince, R. B.; Moore, J. S. *J. Am. Chem. Soc.* **1999**, *121*, 2643-2644.
- (23) Prince, R. B.; Brunsveld, L.; Meijer, E. W.; Moore, J. S. *Angew. Chem. Int. Ed.* **2000**, *39*, 228-230.
- (24) Gin, M. S.; Moore, J. S. *Org. Lett.* **2000**, *2*, 135-138.
- (25) Chan, H. S.; Bromberg, S.; Dill, K. A. *Phil. Trans. Roy. Soc. Lond. B* **1995**, *348*, 61-70.
- (26) (a) Zhao, Y. Cross-conjugated Enyne Oligomers: Synthesis, Properties, and Nonlinear Optical Investigations. Ph.D. Thesis, University of Alberta, Edmonton, AB, June 2002. (b) Slepko, D. A.; Hegmann, F. A.; Zhao, Y.; Tykwinski, R. R.; Kamada, K. *J. Chem. Phys.* **2002**, *116*, 3834-3840. (c) Brunsveld, L.; Meijer, E. W.; Prince, R. B.; Moore, J. S. *J. Am. Chem. Soc.* **2001**, *123*, 7978-7984.
- (27) Stinson, S. C. *Chem. Eng. News* **1997**, *75*, 26-27.
- (28) Julia, S.; Masana, J.; Vega, J. C. *Angew. Chem., Int. Ed. Engl.* **1980**, *19*, 929-931.
- (29) Banfi, S.; Colonna, S.; Molinari, H.; Julia, S.; Guixer, J. *Tetrahedron* **1984**, *40*, 5207-5211.

- (30) Bentley, P. A.; Bergeron, S.; Cappi, M. W.; Hibbs, D. E.; Hursthouse, M. B.; Nugent, T. C.; Pulido, R.; Roberts, S. M.; Wu, L. E. *Chem. Commun.* **1997**, 739-740.
- (31) Gamez, P.; Dunjic, B.; Fache, F.; Lemaire, M. *J. Chem. Soc., Chem. Commun.* **1994**, 1417-1418.
- (32) Canali, L.; Karjalainen, J. K.; Sherrington, D. C.; Hormi, O. *Chem. Commun.* **1997**, 123-124.
- (33) Gravert, D. J.; Janda, K. D. *Chem. Rev.* **1997**, *97*, 489-509.
- (34) Ma, L.; Hu, Q. S.; Vitharana, D.; Wu, C.; Kwan, C. M. S.; Pu, L. *Macromolecules* **1997**, *30*, 204-218.
- (35) Pu, L.; Wagaman, M. W.; Grubbs, R. H. *Macromolecules* **1996**, *29*, 1138-1143.
- (36) Ma, L.; Hu, Q. S.; Pu, L. *Tetrahedron Asymm.* **1996**, *7*, 3103-3106.
- (37) Hu, Q. S.; Zheng, X. F.; Pu, L. *J. Org. Chem.* **1996**, *61*, 5200-5201.
- (38) Hu, Q. S.; Vitharana, D.; Liu, G. Y.; Jain, V.; Wagaman, M. W.; Zhang, L.; Lee, T. R.; Pu, L. *Macromolecules* **1996**, *29*, 1082-1084.
- (39) Huang, W. S.; Hu, Q. S.; Zheng, X. F.; Anderson, J.; Pu, L. *J. Am. Chem. Soc.* **1997**, *119*, 4313-4314.
- (40) Hu, Q. S.; Huang, W. S.; Pu, L. *J. Org. Chem.* **1998**, *63*, 2798-2799.
- (41) Simonson, D. L.; Kingsbury, K.; Xu, M. H.; Hu, Q. S.; Sabat, M.; Pu, L. *Tetrahedron* **2002**, *58*, 8189-8193.
- (42) Seebach, D.; Marti, R. E.; Hintermann, T. *Helv. Chim. Acta* **1996**, *79*, 1710-1740.
- (43) Pu, L. *J. Photochem. Photobiol. A* **2003**, *155*, 47-55.
- (44) Ramos, A. M.; Rispens, M. T.; van Duren, J. K. J.; Hummelen, J. C.; Janssen, R. A. J. *J. Am. Chem. Soc.* **2001**, *123*, 6714-6715.

- (45) (a) Jones, L.; Schumm, J. S.; Tour, J. M. *J. Org. Chem.* **1997**, *62*, 1388-1410.
(b) Martin, R. E.; Diederich, F. *Angew. Chem. Int. Ed.* **1999**, *38*, 1350-1377.
- (46) Segura, J. L. *Acta Polym.* **1998**, *49*, 319-344.
- (47) Prasad, P. N. *Polymer* **1991**, *32*, 1746-1751.
- (48) Tykwinski, R. R.; Gubler, U.; Martin, R. E.; Diederich, F.; Bosshard, C.; Günter, P. *J. Phys. Chem. B* **1998**, *102*, 4451-4465.
- (49) Bosshard, C.; Knopfle, G.; Pretre, P.; Follonier, S.; Serbutoviez, C.; Günter, P. *Opt. Eng.* **1995**, *34*, 1951-1960.
- (50) Nalwa, H. S. *Adv. Mater.* **1993**, *5*, 341-358.
- (51) Cassidy, C.; Halbout, J. M.; Donaldson, W.; Tang, C. L. *Opt. Commun.* **1979**, *29*, 243-246.
- (52) Oudar, J. L.; Chemla, D. S.; Batifol, E. *J. Chem. Phys.* **1977**, *67*, 1626-1635.
- (53) Hopf, H. *Angew. Chem., Int. Ed. Engl.* **1984**, *23*, 948-960.
- (54) Phelan, N. F.; Orchin, M. *J. Chem. Ed.* **1968**, *45*, 633-637. It should be noted that this definition is not completely unambiguous since it can be interpreted to hold as well for linear π -conjugated systems.
- (55) Zhao, Y.; Tykwinski, R. R. *J. Am. Chem. Soc.* **1999**, *121*, 458-459.
- (56) (a) Hopf, H.; Maas, G. *Angew. Chem., Int. Ed. Engl.* **1992**, *31*, 931-954. (b) Fielder, S.; Rowan, D. D.; Sherburn, M. S. *Angew. Chem., Int. Ed. Engl.* **2000**, *39*, 4331-4333.
- (57) Swager, T. M.; Grubbs, R. H. *J. Am. Chem. Soc.* **1987**, *109*, 894-896.
- (58) Klokkenburg, M.; Lutz, M.; Spek, A. L.; van der Maas, J. H.; van Walree, C. A. *Chem. Eur. J.* **2003**, *9*, 3544-3554.
- (59) Ciulei, S. C.; Tykwinski, R. R. *Org. Lett.* **2000**, *2*, 3607-3610.
- (60) Zhao, Y.; Campbell, K.; Tykwinski, R. R. *J. Org. Chem.* **2002**, *67*, 336-344.

- (61) Zhao, Y.; McDonald, R.; Tykwinski, R. R. *Chem. Commun.* **2000**, 77-78.
- (62) Tykwinski, R. R.; Zhao, Y. *Synlett* **2002**, 1939-1953.
- (63) Stang, P. J.; Fisk, T. E. *Synthesis* **1979**, 438-440.
- (64) Stang, P. J.; Treptow, W. *Synthesis* **1980**, 283-284.
- (65) Walton, D. R. M.; Waugh, F. J. *Organomet. Chem.* **1972**, *37*, 45-56.
- (66) Sonogashira, K.; Tohda, Y.; Hagihara, N. *Tetrahedron Lett.* **1975**, 4467-4470.
- (67) Pretsch, E.; Seibl, J.; Simon, W.; Clerc, T. *Tables of Spectral Data for Structure Determination of Organic Compounds*; Springer-Verlag: Berlin, **1989**; page C90.
- (68) Compound **36** showed sintering at 110–112 °C and shrinkage of it accompanied by discolorization (i.e., decomposition) at 169–171 °C.
- (69) Perkins, M. V.; Kitching, W.; Konig, W. A.; Drew, R. A. I. *J. Chem. Soc., Perkin Trans. 1* **1990**, 2501-2506.
- (70) Chiellini, E.; Galli, G.; Carrozzino, S.; Gallot, B. *Macromolecules* **1990**, *23*, 2106-2112.
- (71) Kitaori, K.; Furukawa, Y.; Yoshimoto, H.; Otera, J. *Tetrahedron* **1999**, *55*, 14381-14390.
- (72) Wawrzenczyk, C.; Przepiorka, Z.; Zabza, A. *Pol. J. Chem.* **1981**, *55*, 819-825.
- (73) Rankin, T.; Tykwinski, R. R. *Org. Lett.* **2003**, *5*, 213-216.
- (74) Negishi, E.; Luo, F. T.; Frisbee, R.; Matsushita, H. *Heterocycles* **1982**, *18*, 117-122.
- (75) Bertini, B.; Moineau, C.; Sinou, D.; Gesekus, G.; Vill, V. *Eur. J. Org. Chem.* **2001**, 375-381.

Chapter 2 Synthesis and Characterization of 7,7,8,8-Tetraethynyl-*p*-quinodimethane (TEQ) Derivatives

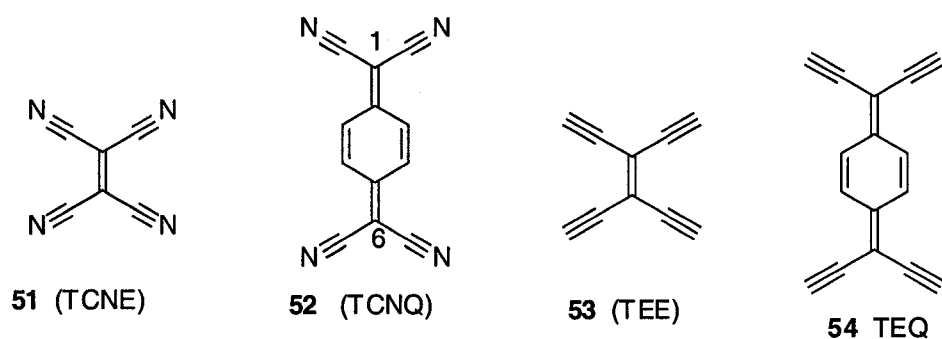
2.1 Introduction

Conjugated organic molecules and polymers show great promise as materials for advanced electronic and photonic applications.¹⁻² The synthesis of π -conjugated oligomers is also of interest because it is anticipated that these oligomers could be important components of molecular electronic devices.³ In addition, they can serve as constrained model systems, whose spectroscopic properties can be extrapolated to enable the electronic, optical, thermal, and morphological properties for the corresponding polymers to be predicted.⁴

Besides linearly conjugated molecules, an alternative form of conjugation which has only sparsely been addressed in materials research is cross-conjugation. Henning Hopf⁵ two decades ago pointed out that, "cross-conjugated molecules have remained a neglected class of compounds, and compared to the extensively studied linearly π -conjugated molecules, cross-conjugated molecules still remain quite unexplored".⁶⁻⁷ This does not mean that cross-conjugated compounds are limited, but rather, cross-conjugated molecules have an unrealized potential for applications in electronic (e.g., organic conducting and semiconducting) and optical (third-order NLO) materials which possesses electronic transparency.

The strong π -electron delocalization in linearly π -conjugated systems can be a disadvantage with respect to optical applications. This is because of the red shift of the maximum electronic absorption in the UV-vis spectrum (λ_{max}) with the increasing conjugation length. Anytime that λ_{max} shifts to the visible region of the UV-vis

spectrum, the operating light beam of the optical devices will be blocked (i.e., absorbed at that wavelength) and, in that event, render their applicability questionable. This disadvantage can, in theory, be eliminated in cross-conjugated systems because of their unique π -electron delocalization. This is because the π -electrons in cross-conjugated systems are not appreciably delocalized along the entire π -electron system as observed for the linearly π -conjugated systems, but rather the delocalization is confined in specified conjugated segments. In this sense, an enormous red shift in λ_{max} is not going to be encountered as a function of increasing length, electronic transparency can be potentially achieved.



Scheme 2.1 A Selection of Important Cross-conjugated Systems⁸

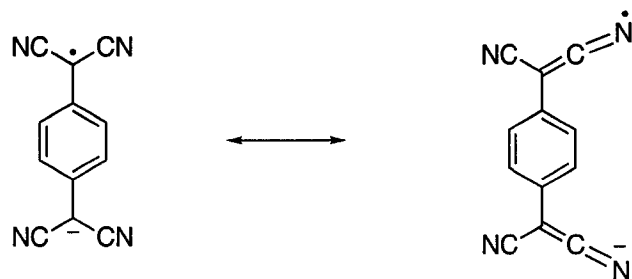
More than 4 decades ago, DuPont Chemists⁹ synthesized the first example of a percyanoolefin, tetracyanoethylene (TCNE) **51**. They reported that TCNE readily undergoes a variety of reactions including addition, substitution and cyclization, to give dyes, strong acids and heterocyclic compounds. They also stated that TCNE is a very active dienophile, condensing quantitatively with butadiene at 0 °C to give 4,4,5,5-tetracyanocyclohexene. Merrifield¹⁰ and co-workers have also done extensive

work with TCNE. They reported that TCNE has the ability to form charge-transfer complexes and that colored complexes are formed between TCNE and aromatic hydrocarbons. For example, TCNE gives an intense yellow color with benzene, orange with toluene and red with xylene.

Only a few years later, another polycyano-substituted compound also destined to have a lasting influence on organic chemistry, 7,7,8,8-tetracyano-*p*-quinodimethane (TCNQ), **52**, was synthesized by Acker and Hertler.¹¹ They reported that TCNQ easily accepts an electron (i.e., is reduced) to form stable anion-radical. They also reported that TCNQ readily undergoes 1,6-addition reactions. The authors concluded by reporting that when crystals are crushed between soft glass melting point cover glasses and heated, a beautiful blue film forms on the glass plates at about 200 °C. They attributed the formation of the blue film to the reaction of TCNQ with bases present in the glass to give the TCNQ anion-radical.

In the same year, Hertler¹² and co-workers made thorough studies of the physical properties of TCNQ. They reported that TCNQ is a strong π -acid which forms stable, crystalline π -complexes (i.e., charge-transfer complexes) with aromatic hydrocarbons, amines, and polyhydric phenols. In addition, TCNQ forms two series of stable, salt-like derivatives, each involving complete transfer of an electron to TCNQ with the formation of the anion-radical $\text{TCNQ}^{\dot{-}}$ represented by the resonance hybrid shown in Scheme 2.2. They presented the first series $\text{M}^+ \text{TCNQ}^{\dot{-}}$ in which M could be a metallic or organic cation and the second series of complex salts represented by $\text{M}^+ (\text{TCNQ}^{\dot{-}})(\text{TCNQ})$ which contain a second, neutral, molecule of TCNQ. They further pointed out that the complex anion-radical salts had the highest electrical conductivities

known for organic compounds at the time, exhibiting volume electrical resistivities as low as 0.01 ohm cm at room temperature.

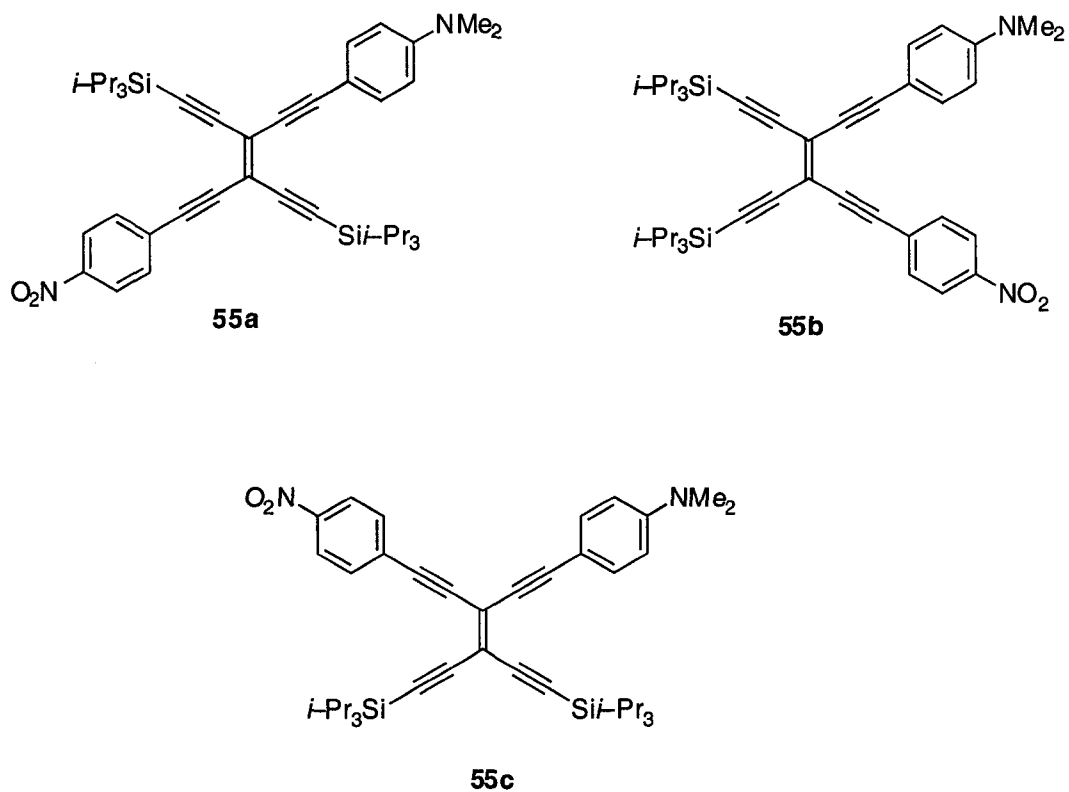


Scheme 2.2 Formation of TCNQ Anion-Radical in Resonance Hybrid

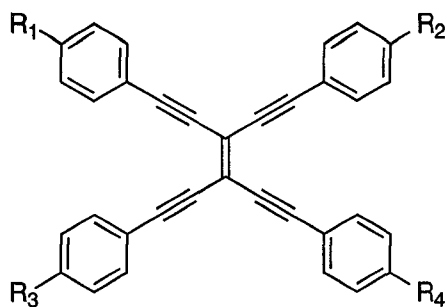
The all-carbon parent systems of tetraethynylethene (TEE, 3,4-diethynylhex-3-ene-1,5-diyne), **53**, was first synthesized by Diederich and co-workers.¹³ They outlined the importance for synthesizing TEE, the only known isomer of molecular formula $C_{10}H_4$ as: (1) it is an interesting example of cross-conjugated π -systems,¹⁴ (2) it can serve as a direct precursor of new carbon networks,¹⁵ (3) it can undergo double Bergman cyclization¹⁶ which could lead to a convenient route to poly(*peri*-naphthalenes), which have been predicted to possess a low-lying bandgap, and (4) its derivatives could show the potent anticancer activity observed for strained *cis*-enediynes.^{17,18}

Five years later, Diederich and co-workers¹⁹ reported a full account of the synthesis and characterization of a library of donor/acceptor-functionalized TEEs. They reported that intramolecular donor-acceptor interactions, as evidenced by a long-wavelength charge-transfer band, were considerably more effective in TEEs **55a** and **55b**, with

trans- and *cis*-linearly-conjugated electronic pathways between donor and acceptor, than in **55c**, with a geminal cross-conjugated electronic pathway.



The same group has done a comprehensive investigation of the second-²⁰ and third-order²¹ nonlinear optical properties of donor/acceptor substituted TEEs as well as comparative discussions of the obtained structure-property relationships for third-order effects on **56a-c**.²²

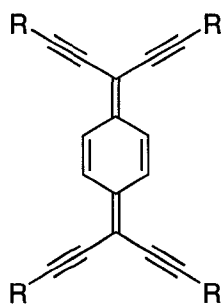


56a R₁ = R₂ = NMe₂, R₃ = R₄ = NO₂

56b R₁ = R₄ = NO₂, R₂ = R₃ = NMe₂

56c R₁ = R₃ = NMe₂, R₂ = R₄ = NO₂

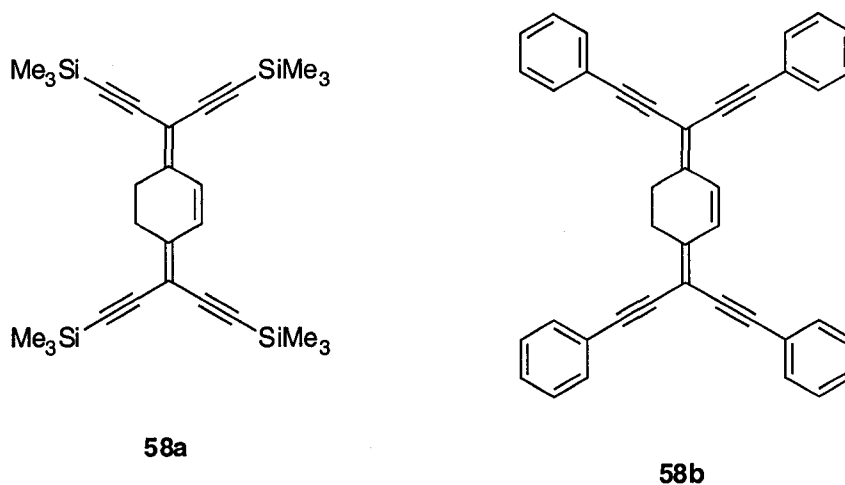
A major breakthrough in the synthesis of an all-carbon analogue of **54** with tetrakis(trimethylsilyl) protected alkynes, TEQ **57a**, was first reported by Neidlein and Winter in 1998.²³



57a R = SiMe₃

57b R = Ph

During the course of my work, Hopf and co-workers²⁴ reported a successful synthesis of the dihydro derivatives of TEQ (2H-TEQ), with pendent trimethylsilyl and phenyl groups, **58a** and **58b**, respectively. They reported that all efforts to further dehydrogenate **58a** and **58b** to **57a** and **57b**, respectively, have been unsuccessful. Compounds **57** thus remain elusive.



An interesting challenge to synthetic and materials chemists is thus the preparation of the carbon-rich target **TEQ 54**. **TEQ 54** and its derivatives would serve as interesting building blocks for the construction of very large extended conjugated structures that could show promise for applications in materials science. In this chapter, the description of a series of 2H-TEQ derivatives with different silyl protecting groups patterns is outlined in the discussion below.

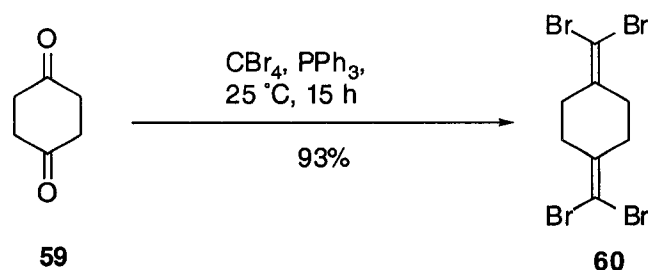
2.2 Results and Discussion

2.2.1 *Synthesis of Tetrakis(trimethylsilyl) Protected Derivative of 7,7,8,8-Tetraethynyl-p-quinodimethane (TEQ)*

In this section are described efforts to synthesize derivatives of and precursors for TEQ. As will be shown, the most highly unsaturated derivatives of TEQ that we have so far been able to synthesize are the dihydro derivatives of the silyl protective analogue **58a**.

In order to synthesize precursors for the carbon-rich target **54**, we chose to begin with cyclohexane-1,4-dione **59** and transform it into the corresponding 1,4-bis(dibromomethylene)-cyclohexane **60** via modification of the procedure

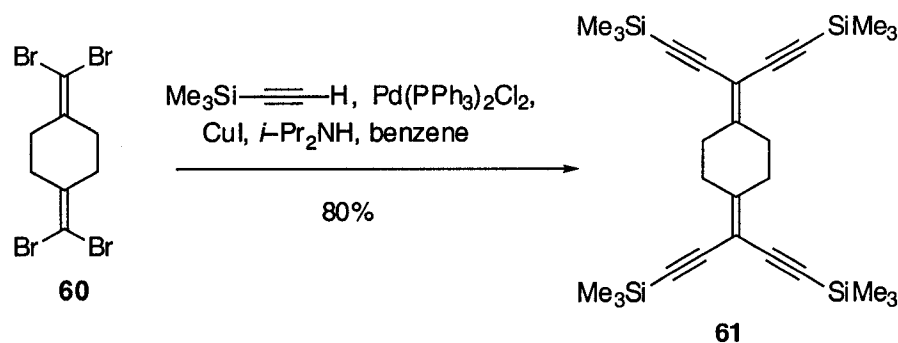
described by Neidlein.^{23,25} This dibromoalkene can serve as a suitable starting material for the catalytic alkynylation resulting in novel cyclic geminal enediynes. In this procedure, **59**, was reacted with a mixture of PPh_3 and CBr_4 in anhydrous benzene. After reaction at room temperature for 15 h, **60** was isolated by a sequence of filtration of the reaction mixture, evaporation of the filtrates and column chromatography (silica gel). This compound was stable to air at ambient temperature, and spectral characteristics were consistent with literature values.^{23,24}



Scheme 2.3 Formation of Dibromoalkene **60**

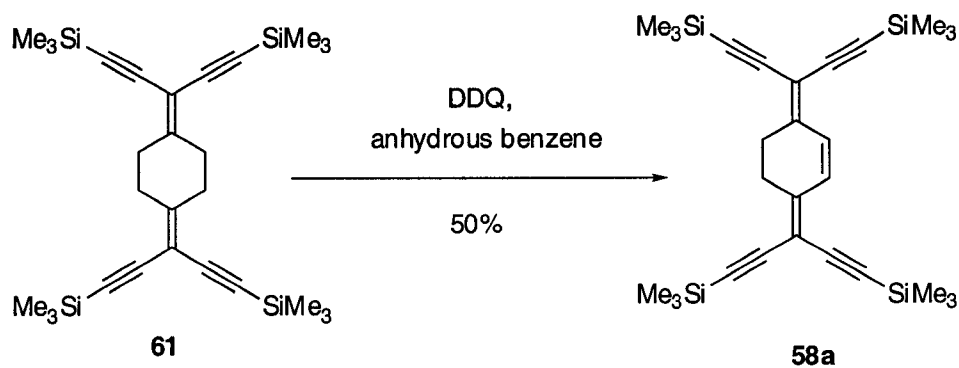
Next, synthesis of 1,4-bis[bis-(trimethylsilylethynyl)methylene]cyclohexane **61**, was accomplished under modification of Sonogashira²⁶ Pd-catalyzed cross-coupling conditions. 1,4-Bis(dibromomethylene)cyclohexane **60** was cross-coupled with trimethylsilylacetylene (TMSA) using $\text{PdCl}_2(\text{PPh}_3)_2$ as catalyst, CuI as co-catalyst, and $i\text{-Pr}_2\text{NH}$ base in anhydrous benzene at room temperature for 48 h under N_2 atmosphere. Pure product **61** was isolated by evaporation of the volatile portion of the reaction mixture, column chromatography (silica gel) and recrystallization from Et_2O /hexanes gave pure **61** as bright yellow crystals in 80% yield. This compound was stable to air and can be stored for extended periods of time at ambient temperature. It also displays fluorescence in hexane solution. The structure of **61** was verified by IR spectroscopic analysis, ^1H and ^{13}C NMR spectroscopy as well as EIMS analysis, and the spectral characteristics were consistent with those reported in the literature.^{23,24} This

bis(cyclohexylidene) backbone is thus the direct precursor toward the formation of the *p*-quinoid system **57a** (TEQ).



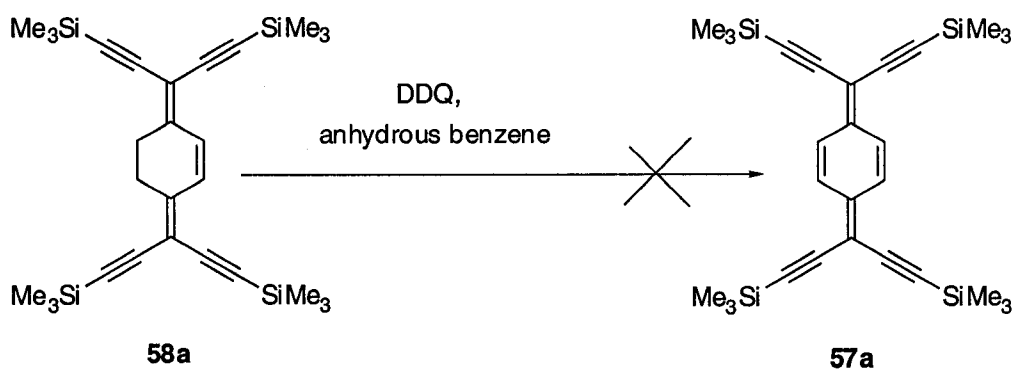
Scheme 2.4 Formation of Geminal Eneyne **61**

On heating a solution of **61** in xylene or toluene under reflux in the presence of a fourfold excess of 2,3-dichloro-5,6-dicyano-*p*-benzoquinone (DDQ) for 24 h, dehydrogenation took place to furnish the dihydro-TEQ derivative **58a** in 40% yield, as well as recovered **61** in 20% yield. On changing the solvent to benzene and refluxing in the presence of a fourfold excess of DDQ, for 2 to 4 h, dehydrogenation took place to furnish the dihydro-TEQ derivative **58a**, in 50% yield. Pure product of **58a**, was isolated by evaporation of the volatile portion of the reaction mixture, subjecting the resulting residue in column chromatography (silica gel) and recrystallization from Et_2O /hexanes. The resulting dihydro-TEQ derivative **58a** was a bright yellow zone in hexane, and isolated as orange needles. This compound was stable to air and can be stored for extended periods of time at ambient temperature. It also displays fluorescence in hexane solution. The structure of this compound was confirmed by IR, ^1H and ^{13}C NMR spectroscopy as well as EIMS analysis. In addition, spectral characteristics were consistent with literature values.²⁴



Scheme 2.5 Formation of dihydro-TEQ derivative 58a

While the report by Neidlein describes the formation of **57a** via the conditions outlined above, all efforts to further oxidize this orange colored solid **58a** to **57a** have proved futile. When the amount of the oxidant or the reaction conditions were varied, only a black material that could not be identified by physical or chemical methods was obtained. During the course of this investigation, similar results have been reported by Hopf, in which their efforts toward **57a** have been equally as ineffective using the Neidlein protocol.



Scheme 2.6 Ineffective oxidation of 58a

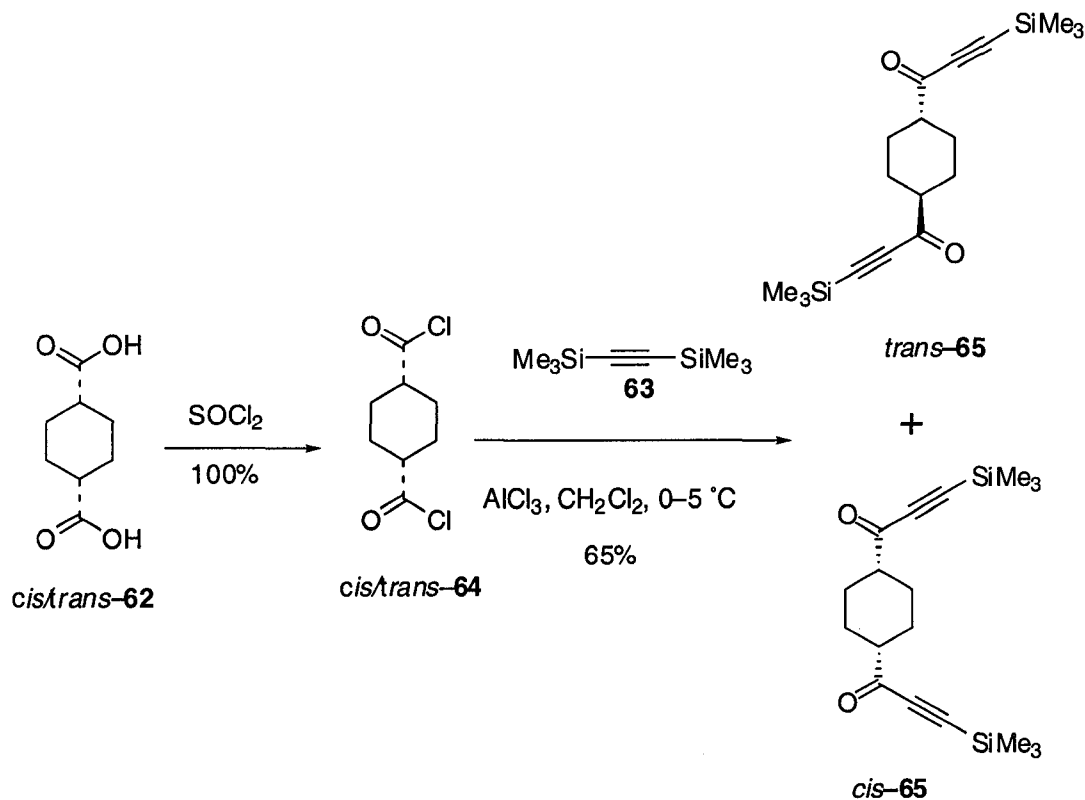
2.2.2 Toward the Synthesis of Bis(trimethylsilyl) and Bis(triisopropyl-, tert-butyl dimethylsilyl-, and triethylsilyl) Protected Derivatives of 7,7,8,8-Tetraethynyl-p-quinodimethane (TEQ)

Having established the basic synthetic operations required in this area, the more demanding goal of synthesizing TEQ derivatives or precursors with different silyl protecting groups was addressed next. In this section, we describe our efforts to synthesize precursors for and derivatives of TEQ having different silyl protecting groups. The essence of synthesizing TEQ having different silyl protecting groups was: (a) this molecular architecture will be a more versatile building block compared to the tetrakis(trimethylsilyl) derivatives, due to the differentially protected alkyne groups, (b) these derivatives would serve as interesting building blocks for the construction of very large extended, conjugated, and carbon-rich structures, (c) these derivatives would be interesting examples of cross-conjugated π -systems. As described below, the most highly unsaturated derivatives of TEQ that we have so far been able to synthesize are the dihydro derivatives with different silyl protective analogues.

We began by transforming 1,4-cyclohexanedicarboxylic acid **62** (mixture of *cis/trans*) to acyl halide **64**. Compound **64** was transformed to the required ketone **65** through the modification of the procedure described by Stang.²⁷ During the Friedel-Crafts²⁸ type acylation of silyl-protected acetylenes, bis(trimethylsilylacetylene)²⁹ **63** was reacted with cyclohexane-1,4-dicarbonyl dichloride **64**, in the presence of aluminium chloride at 0 °C for 3 h. Aqueous reaction work-up, followed by purification via column chromatography (silica gel) gave ketone **65** in 65% yield as a colorless solid (as a mixture of isomers i.e., *trans-65*, *cis-65*). The stereochemistry of the two isomers was determined to be in an approximate ratio of 4.8:5.2 based on NMR spectroscopic analysis. Chromatographic separation of the two isomers was extremely difficult due to

their nearly identical polarities and they were therefore characterized as a mixture. This mixture was stable to air at room temperature.

Confirmation of the structure of isomers **65** is based on analysis of the spectroscopic data. In the ^1H NMR spectrum, the protons of cyclohexane backbone show up at δ 2.38–1.42 and those of the TMS group at δ 0.42. The ^{13}C NMR (APT) spectrum also supports the structural assignment. The resonance of the carbonyl carbon of the ketone is observed at 190.2 ppm, and the resonances for the acetylene carbons are discernible at 101.2 and 99.3 ppm. The resonances for the methine and methylene carbons of the cyclohexane backbone were observed at 51.3 and 27.2 ppm, respectively. The TMS carbons are observed at -0.7 ppm. The IR spectrum shows a medium peak at 2151 cm^{-1} correspond to $\text{C}\equiv\text{C}$ stretches whereas the strong peak at 1671 cm^{-1} correspond to the stretching of the $\text{C}=\text{O}$ bonds. The mass spectrum shows a molecular ion peak at m/z 332.3 corresponding to the molecular mass of **65**. Combustion analysis is also consistent with the proposed molecular composition.

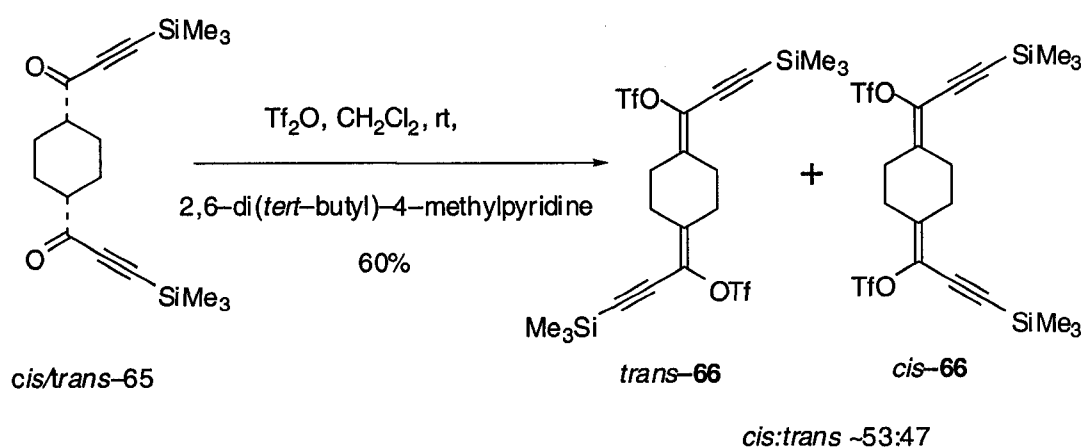


Scheme 2.7 Formation of ketone 65 (mixture of *trans*-65, *cis*-65)

Triflation of ketones 65 took place in the presence of excess triflic anhydride and 2,6-di(*tert*-butyl)-4-methylpyridine in CH_2Cl_2 at room temperature for 3–4 days (Scheme 2.8). After aqueous reaction work-up, followed by purification via column chromatography (silica gel), triflate 66 was isolated in 60% yield as a colorless solid (as a mixture of isomers i.e., *trans*-66:*cis*-66 ~ 47:53). Separation of the two isomers was extremely difficult due to their nearly identical polarities. Repeated column chromatography, however, yielded small quantities of pure *trans*-66 and *cis*-66. Both compounds were stable to air at ambient temperature and both melted at $131-132^\circ\text{C}$.

The proposed structures of the triflates 66 (i.e., *trans*-66, *cis*-66) are consistent with the spectroscopic data. In the ^1H NMR spectrum, the protons of the cyclohexane backbone show as a singlet at δ 2.56 for *trans*-66 and as two singlets at δ 2.60 and δ

2.51 for *cis*-**66**. In the same respect, the TMS protons show a singlet at δ 0.21 for *trans*-**66**, a singlet at δ 0.20 for *cis*-**66**. The ^{13}C NMR (APT) spectrum also supports this assignment. The in-chain vinylidene carbons of the main chain ($[\text{CH}_2]_2\text{C}=\text{C}$) are quite deshielded, resonating at 140.4 ppm for *trans*-**66**, and 140.5 ppm for *cis*-**66**. The vinylidene carbons outside of the main chain ($[\text{CH}_2]_2\text{C}=\text{C}$) are quite shielded, resonating at 125.1 ppm for *trans*-**66** and 125.0 ppm for *cis*-**66**. The resonances of the triflate (CF_3) groups is observed as a quartets ($^1J_{\text{C,F}} \sim 320$ Hz) at δ 118.2 for both *trans*- and *cis*-**66**. The resonances for the acetylene carbons are discernible at δ 104.6 and 93.4 for *trans*-**66** and at δ 104.5 and 93.5 for *cis*-**66**. The resonances for the methylene carbons of the cyclohexane backbone are observed at δ 29.7 and 27.5 for *trans*-**66** and δ 29.9 and 27.1 for *cis*-**66**. The TMS carbons are observed at -0.6 ppm for *trans*-**66** and -0.5 ppm for *cis*-**66**. The IR spectrum shows the presence of acetylene functional group, with a medium peak at 2154 cm^{-1} in both *trans*- and *cis*-**66**. The mass spectrum shows a molecular ion peak at m/z 596.1 corresponding to the molecular mass of both isomers.



Scheme 2.8 Formation of Triflate **66** (mixture of *trans*-**66**, *cis*-**66**)

Single crystal X-ray analysis was performed to reveal the solid-state structural properties and isomeric identity of *trans*-**66**, and the ORTEP diagram is found in Fig. 2.1. Single crystals of *trans*-**66** were obtained by diffusion of MeOH into a CH₂Cl₂ solution at 4 °C, and the structure was solved at -80 °C. The molecule displays a crystallographic inversion centre. The structural data show that the dihedral angle of 46.84° between the plane composed of Si, C(6), C(5), C(4), O(1), and C(1) and the plane composed of C(2), C(3), C(2'), and C(3'), which is comparable to similar compounds.^{24,30} The vinylidene angles of O(1)-C(4)-C(5) at 112.5° and 115.5° for C(2)-C(1)-C(3') are slightly distorted from 120° for an sp² hybridized carbon center. The Si-C≡C bonds at 177.6° are slightly distorted from linearity. Single bonds of the conjugated framework, e.g., C(4)-C(5) at 1.426(2) Å, are in the expected range for single bonds linking sp-sp² carbons. The C≡C bond at 1.202(2) Å and the C=C bond at 1.327(2) Å are also within the expected range. The C-O bond at 1.4409(19) Å is within the expected range of a vinyl triflate.^{30,31}

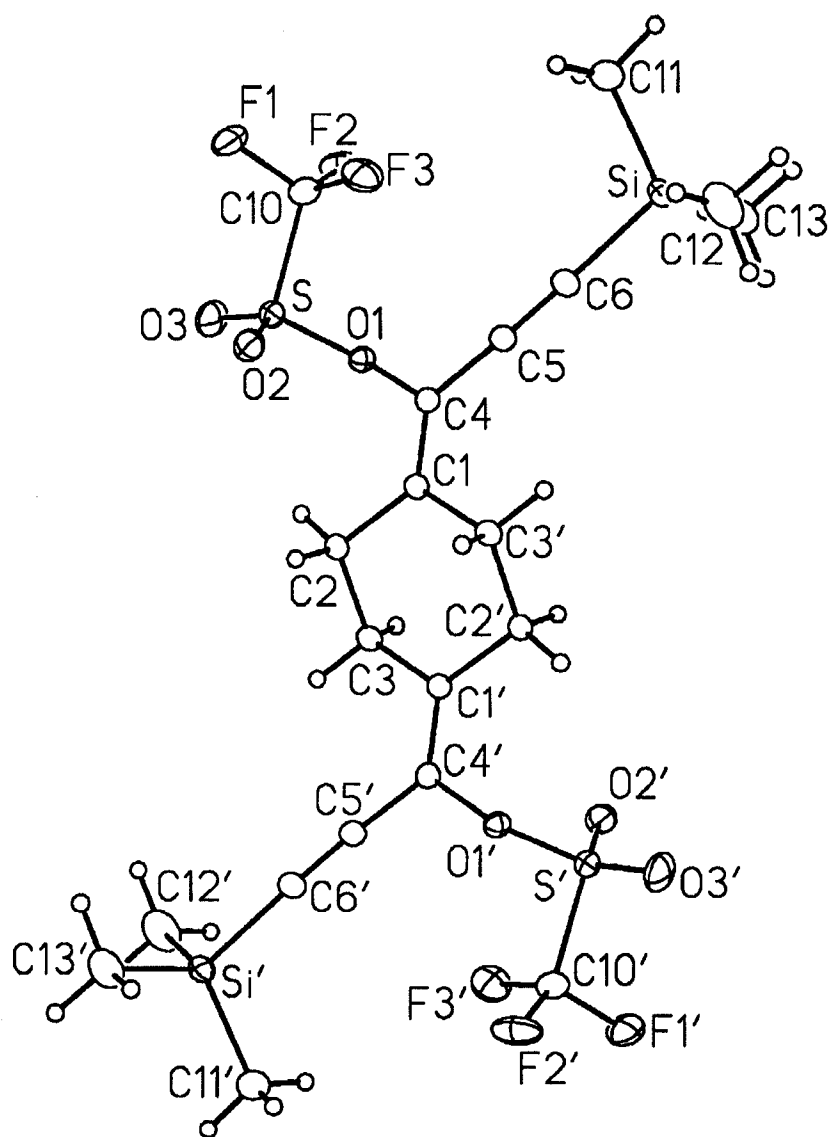
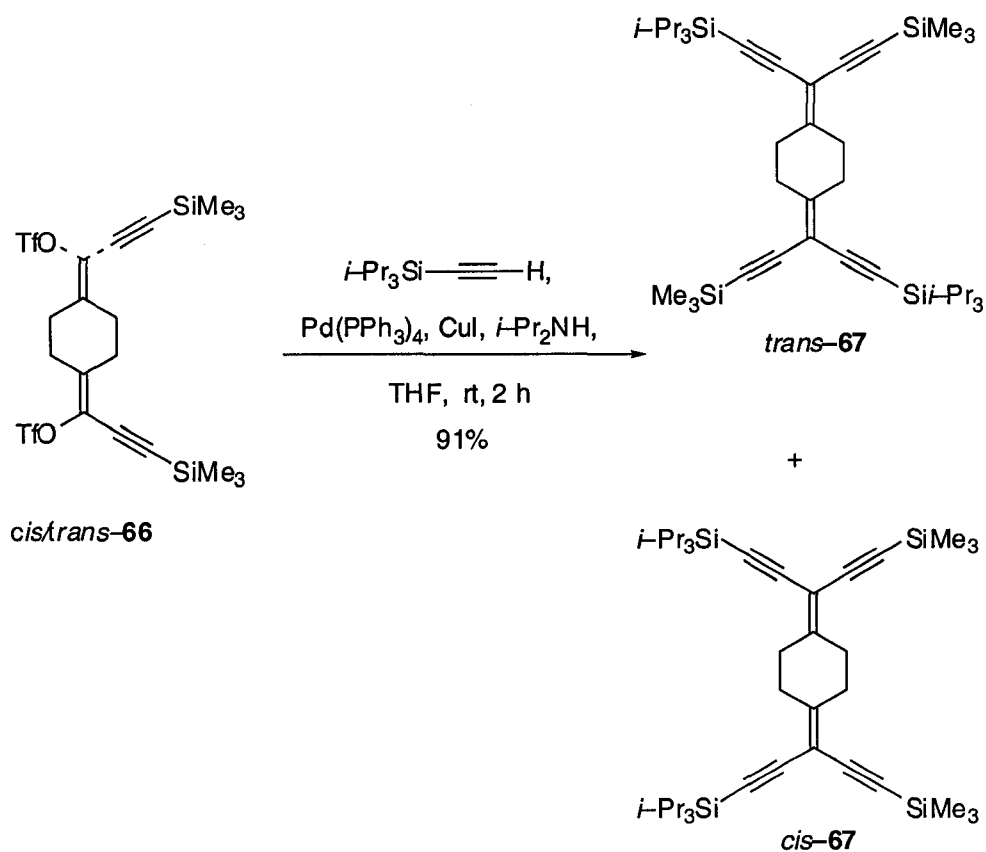


FIG. 2.1 ORTEP drawing (20% probability level) of **66a**. Selected bond lengths (Å) and bond angles (°): C(1)–C(2) 1.504(2), C(1)–C(4) 1.327(2), C(2)–C(3) 1.537(2), C(4)–C(5) 1.426(2), C(5)–C(6) 1.202(2), S–O(1) 1.577(13), S–O(3) 1.406(15), Si–C(6) 1.853(18), C(4)–C(5)–C(6) 177.3(19), Si–C(6)–C(5) 177.6(17), O(1)–C(4)–C(5) 112.5(14), C(2)–C(1)–C(3') 115.4(14), O(1)–C(4)–C(1) 119.8(14), C(3')–C(1)–C(4) 120.0(14).

Next, the geminal enediyne **67**, was formed under modification of Sonogashira²⁶ Pd-catalyzed cross-coupling conditions. Triflate **66** (i.e., mixture of *trans*-**66**, *cis*-**66**) was cross-coupled with triisopropylsilylacetylene (TIPSA) using Pd(PPh₃)₄ as catalyst, CuI as co-catalyst, and *i*-Pr₂NH base in anhydrous THF at room temperature for 2 h under N₂ atmosphere (Scheme 2.9). After aqueous work-up, followed by purification via column chromatography (silica gel), geminal enediyne **67** (as a mixture of isomers i.e., *trans*-**67**, *cis*-**67**) was isolated in pure form as a light yellow solid with defined melting point of 104–106 °C. Separation of the two isomers was impossible because of their identical polarities, but the mixture was determined to be an approximate ratio of 47:53 based on NMR spectroscopic analysis. This compound was stable to air and could be stored for extended periods of time at room temperature without any sign of decomposition by either TLC or NMR spectroscopic analysis.

Confirmation of the structure of **67** (as a mixture) is based on analysis of the spectroscopic data. In the ¹H NMR spectrum, the protons of the cyclohexane backbone show as a singlet at δ 2.64. The TIPS protons show two singlets at δ 1.09 and 1.08 whereas the TMS protons also show two singlets at δ 0.19 and 0.18. The ¹³C NMR (APT) spectrum also supports this assignment. The in-chain vinylidene carbons ([CH₂]₂C=C) are quite deshielded, resonating at 158.7 and 158.5 ppm. The vinylidene carbons outside of the main chain ([CH₂]₂C=C) fall into the chemical shift range of the acetylenic carbons, from 94–103 ppm and all are not assignable. It is known that alkyl substituents increase the chemical shift of the adjacent carbon atom and decrease the chemical shift of the other carbon in the vinyl moiety, whereas acetylene substituents have an opposite effect.³³ The synergetic effect of the two ethynyl bonds and the two geminal methylene groups in the cyclohexane backbone polarizes the vinylidene bonds, resulting in the shielding of the vinylidene carbons outside of the main chain

($[\text{CH}_2]_2\text{C}=\text{C}$). Four peaks are discernible at 31.4–31.6 ppm corresponding to the resonances of the methylene carbons of the cyclohexane backbone. The resonances for the TIPS carbons are observed at 18.7 and 11.4 ppm whereas the TMS carbons are found at 0.0 ppm. The IR spectrum shows a medium peak at 2150 cm^{-1} corresponding to $\text{C}\equiv\text{C}$ stretches, whereas a medium peak at 1598 cm^{-1} corresponds to the stretching of the $\text{C}=\text{C}$ bonds. The mass spectrum shows a molecular ion peak at m/z 660.4 corresponding to the molecular mass of both isomers of **67**.

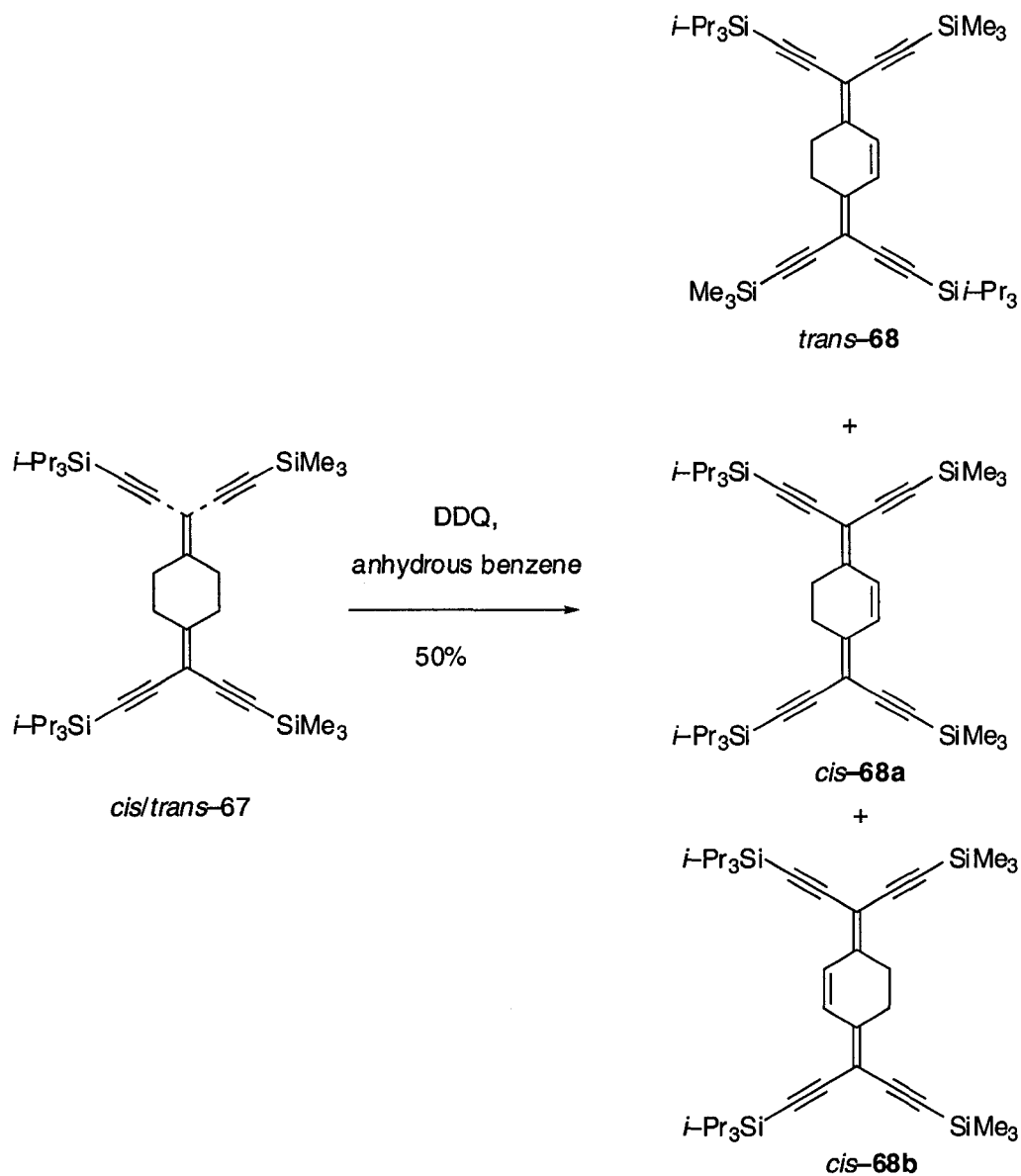


Scheme 2.9 Formation of Geminal Eneyne, **67** (mixture of *trans-67*, *cis-67*)

On heating of a benzene solution of **67** at reflux in the presence of a fourfold excess of DDQ for 4 h, dehydrogenation took place to furnish the dihydro-TEQ derivatives **68**

(Scheme 2.10). Pure **68** (as a mixture of stereoisomers i.e., *trans*-**68**, *cis*-**68a**, and *cis*-**68b**), was isolated by evaporation of the volatile portion of the reaction mixture and subjecting the resulting residue to column chromatography (silica gel). The dihydro-TEQ derivatives **68** were obtained as a mixture, in 50% yield. Separation of the three isomers was impossible due to their identical polarities, but was determined to be in an approximate isomeric ratio of 24:14:62 based on NMR spectroscopic analysis. This mixture was thermally stable and can be stored for months as solid in the air at ambient temperature.

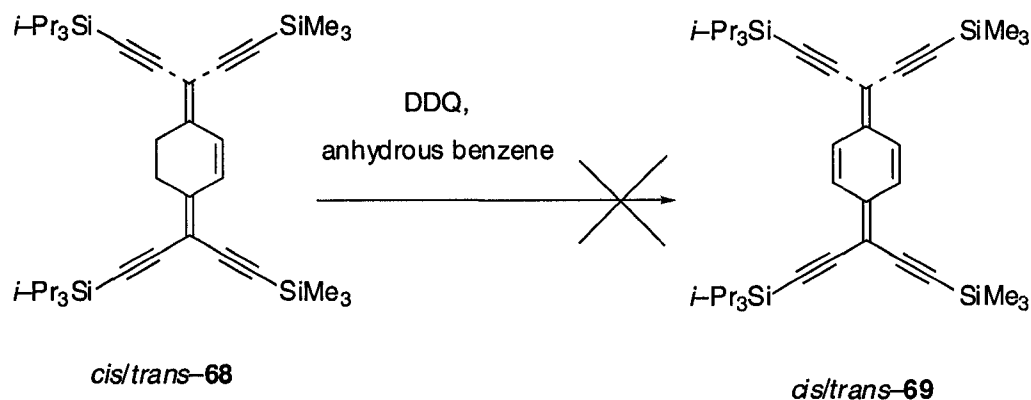
The proposed structure of the dihydro-TEQ derivatives **68** (as a mixture) is consistent with the spectroscopic data. In the ^1H NMR spectrum, the vinyl protons in the cyclohexene ring show a multiplet at δ 6.96, whereas the methylene protons resonate at δ 2.72. The TIPS protons show two singlets at δ 1.09 and 1.08, whereas the TMS protons show two singlets at δ 0.22 and 0.21. The ^{13}C NMR (APT) spectrum also supports this assignment. The three in-chain vinylidene carbons $[(\text{CH}_2)(\text{CH})\text{C}=\text{C}]$ are quite deshielded, resonating in a range of 150.4–150.6 ppm, whereas the vinylidene carbons outside of the main chain $[(\text{CH}_2)(\text{CH})\text{C}=\text{C}]$ fall into the chemical shift range of the acetylenic carbons, from 97–104 ppm and are not assignable. The vinyl carbons for **68** are degenerate, resonating at 130.5 ppm, whereas the methylene carbons show in the range of 27–30 ppm. The resonances for the TIPS carbons are observed at 18.9 and 11.6 ppm and the TMS carbons at 1.3 and 0.1 ppm. The IR spectrum shows medium peaks at 2149 and 2063 cm^{-1} corresponding to $\text{C}\equiv\text{C}$ stretches, whereas the medium peak at 1651 cm^{-1} corresponds to the stretching of the $\text{C}=\text{C}$ bonds. The mass spectrum shows a molecular ion peak at m/z 658.4 corresponding to the molecular mass of **68**. Combustion analysis was also consistent with the proposed molecular composition.



Scheme 2.10 Attempted oxidation of dihydro-TEQ derivative **68** (*cis-trans*)

Frustratingly, all efforts to further oxidize this bright yellow solid to TEQ **69** (Scheme 2.11) have to date failed. When the amount of the oxidant or the reaction conditions were varied (i.e., increasing or decreasing the reaction time, the temperature

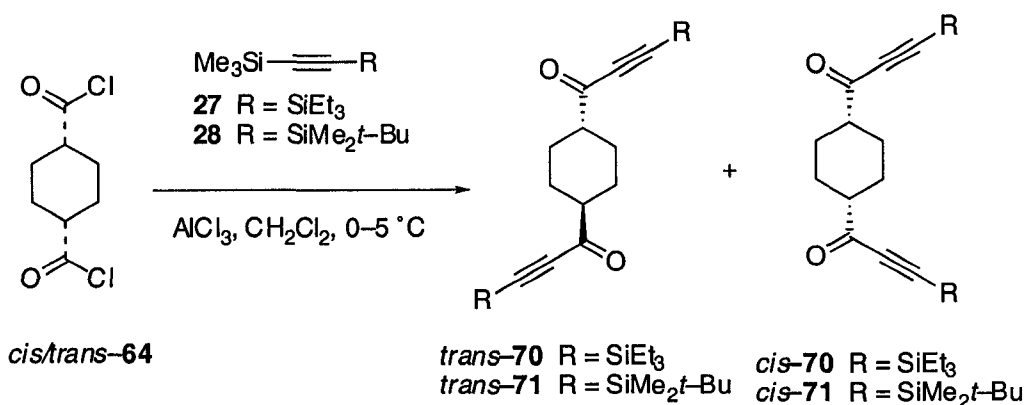
and the oxidant) only a black material that could not be identified by physical or chemical methods was obtained.



Scheme 2.11 Ineffective Oxidation of 68

It has been reported that using bistrimethylsilylacetylene as the starting material in the Friedel–Crafts²⁸ type acylation of silyl-protected acetylenes can result in a mixture of bis-acylated and mono-acylated products.³⁴ In addition, desilylation of the newly formed ketone under the reaction conditions has been also observed. Changing the alkynyl protecting group to a more robust silyl group, such as TES **27** and TBDMS **28** groups, actually limited the formation of the side-products, with increasing thermal stability, especially with the TBDMS groups. The ketones **70** (as a mixture of isomers i.e., *trans*-**70**, *cis*-**70**) and **71** (as a mixture of isomers i.e., *trans*-**71**, *cis*-**71**) were thus formed in 64% and 62% yields, respectively, through a modification of the procedure described by Stang²⁷ as shown in Scheme 2.12. Separation of the *cis/trans* isomers was in each case impossible due to their nearly identical polarities. *Cis/trans*-**70** was a yellow oily solid which was stable to air at ambient temperature (isolated in an approximate ratio of 4:6), whereas **71** was a colorless solid that was also very stable to air at room temperature and melted at 126–128 °C (isolated in a ratio of ~2:8).

Confirmation of the structures of *cis/trans*-**70** and **71** is based on analysis of spectroscopic data done as a mixture. In the ^1H NMR spectrum, the protons of the cyclohexane backbone show up at δ 1.44–2.46 for *cis/trans*-**70** and δ 1.42–2.35 for *cis/trans*-**71**. The TES protons show a triplet at δ 0.99 and a quartet at δ 0.65 for *cis/trans*-**70**, whereas for *cis/trans*-**71** the TBDMS protons show two singlets at δ 0.95 and 0.15. The ^{13}C NMR (APT) spectrum also supports this structural assignment. The resonances of the carbonyl carbons of the ketones are observed at 189.9 ppm for *cis/trans*-**70** and 188.8 ppm for *cis/trans*-**71**. The resonances for the acetylene carbons are discernible at δ 102.4, 102.3, 97.6 and 97.2 for the isomers of *cis/trans*-**70** and at δ 101.6, 97.6 for *cis/trans*-**71**. The resonances for the methine and methylene carbons of the cyclohexane backbone are observed in a range of 49.2–51.7 ppm and 25.1–27.4 ppm, respectively, for both *cis/trans*-**70** and **71**. The TES carbons are observed at 7.3, and 3.8 ppm for *cis/trans*-**70** and for *cis/trans*-**71**, the TBDMS carbons are at 25.9, 24.4, and 16.8 ppm. The IR spectrum shows the presence of a medium peak at 2146 cm^{-1} corresponding to $\text{C}\equiv\text{C}$ stretches for both *cis/trans*-**70** and **71**, whereas the strong peaks at 1672 cm^{-1} and 1668 cm^{-1} correspond to the stretching of the $\text{C}=\text{O}$ bonds for *cis/trans*-**70** and **71**, respectively. The mass spectrum shows a weak molecular ion peak at m/z 416.3 for *cis/trans*-**70**, whereas the signal at m/z 359.2 ($\text{M} - t\text{-Bu}$) $^+$ corresponds to the molecular ion observed for the *cis/trans*-**71** fragment less a *tert*-butyl group.

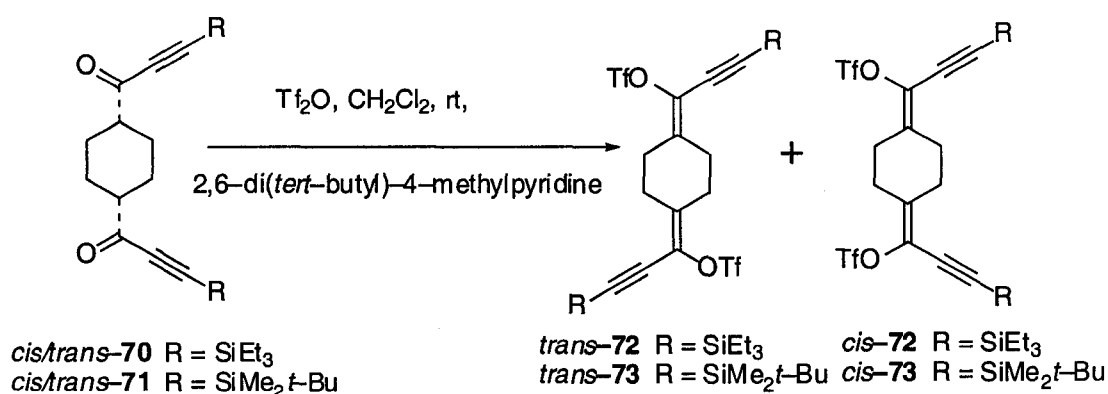


Scheme 2.12 Formation of ketones **70** and **71** (mixture of *cis/trans*-**70** [\sim 4:6] and **71** [\sim 2:8])

Triflation of ketones **70** and **71** took place in the presence of excess triflic anhydride and 2,6-di(*tert*-butyl)-4-methylpyridine in CH_2Cl_2 at room temperature for 3–4 days (Scheme 2.13). Aqueous reaction work-up followed by purification via column chromatography (silica gel) gave triflates **72** (as a mixture of *trans*-**72**:*cis*-**72** \sim 46:54) and **73** (as a mixture of *trans*-**73**:*cis*-**73** \sim 45:55) in 72% and 66% yields, respectively, both as colorless solids. Separation of the two isomers was difficult due to their nearly identical polarities. Compounds **72** and **73** melted (as mixtures) at 94–96 °C and 93–94 °C, respectively, and both were stable to air at ambient temperature.

The structures of the triflates **72** and **73** are consistent with the spectroscopic data. In the ^1H NMR spectrum, the protons of the cyclohexane backbone show three singlets at δ 2.64, 2.60, and 2.55 for *cis/trans*-**72** and at δ 2.61, 2.58, and 2.52 for *cis/trans*-**73**. The TES protons show a triplet at δ 1.01 and a quartet at δ 0.68 for *cis/trans*-**72**, whereas for *cis/trans*-**73**, the TBDMS protons show as three singlets at δ 0.96, 0.16, and 0.15. The ^{13}C NMR (APT) spectrum also supports this assignment. The in-chain vinylidene carbons ($[\text{CH}_2]_2\text{C}=\text{C}$) are quite deshielded, resonating at 140.4 and 140.3

ppm for *cis/trans*-**72** and at 140.5 and 140.4 ppm for *cis/trans*-**73**. The vinylidene carbons outside of the main chain ($[\text{CH}_2]_2\text{C}=\text{C}$) are quite shielded, resonating 125.2 and 125.1 ppm for *cis/trans*-**72** and at 125.1 and 125.0 ppm for *cis/trans*-**73**. The resonances of the triflate (CF_3) groups are observed as a quartet at δ 118.3 for *cis/trans*-**72** and δ 119.2 for *cis/trans*-**73**. The resonances for the acetylene carbons are discernible at δ 102.7, 102.6, 94.6 and 94.5 for *cis/trans*-**72** and at δ 103.6, 103.2, 94.3 and 94.2 for *cis/trans*-**73**. The resonances for the four methylene carbons of the cyclohexane backbone are observed in the range of 26.0–29.9 ppm for both *cis/trans*-**72** and **73**. The TES carbons are observed at 7.2, 3.9 and 3.7 ppm for *cis/trans*-**72**, whereas for *cis/trans*-**73** the TBDMS carbons are at 25.9, 16.6 and 16.5 ppm. The IR spectrum shows the presence of medium peaks at 2148 and 2152 cm^{-1} corresponding to $\text{C}\equiv\text{C}$ stretches whereas the medium peaks at 1650 and 1651 cm^{-1} correspond to the stretching of the $\text{C}=\text{C}$ bonds for *cis/trans*-**72** and **73**, respectively. The mass spectrum shows a molecular ion peaks at m/z 680.2 corresponding to the molecular mass of both derivatives *cis/trans*-**72** and **73**.

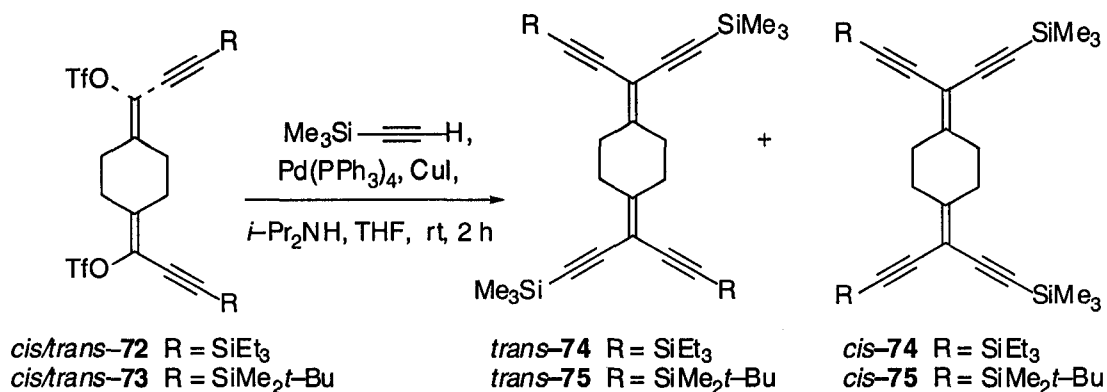


Scheme 2.13 Formation of Triflates **72** and **73** (mixture of *cis/trans*-**72** [~54:46] and **73** [~55:45])

Next, the geminal enediynes **74** and **75** were formed under modification of Sonogashira²⁶ Pd-catalyzed cross-coupling conditions (Scheme 2.14). Triflates *cis/trans*-**72** and **73**, were cross-coupled with TMSA using Pd(PPh₃)₄ as catalyst, CuI as co-catalyst, and *i*-Pr₂NH base in anhydrous THF at room temperature for 2 h under a N₂ atmosphere. After aqueous work-up and purification via column chromatography (silica gel), geminal enediyne **74** (as a mixture of *trans*-**74**, and *cis*-**74**) and **75** (as a mixture of *trans*-**75**, and *cis*-**75b**) were isolated in pure form as light yellow solids with defined melting points of 106–108 and 146–148 °C, respectively. Separation of the *cis/trans* isomers in both cases was impossible as a result of their identical polarities. An approximate isomeric ratio of 47:53 was determined for **75** based on NMR analysis. The ratio for **74** was not determined. These compounds were stable to air and could be stored for extended periods of time at room temperature without noticing any sign of decomposition by either TLC or NMR spectroscopic analysis.

Confirmation of the structures of *cis/trans*-**74** and **75** is based on analysis of their spectroscopic data. In the ¹H NMR spectrum, the protons of the cyclohexane backbone show a singlet at δ 2.63 for *cis/trans*-**74** and at δ 2.62 for *cis/trans*-**75**. The TES protons show a triplet at δ 0.99 and a quartet at δ 0.62 for *cis/trans*-**74**, whereas for *cis/trans*-**75**, TBDMS protons show four singlets at δ 0.96, 0.93, 0.13, and 0.11. The TMS protons show a singlet at δ 0.18 for *cis/trans*-**74** and two singlets at δ 0.19, and 0.18 for *cis/trans*-**75**. The ¹³C NMR (APT) spectrum also supports this assignment. The in-chain vinylidene carbons ([CH₂]₂C=C) are quite deshielded, resonating at 159.1 and 159.0 ppm for both *cis/trans*-**74** and **75**. The vinylidene carbons outside of the main chain ([CH₂]₂C=C) fall into the chemical shift range of the acetylenic carbons, from 94.9–101.9 ppm for both *cis/trans*-**74** and **75** and are not assignable. This

upfield shift is due to the synergistic effect of the two ethynyl bonds and the two geminal methylene groups in the cyclohexane backbone which polarize the vinylidene bonds resulting in the shielding of the vinylidene carbons outside of the main chain ($[\text{CH}_2]_2\text{C}=\text{C}$). The resonances for the methylene carbons of the cyclohexane backbone are observed in the range of 31.2–31.4 ppm for both *cis/trans*-**74** and **75**. The TES carbons are observed at 7.4 and 4.4 ppm for *cis/trans*-**74**, whereas for *cis/trans*-**75** the TBDMS carbons are at 26.1 and 16.8 ppm. The resonances for the TMS carbons are observed in the range of -0.5–(-0.1) ppm for both *cis/trans*-**74** and **75**. The IR spectrum shows the presence of a medium peak at 2149 cm^{-1} corresponding to $\text{C}\equiv\text{C}$ stretches for both *cis/trans*-**74** and **75**, whereas the medium peaks at 1591 cm^{-1} and 1588 cm^{-1} correspond to the stretching of the $\text{C}=\text{C}$ bonds for *cis/trans*-**74** and **75**, respectively. The mass spectrum shows a molecular ion peaks at m/z 576.3 corresponding to the molecular mass of both *cis/trans*-**74** and **75**.

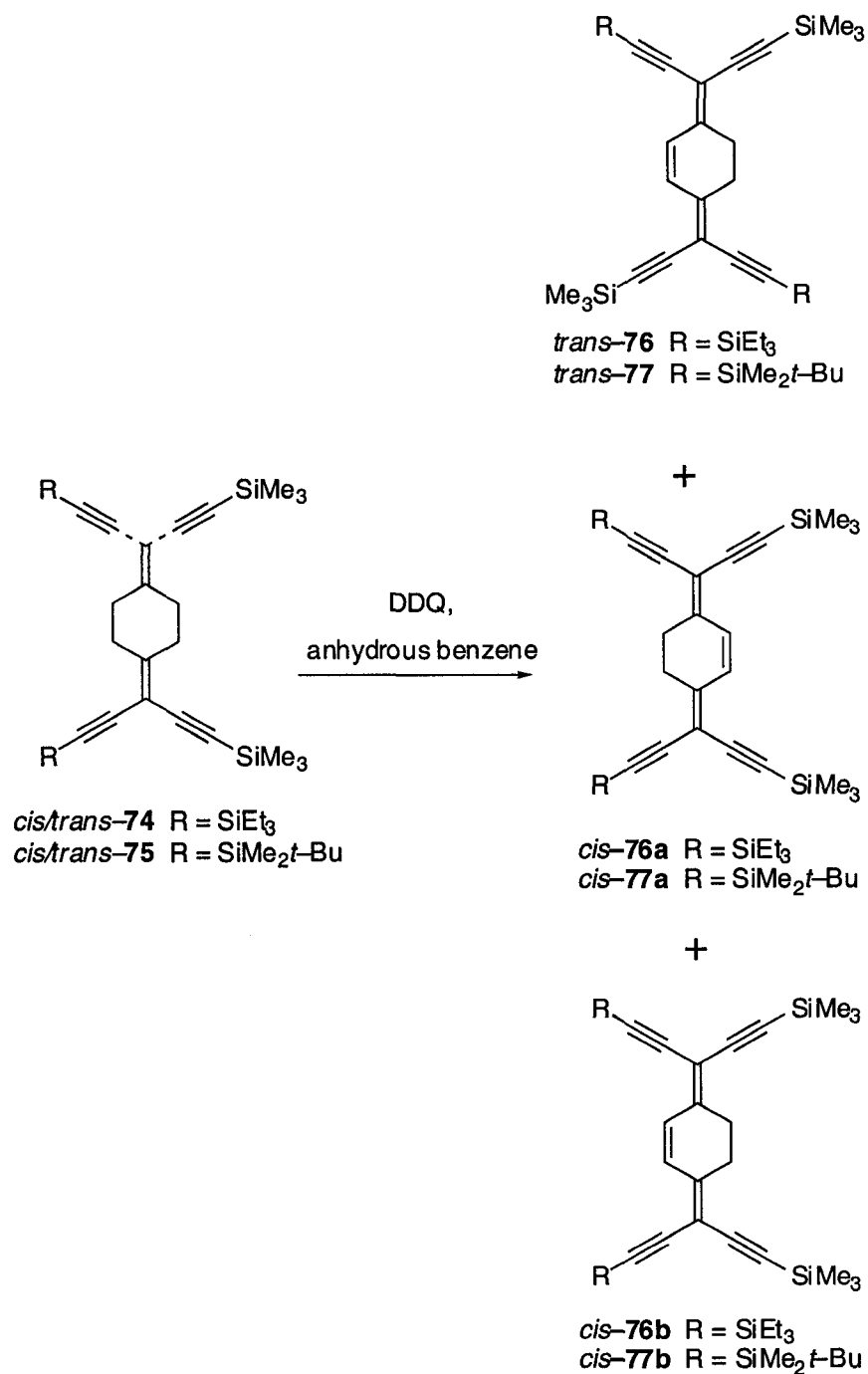


Scheme 2.14 Formation of Geminal Eneynes, **74** and **75** (mixture of *cis/trans*-**74** and **75**).

On heating of a benzene solution of *cis/trans*-**74** and **75** at reflux in the presence of a fourfold excess of DDQ for 2–4 h, dehydrogenation took place to furnish the dihydro-TEQ derivatives **76** and **77**, respectively (Scheme 2.15). Pure products of **76** (as a mixture of isomers i.e., *trans*-**76**, *cis*-**76a**, and *cis*-**76b**) and **77** (as a mixture of isomers i.e., *trans*-**77**, *cis*-**77a**, and *cis*-**77b**) were isolated by evaporation of the volatile portion of the reaction mixture and subjecting the resulting residue to column chromatography (silica gel). The dihydro-TEQ derivatives **76** and **77** were obtained as mixtures in 28% and 52% yields, respectively. In each case, separation of the three isomers was impossible because of their identical polarities. An approximate isomeric ratio of 49:16:35 was determined for **77** based on NMR spectroscopic analysis. Ratios for **76** were not determined. These compounds were thermally stable and could be stored for months as solids in the air at room temperature.

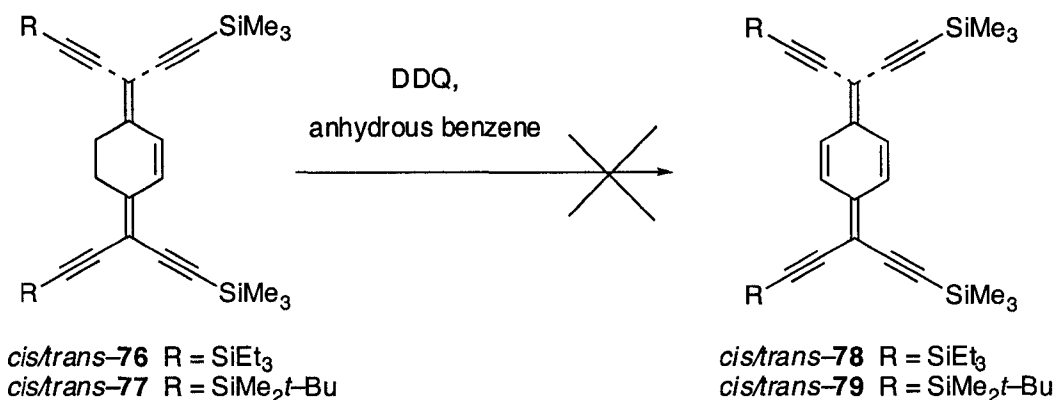
The structures of the dihydro-TEQ derivatives *cis/trans*-**76** and **77** are consistent with their spectroscopic data. In the ¹H NMR spectrum, the vinyl protons in the cyclohexene ring show a multiplet at δ 6.92 for both *cis/trans*-**76** and **77**, whereas the methylene protons resonate at δ 2.70 for *cis/trans*-**76** and δ 2.70 for *cis/trans*-**77**. The TES protons show as a triplet at δ 1.01 and a quartet at δ 0.64 for *cis/trans*-**76**, whereas for *cis/trans*-**77** the TBDMS protons show four singlets at δ 0.96, 0.95, 0.16 and 0.15. The TMS protons show as a singlet at δ 0.18 for *cis/trans*-**76** and two singlets at δ 0.22 and 0.21 for *cis/trans*-**77**. The ¹³C NMR (APT) spectrum also supports this assignment. The in-chain vinylidene carbons [(CH₂)(CH)C=C] are quite deshielded, resonating in the range of 150.6–150.8 ppm for both *cis/trans*-**76** and **77**, whereas the vinylidene carbons outside of the main chain [(CH₂)(CH)C=C] fall into the chemical shift range of the acetylenic carbons, from 97.7–103.2 ppm for both *cis/trans*-**76** and

77. The vinyl carbons for *cis/trans*-**76** and **77** are degenerate, resonating at 130.3 ppm, whereas the methylene carbons show in the range of 26.2–29.8 ppm. The TES carbons are observed at 7.4 and 4.4 ppm for *cis/trans*-**76**, whereas for *cis/trans*-**77** the TBDMS carbons are at 26.2 and 16.9 ppm. The resonances for the TMS carbons are observed in the range of –4.5–0.0 ppm for both *cis/trans*-**76** and **77**. The IR spectrum shows the presence of medium peaks at 2145 and 2126 cm^{-1} for *cis/trans*-**76** and at 2142 and 2124 cm^{-1} for *cis/trans*-**77** corresponding to $\text{C}\equiv\text{C}$ stretches, whereas the medium peaks at 1652 and 1462 cm^{-1} correspond to the stretching of the $\text{C}=\text{C}$ bonds in *cis/trans*-**76** and **77**, respectively. The mass spectrum shows a molecular ion peaks at m/z 574.3 corresponding to the molecular mass of both *cis/trans*-**76** and **77**.



Scheme 2.15 Attempted oxidation of dihydro-TEQ derivatives **76** and **77**
 (mixture of *cis/trans-76* and *77*)

All efforts to further oxidize these bright yellow solids **76** and **77** to **78** and **79**, respectively, (Scheme 2.16), have to date failed. When the amount of the oxidant or the reaction conditions were varied (i.e., increasing or decreasing the reaction time, the temperature and the oxidant), only a black material that could not be identified by physical or chemical methods was obtained.



Scheme 2.16 Ineffective oxidation of 76 and 77

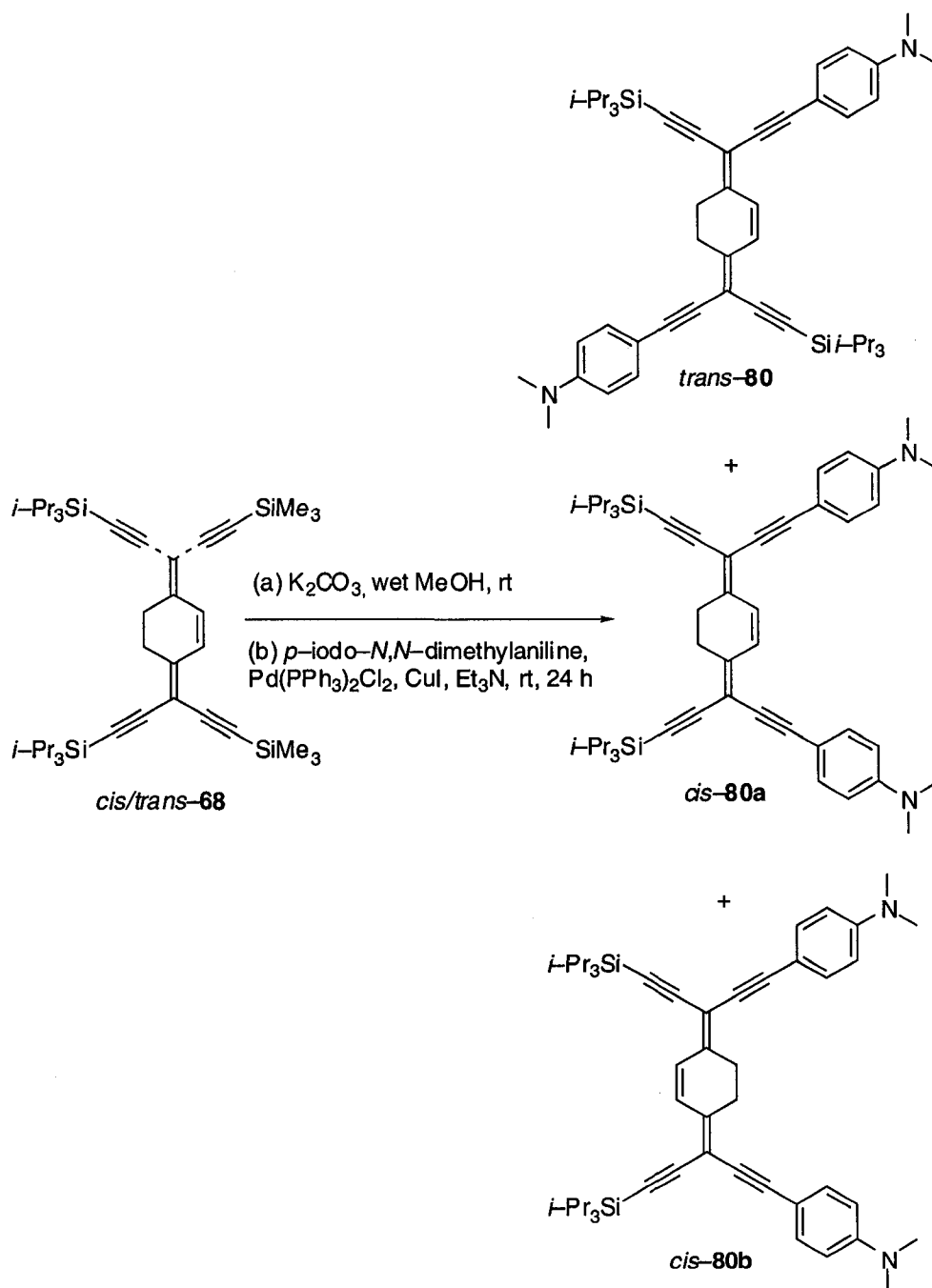
The ability to selectively and sequentially remove the Me₃Si groups in the presence of Et₃Si, *t*-BuMe₂Si and *i*-Pr₃Si groups in effect makes **68**, **76** and **77** more versatile building blocks in comparison to tetrakis(trimethylsilyl) dihydro-TEQ derivative **62**. Based on this, one can confidently say that the dihydro-TEQ derivatives **68**, **76** and **77** represent important precursors for the synthesis of differentially di- and tetra-functionalized dihydro-TEQ derivatives through stepwise deprotection-cross-coupling sequences. Our attention was thus drawn to the synthesis of a series of dihydro-TEQ derivatives bearing electron donating (*p*-dimethylaminophenyl) and/or electron accepting (*p*-nitrophenyl) groups.

Protodesilylation of **68** with K₂CO₃ in wet MeOH selectively removed the Me₃Si groups in the presence of the *i*-Pr₃Si groups, and the formed terminally deprotected

alkyne was directly coupled with *p*-iodo-*N,N*-dimethylaniline³⁵ in degassed Et₃N, using PdCl₂(PPh₃)₂ as catalyst and CuI as co-catalyst at room temperature for 24 h under N₂ atmosphere to afford **80** (Scheme 2.17). Pure **80** (as a mixture of isomers i.e., *trans*-**80**, and *cis*-**80a**, and *cis*-**80b**), was isolated by evaporation of the volatile portion of the reaction mixture and subjecting the resulting residue to column chromatography (silica gel). The dihydro-TEQ derivatives **80** were obtained as a mixture in a combined 20% yield as deep red needles. Separation of the three isomers was impossible because of their nearly identical polarities. An approximate isomeric ratio of 31:33:36 was determined based on NMR spectroscopic analysis. This compound was stable to air at ambient temperature, and shows strong fluorescence as a CH₂Cl₂ solution.

The structure of the dihydro-TEQ derivatives **80** (as a mixture) is consistent with the spectroscopic data. In the ¹H NMR spectrum, the four aromatic protons ortho to the acetylene are deshielded and show up at δ 7.34. The other four protons ortho to the amino group are shielded, and their signal appears at δ 6.65. The vinyl protons of the cyclohexene ring are quite deshielded and show as a multiplet at δ 7.02, whereas the methylene protons are shielded and their signal appears at δ 2.81. The methyl protons on the amine show as two singlets at δ 2.98 and 2.99. The TIPS protons show as three singlets in the range of δ 1.11–1.13. Recording a ¹³C NMR spectrum of this product has not been possible because of insufficient material. The IR spectrum shows the presence of medium peaks at 2185 and 2136 cm⁻¹ corresponding to C≡C stretches, whereas the medium peaks at 1608, 1547 and 1520 cm⁻¹ correspond to the stretching of

the C=C bonds. The ESI MS analysis shows a molecular ion peak at m/z 751 ($[M + H]^+$, 38) corresponding to the molecular mass of all three isomers of **80**.

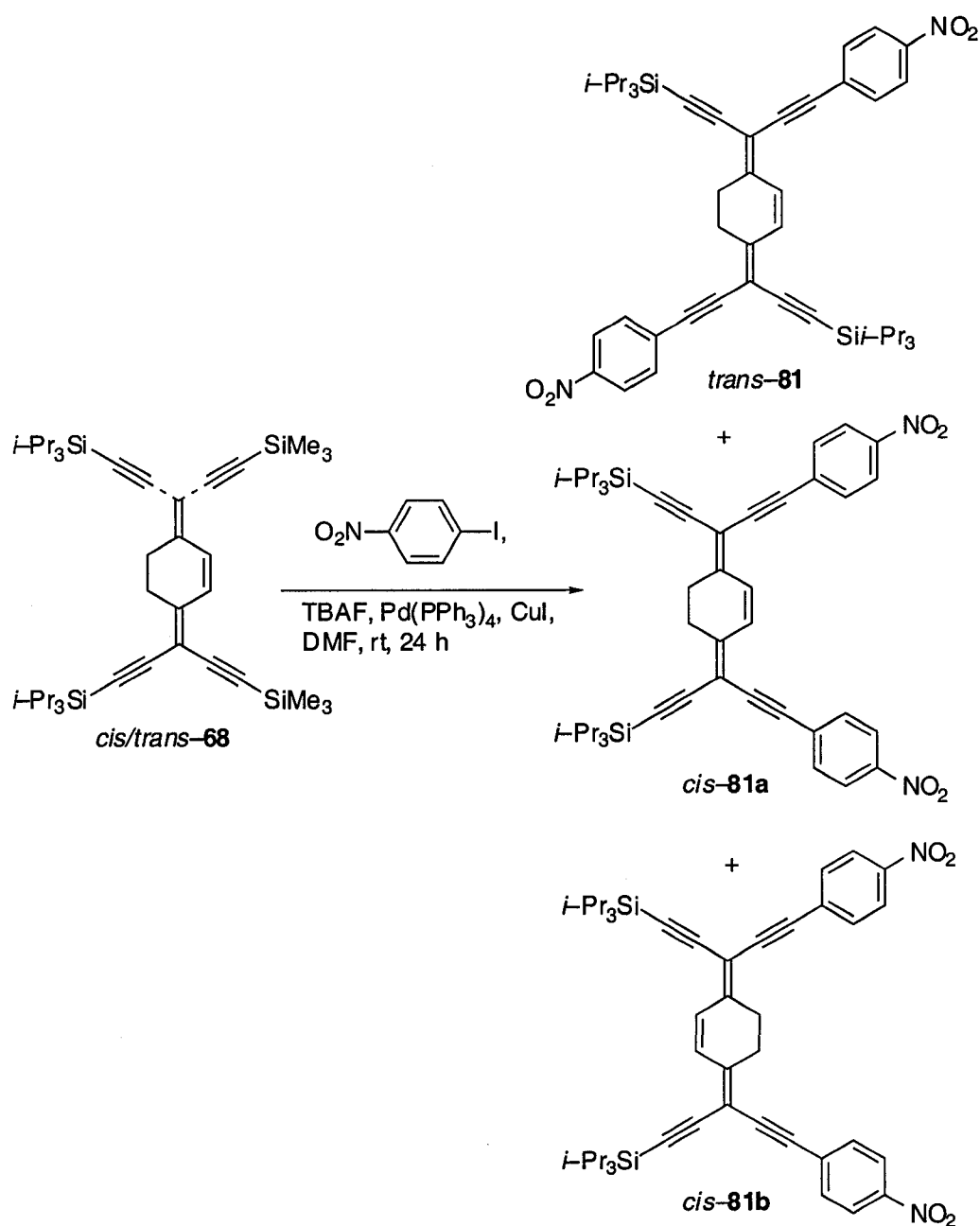


Scheme 2.17 Formation of di-donor dihydro-TEQ derivative **80** (mixture of *trans*-**80**, *cis*-**80a** and *cis*-**80b**)

In our effort to synthesize a dihydro-TEQ derivative bearing electron accepting (*p*-nitrophenyl) groups, **68** was transformed into **81**, using Hiyama³⁶ Pd(0)-mediated cross-coupling reaction. For this synthesis, **68** was cross-coupled with *p*-iodonitrobenzene in the presence of tetrabutylammonium fluoride (TBAF) as a desilylating reagent, Pd(PPh₃)₄ as catalyst, CuI as co-catalyst and DMF as a solvent at room temperature for 24 h under a N₂ atmosphere to afford **81** (Scheme 2.18). Pure **81** (as a mixture of isomers i.e., *trans*-**81**, *cis*-**81a**, and *cis*-**81b**) was isolated by evaporation of the volatile portion of the reaction mixture and subjecting the resulting residue to column chromatography (silica gel). Separation of the three isomers was impossible due to their nearly identical polarities, but an approximate isomeric ratio of 28:28:44 was determined based on NMR spectroscopic analysis. The dihydro-TEQ derivatives **81** were obtained as a mixture in 25% yield as deep red solid. This compound was thermally stable and could be stored for months as a solid in the air at room temperature.

Confirmation of the structure of **81** is based on analysis of the spectroscopic data. In the ¹H NMR spectrum, the four aromatic protons ortho to the nitro group are deshielded and show up at δ 8.21. The other four protons ortho to the acetylene group appear at δ 7.60. The vinyl protons of the cyclohexene ring are quite deshielded and show as a multiplet at δ 7.09, whereas the methylene protons appear at δ 2.87. The TIPS protons show as three singlets at δ 1.13. The ¹³C NMR (APT) spectrum also supports this assignment. The in-chain vinylidene carbons [(CH₂)(CH)C=C] are quite deshielded, resonating at 150.8 ppm, whereas the vinylidene carbons outside of the main chain [(CH₂)(CH)C=C] fall into the chemical shift range of the acetylenic carbons, from 91–102 ppm. The resonances of the deshielded aromatic quaternary carbons are observed at 147.0 ppm, whereas the vinyl carbons in the cyclohexene ring fall into the

chemical shift range of the methine aromatic carbons, from 123.6–133.2 ppm. The methylene carbons in the cyclohexene ring are observed at 27.2 ppm. The resonances for the TIPS carbons are observed at 18.8 and 11.4 ppm. The IR spectrum shows the presence of medium peaks at 2194 and 2138 cm^{-1} that correspond to $\text{C}\equiv\text{C}$ stretches, whereas the medium peaks at 1654, 1593 and 1517 cm^{-1} correspond to the stretching of the $\text{C}=\text{C}$ bonds. The ESI MS analysis shows a molecular ion peak at m/z 756.4 (M^+ , 100) corresponding to the molecular mass of the three isomers **81**.

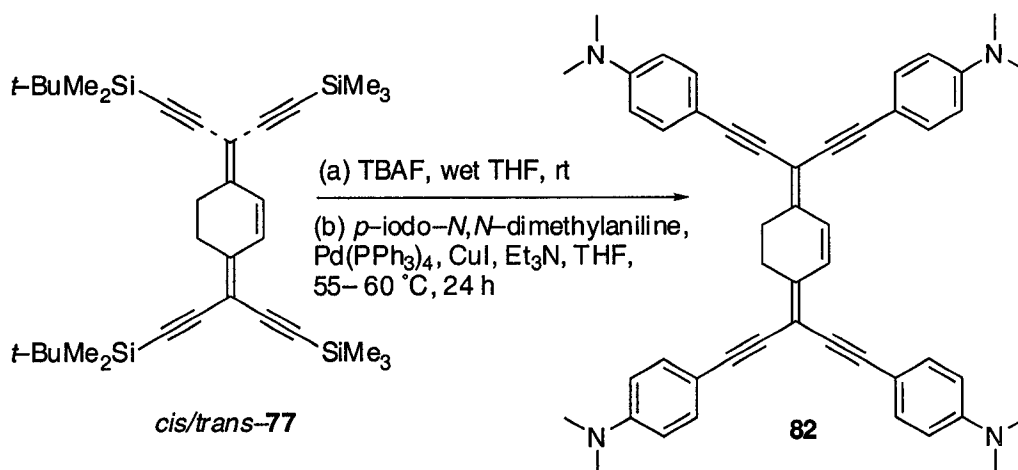


Scheme 2.18 Formation of di-acceptor dihydro-TEQ derivative **81** (mixture of *trans*-**81**, *cis*-**81a** and *cis*-**81b**)

The synthesis of tetra-functionalized dihydro-TEQ derivative bearing electron donating (*p*-dimethylaminophenyl) groups **82** was targeted. During this synthesis, **77**

was desilylated with TBAF. The terminally deprotected alkyne product was directly coupled with *p*-iodo-*N,N*-dimethylaniline in degassed THF, using Pd(PPh₃)₄ as catalyst, CuI as co-catalyst and Et₃N as base, under reflux for 24 h under N₂ atmosphere to afford **82** (Scheme 2.19). Pure **82** was isolated by evaporation of the volatile portion of the reaction mixture and subjecting the resulting residue to column chromatography (silica gel). The resulting tetra-functionalized dihydro-TEQ derivative bearing electron donating (*p*-aminophenyl) groups **82**, was obtained in only 5% yield as deep red needles. This compound was stable to air at room temperature and showed fluorescence in CH₂Cl₂ solution.

The structure of the dihydro-TEQ derivative **82** is consistent with the spectroscopic data. In the ¹H NMR spectrum, the eight aromatic protons ortho to the acetylene group are deshielded and show up at δ 7.41. The other eight protons ortho to the amino group are shielded and their signal appears at δ 6.66. The vinyl protons of the cyclohexene ring are quite deshielded and show a multiplet at δ 7.08, whereas the methylene protons appear at δ 2.89. The methyl protons on the amino group show two singlets at δ 2.98. The ¹³C NMR spectroscopic analysis has not been possible because of insufficient material. The IR spectrum shows a medium peak at 2175 cm⁻¹ that corresponds to C≡C stretches, whereas the medium peaks at 1604 and 1520 cm⁻¹ correspond to the stretching of the C=C bonds. The ESI MS analysis shows a molecular ion peak at *m/z* 679.4 ([M + H]⁺, 100) confirming to the molecular mass of **82**.



Scheme 2.19 Formation of tetra-donor dihydro-TEQ derivative 82

2.3 Conclusions

In this chapter, we have described the importance of conjugated molecules, especially for optical and electronic applications. Besides linearly conjugated molecules, an alternative form of conjugation which has only sparsely been addressed in material research has also been described, namely cross-conjugation. Some practical applications of cross-conjugated molecules in electronic and optical devices, as well as examples of recent investigations have also been discussed.

We describe in this chapter an efficient synthesis of the precursors for and derivatives of 7,7,8,8-tetraethynyl-*p*-quinodimethane (TEQ) having different silyl protecting groups. These compounds are stable to air and can be stored for months at room temperature without any noticeable sign of decomposition by either TLC or NMR spectroscopic analysis.

Finally, we describe the synthesis and characterization of differentially di- and tetra-functionalized dihydro-TEQ derivatives bearing electron donating (*p*-dimethylaminophenyl) and/or electron accepting (*p*-nitrophenyl) groups through stepwise deprotection-cross-coupling sequences.

2.4 References and Notes

- (1) Marder, S. R.; Perry, J. W. *Adv. Mater.* **1993**, *5*, 804-815.
- (2) Nalwa, H. S. *Adv. Mater.* **1993**, *5*, 341-358.
- (3) Martin, R. E.; Diederich, F. *Angew. Chem. Int. Ed.* **1999**, *38*, 1350-1377.
- (4) Jones, L.; Schumm, J. S.; Tour, J. M. *J. Org. Chem.* **1997**, *62*, 1388-1410.
- (5) Hopf, H. *Angew. Chem., Int. Ed. Engl.* **1984**, *23*, 948-960.
- (6) Lehrich, F.; Hopf, H. *Tetrahedron Lett.* **1987**, *28*, 2697-2700.
- (7) Faust, R.; Gobelt, B.; Weber, C.; Krieger, C.; Gross, M.; Gisselbrecht, J. P.; Boudon, C. *Eur. J. Org. Chem.* **1999**, 205-214.
- (8) For a comprehensive review on cross conjugation and cross-conjugated systems, see Chapter 1.
- (9) Cairns, T. L.; Carboni, R. A.; Coffman, D. D.; Engelhardt, V. A.; Heckert, R. E.; Little, E. L.; McGeer, E. G.; McKusick, B. C.; Middleton, W. J.; Scribner, R. M.; Theobald, C. W.; Winberg, H. E. *J. Am. Chem. Soc.* **1958**, *80*, 2775-2778.
- (10) Merrifield, R. E.; Phillips, W. D. *J. Am. Chem. Soc.* **1958**, *80*, 2778-2782.
- (11) Acker, D. S.; Hertler, W. R. *J. Am. Chem. Soc.* **1962**, *84*, 3370-3374.
- (12) Melby, L. R.; Harder, R. J.; Hertler, W. R.; Mahler, W.; Benson, R. E.; Mochel, W. E. *J. Am. Chem. Soc.* **1962**, *84*, 3374-3387.
- (13) Rubin, Y.; Knobler, C. B.; Diederich, F. *Angew. Chem., Int. Ed. Engl.* **1991**, *30*, 698-700.
- (14) Hauptmann, H. *Angew. Chem., Int. Ed. Engl.* **1975**, *14*, 498.
- (15) Neenan, T. X.; Whitesides, G. M. *J. Org. Chem.* **1988**, *53*, 2489-2496.
- (16) Lockhart, T. P.; Comita, P. B.; Bergman, R. G. *J. Am. Chem. Soc.* **1981**, *103*, 4082-4090.
- (17) Nicolaou, K. C.; Hwang, C. K.; Smith, A. L.; Wendeborn, S. V. *J. Am. Chem. Soc.* **1990**, *112*, 7416-7418.

- (18) Porco, J. A.; Schoenen, F. J.; Stout, T. J.; Clardy, J.; Schreiber, S. L. *J. Am. Chem. Soc.* **1990**, *112*, 7410-7411.
- (19) Tykwinski, R. R.; Schreiber, M.; Carlon, R. P.; Diederich, F.; Gramlich, V. *Helv. Chim. Acta* **1996**, *79*, 2249-2281.
- (20) Spreiter, R.; Bosshard, C.; Knopfle, G.; Gunter, P.; Tykwinski, R. R.; Schreiber, M.; Diederich, F. *J. Phys. Chem. B* **1998**, *102*, 29-32.
- (21) Bosshard, C.; Spreiter, R.; Gunter, P.; Tykwinski, R. R.; Schreiber, M.; Diederich, F. *Adv. Mater.* **1996**, *8*, 231-234.
- (22) Tykwinski, R. R.; Gubler, U.; Martin, R. E.; Diederich, F.; Bosshard, C.; Gunter, P. *J. Phys. Chem. B* **1998**, *102*, 4451-4465.
- (23) Neidlein, R.; Winter, M. *Synthesis* **1998**, 1362-1366.
- (24) Hopf, H.; Kampen, J.; Bubenitschek, P.; Jones, P. G. *Eur. J. Org. Chem.* **2002**, 1708-1721.
- (25) Corey, E. J.; Fuchs, P. L. *Tetrahedron Lett.* **1972**, 3769-3772.
- (26) Sonogashira, K.; Tohda, Y.; Hagihara, N. *Tetrahedron Lett.* **1975**, 4467-4470.
- (27) Stang, P. J.; Treptow, W. *Synthesis* **1980**, 283-284.
- (28) Walton, D. R. M.; Waugh, F. *J. Organomet. Chem.* **1972**, *37*, 45-56.
- (29) Brandsma, L. *Preparative Acetylene Chemistry*; 2nd ed.; Elsevier Science: Amsterdam, 1998.
- (30) Wasaki, F. I.; Aihara, A. *Acta Crystallogr., Sect. B: Struct. Crystallogr. Cryst. Chem.* **1970**, *26*, 91.
- (31) Maas, G.; Lorenz, W. *J. Org. Chem.* **1984**, *49*, 2273.
- (32) Wood, J. L.; Moniz, G. A. *Org. Lett.* **1999**, *1*, 371,
- (33) Pretsch, E.; Seibl, J.; Simon, W.; Clerc, T. *Tables of Spectral Data for Structure Determination of Organic Compounds*; Springer-Verlag: Berlin, **1989**; page C90.

- (34) Zhao, Y. Cross-conjugated Enyne Oligomers: Synthesis, Properties, and Nonlinear Optical Investigations. Ph.D. Thesis, University of Alberta, Edmonton, AB, June 2002.
- (35) Dawson, D. J.; Frazier, J. D.; Brock, P. J.; Twieg, R. J. in *Polymers for High Technology*; ACS: Washington, D.C., **1987**; Vol. 346, page 445.
- (36) Hatanaka, Y.; Hiyama, T. *J. Org. Chem.* **1989**, *54*, 265-270.

Chapter 3 EXPERIMENTAL SECTION

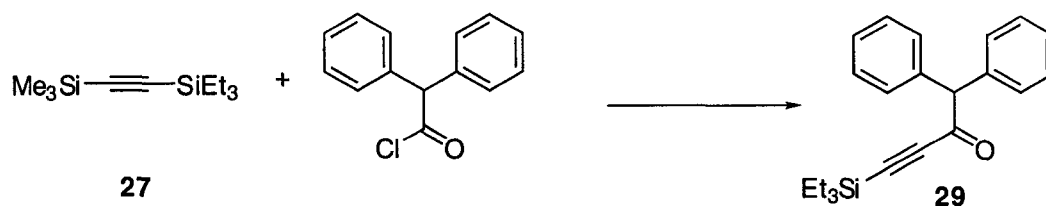
General. Reagents were purchased reagent grade from commercial suppliers and used without further purification. *p*-iodo-*N,N*-dimethylaniline, was made as previously described.¹ Bistrimethylsilylacetylene and compounds **27–28**² were prepared as previously described. Anhydrous MgSO₄ was used as the drying agent after aqueous work-up. Evaporation and concentration *in vacuo* was done at H₂O-aspirator pressure. All reactions were performed in standard, dry glassware under an inert atmosphere pressure of Ar or N₂ unless otherwise stated. A positive pressure of N₂ or Ar was essential to the success of all Pd-catalyzed reactions. Degassing of solvents was accomplished by vigorously bubbling N₂ or Ar through the solution for at least 45 min. Flash column chromatography: *silica gel–60* (230–400 mesh) from *General Intermediates of Canada*. Size-exclusion chromatography (SEC): *Bio-Beads S–X2* (200–400 mesh) from *Bio-Rad Laboratories*. Thin Layer Chromatography (TLC): plastic sheets coated with *silica gel–60* F₂₅₄ with fluorescent indicator UV₂₅₄ from Macherey–Nagel and aluminium sheets coated with *silica gel–60* F₂₅₄ from E. Merck; visualization by UV light or KMnO₄ stain. Mp: *Gallenkamp* apparatus; uncorrected. UV–vis spectra: *Varian Cary 400* at rt; λ_{max} in nm (ϵ in L mol⁻¹ cm⁻¹). IR spectra (cm⁻¹): *Nicolet Magna–IR 750* or *Nic–Plan IR Microscope* (solids). ¹H and ¹³C NMR: *Varian Inova 300, 400, or 500 MHz* instruments, at rt in CDCl₃ (solvent peaks: 7.24 ppm for ¹H and 77.0 ppm for ¹³C as reference). EI MS (*m/z*): *Kratos MS 50* instrument. ESI MS (*m/z*): *Micromass Zabspec Hybrid Sector–TOF*, in either positive or negative ion mode or *PE Biosystems Mariner TOF* instruments; solvents: MeOH, MeOH/toluene 3:1, CH₃NO₂, and C₂H₄Cl₂. Optical Rotation [α]_D: *Perkin–Elmer 241* Polarimeter (10 cm cell). X-ray crystallographic analysis was done on a *Bruker PLATFORM/SMART 1000 CCD* X-ray diffractometer. Elemental analyses were effected by Spectral Services at the

Department of Chemistry–University of Alberta, using a *Carlo Erba EA 1108* Elemental Analyzer. For simplicity, the coupling constants of the aryl protons for the oligomers, *p*-*N,N*-dimethylaminophenyl and *p*-nitrophenyl moieties have been reported as pseudo first-order, even though they are second-order spin systems.

General Desilylation and Palladium-catalyzed Cross-coupling Procedure.

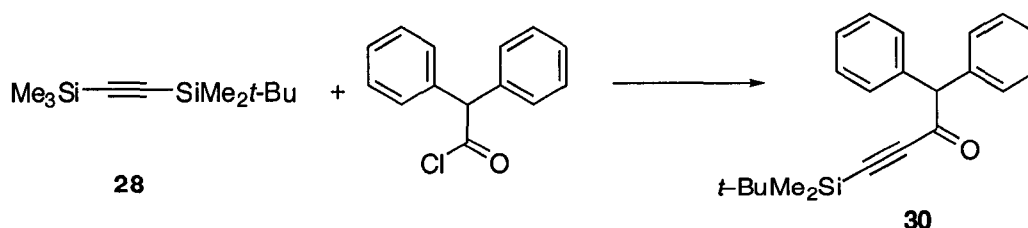
A mixture of the appropriate trimethylsilyl- or tert-butyldimethylsilyl-, triisopropylsilyl-, triethylsilyl-protected polyynes and K_2CO_3 (ca. 0.2 equiv.) or TBAF (2.2 equiv.) in wet THF/MeOH (1:1, 20 mL) or THF (20 mL), respectively, was stirred at rt for 2 h. Ether and saturated aqueous NH_4Cl were added, the organic phase separated, washed with saturated aqueous NH_4Cl (2 x 50 mL), dried, reduced to ca. 1 mL, and added to a degassed solution of vinyl triflate or aryl halide in THF or DMF (20 mL). $Pd(PPh_3)_4$ or $PdCl_2(PPh_3)_2$ (ca. 0.05 equiv.) and *i*-Pr₂NH or Et₃N were sequentially added, the solution stirred for 5 min, CuI (ca. 0.1 equiv.) was added and the solution stirred under conditions described in the individual procedures until TLC analysis no longer showed the presence of the deprotected polyynes starting material. Ether and H₂O were added, the organic phase separated, washed with saturated aqueous NH_4Cl (2 x 50 mL), dried and the solvent removed *in vacuo*. Flash column chromatography or size-exclusion chromatography, and/or precipitation from MeOH gave the desired endiynes oligomer or geminal endiynes derivatives of TEQ.

1,1-Diphenyl-4-triethylsilylbut-3-yn-2-one (29)



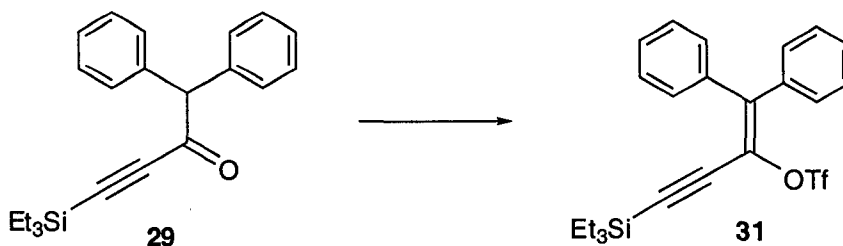
*1-Triethylsilyl-2-trimethylsilylacetylene (2.78 g, 13.1 mmol) **27** and diphenyl acetyl chloride (3.01 g, 13.1 mmol) in CH_2Cl_2 (200 mL) were placed into a flask at 0 °C under nitrogen atmosphere. Aluminium chloride (1.75 g, 13.1 mmol) was slowly added in portions, the solution was stirred at 0 °C for 3 h and then poured into a mixture of 10% HCl solution (200 mL) and ice (200 g). The aqueous layer was extracted with ethyl acetate (3 x 50 mL) and the combined organic phases were subsequently washed with saturated aqueous NaHCO_3 and saturated aqueous NaCl, and then dried with MgSO_4 . Solvent removal and purification of the resulting crude product by column chromatography (silica gel, hexanes/ CH_2Cl_2 2:1) afforded **29** (3.33 g, 76%) as a yellow oil. $R_f = 0.4$ (hexanes/ CH_2Cl_2 2:1). *Spectral data were consistent with literature values.³

1,1-Diphenyl-4-tert-butyl dimethylsilylbut-3-yn-2-one (30)



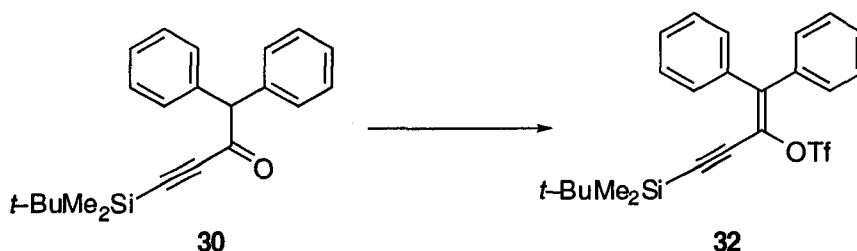
1-Tert-butyltrimethylsilyl-2-trimethylsilylacetylene (4.76 g, 22.4 mmol) **28** and diphenyl acetyl chloride (5.15 g, 22.4 mmol) in CH₂Cl₂ (200 mL) were placed into a flask at 0 °C under nitrogen atmosphere. Aluminium chloride (3.29 g, 24.6 mmol) was slowly added in portions, while the solution was stirred at 0 °C. The solution was kept stirring at 0 °C for 3 h, then poured into a mixture of 10% HCl solution (200 mL) and ice (200 g). The aqueous layer was extracted with ethyl acetate (3 x 50 mL) and the combined organic phases were subsequently washed with saturated aqueous NaHCO₃ and saturated aqueous NaCl, and then dried with MgSO₄. Solvent removal and purification by column chromatography (silica gel, hexanes/CH₂Cl₂ 2:1) afforded **30** (5.52 g, 74%) as a yellow oil. *R_f* = 0.4 (hexanes/CH₂Cl₂ 2:1). IR (CHCl₃, cast) 3062, 3029, 2953, 2929, 2857, 2147, 1682, 1601, 1496, 1252, 1096, 827 cm⁻¹; ¹H NMR (400 MHz, CDCl₃) δ 7.33–7.27 (m, 10H), 5.16 (s, 1H), 0.81 (s, 9H), 0.07 (s, 6H); ¹³C NMR (100 MHz, CDCl₃) δ 185.3, 137.4, 129.2, 128.6, 127.4, 102.8, 100.1, 66.3, 25.9, 16.5, 0.5. EIMS *m/z* 334.2 (M⁺, 1.13), 167.1 ([Ph₂CH]⁺, 100); HRMS calcd. for C₂₂H₂₆OSi (M⁺) 334.1753, found 334.1743. Anal. calcd. for C₂₂H₂₆OSi: C, 79.06; H, 7.84. Found: C, 78.27; H, 7.92.

Trifluoromethanesulfonic acid 1-diphenylmethylenediphenyl-3-triethylsilylprop-2-ynyl ester (31)



*Reaction of **29** (2.34 g, 7.01 mmol) with trifluoromethane-sulfonic anhydride (1.77 mL, 2.97 g, 10.5 mmol) and 2,6-di-*t*-butyl-4-methyl pyridine (2.16 g, 10.5 mmol) in CH₂Cl₂ (50 mL) was conducted under nitrogen atmosphere for 3 days. The CH₂Cl₂ was removed *in vacuo* and the residue extracted with hexanes. The organic solution was washed with 10% HCl, saturated aqueous NaHCO₃, saturated aqueous NaCl, and dried with MgSO₄. Solvent removal and purification by column chromatography (silica gel, hexanes/CH₂Cl₂ 2:1) afforded **31** (2.64 g, 81%) as a clear light yellow oil. *R_f* = 0.6 (hexanes/CH₂Cl₂ 2:1). *Spectral data were consistent with literature values.³

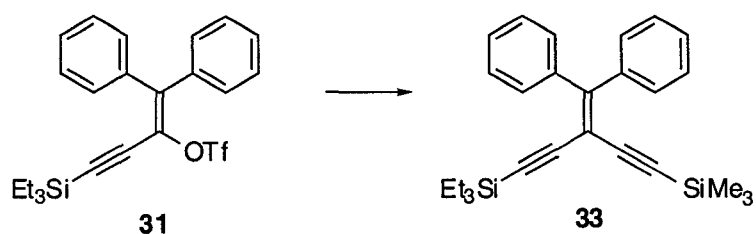
Trifluoromethanesulfonic acid 1-diphenylmethyldene-3-tert-butyl dimethylsilyl-prop-2-ynyl ester (32)



Reaction of **30** (3.41 g, 10.2 mmol) with trifluoromethane-sulfonic anhydride (2.58 mL, 4.32 g, 15.3 mmol) and 2,6-di-*t*-butyl-4-methyl pyridine (3.15 g, 15.3 mmol) in CH₂Cl₂ (50 mL) was conducted under nitrogen atmosphere for 3 days. The CH₂Cl₂ was removed *in vacuo* and the residue extracted with hexanes. The organic solution was washed with 10% HCl, saturated aqueous NaHCO₃, saturated aqueous NaCl, and dried with MgSO₄. Solvent removal and purification by column chromatography (silica gel, hexanes/CH₂Cl₂ 2:1) afforded **32** (3.80 g, 80%) as a clear light yellow oil. *R_f* = 0.6 (hexanes/CH₂Cl₂ 2:1). IR (CHCl₃, cast) 3060, 2954, 2930, 2858, 2150, 1599, 1424,

1212, 1140 cm^{-1} ; ^1H NMR (500 MHz, CDCl_3) δ 7.35–7.24 (m, 10H), 0.86 (s, 9H), 0.07 (s, 6H); ^{13}C NMR (125 MHz, CDCl_3) δ 144.0, 136.7, 136.0, 130.4, 130.0, 129.3, 129.2, 128.4, 128.1, 126.3, 118.3 (q, $J = 326$ Hz), 103.6, 97.2, 26.0, 16.7, –5.3. EIMS m/z 466.1 (M^+ , 62), 333.2 ($[\text{M} - \text{CF}_3\text{SO}_2]^+$, 100); HRMS calcd. for $\text{C}_{23}\text{H}_{25}\text{O}_3\text{F}_3\text{SiS}$ (M^+) 466.1246, found 466.1247. Anal. calcd. for $\text{C}_{23}\text{H}_{25}\text{O}_3\text{F}_3\text{SiS}$: C, 59.26; H, 5.41; S, 6.88. Found: C, 59.43; H, 5.37; S, 6.78.

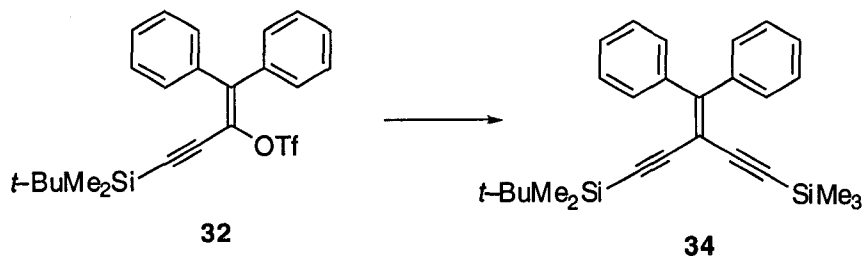
3-Diphenylmethylidene-1-triethylsilyl-5-trimethylsilyl-1,4-pentadiyne
(**33**)



*Triflate **31** (885 mg, 1.91 mmol) was cross-coupled with trimethylsilylacetylene (0.54 mL, 3.8 mmol) in degassed THF (20 mL) in the presence of $\text{PdCl}_2(\text{PPh}_3)_2$ (67 mg, 0.11 mmol), $i\text{-Pr}_2\text{NH}$ (3 mL), CuI (36 mg, 0.2 mmol) for 12 h under reflux as described in the general procedure. Flash column chromatography (hexanes/ CH_2Cl_2 2:1) afforded **33** (754 mg, 96%) as a pale yellow solid. $R_f = 0.5$ (hexanes/ CH_2Cl_2 2:1).

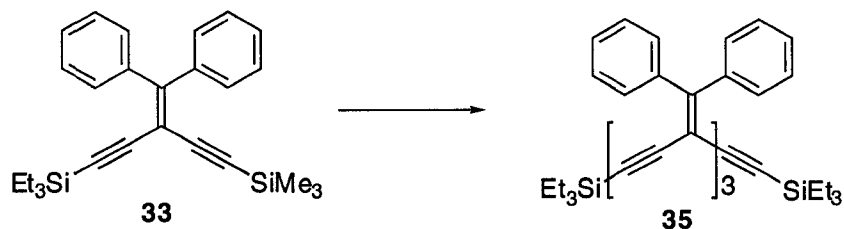
*Spectral data were consistent with literature values.³

3-Diphenylmethylidene-1-tert-butyldimethylsilyl-5-trimethylsilyl-1,4-pentadiyne (34)



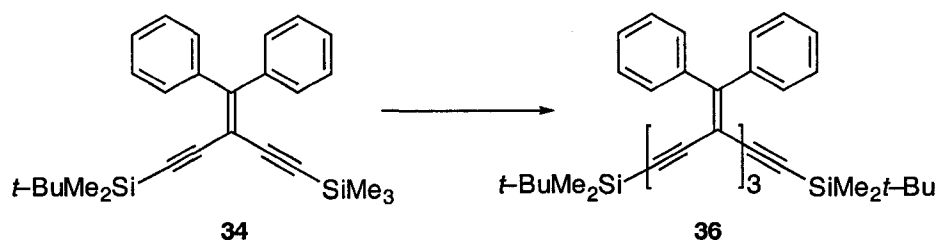
Triflate **32** (182 mg, 0.391 mmol) was cross-coupled with trimethylsilylacetylene (0.11 mL, 77 mg, 0.78 mmol) in degassed THF (20 mL) in the presence of $\text{PdCl}_2(\text{PPh}_3)_2$ (13.7 mg, 0.0211 mmol), *i*-Pr₂NH (3 mL), CuI (11 mg, 0.059 mmol) for 12 h under reflux as described in the general procedure. Flash column chromatography (hexanes/ CH_2Cl_2 2:1) afforded **34** (154 mg, 95%) as a pale yellow solid. Mp 100-102 °C. R_f = 0.5 (hexanes/ CH_2Cl_2 2:1); UV-vis (CHCl_3) λ_{max} (ϵ) 246 (18000), 330 (18100) nm; IR (CH_2Cl_2 , cast) 3057, 2955, 2927, 2856, 2151, 1492, 1470, 1442, 1250, 1213 cm^{-1} ; ^1H NMR (400 MHz, CDCl_3) δ 7.42-7.39 (m, 4H), 7.29-7.27 (m, 6H), 0.83 (s, 9H), 0.10 (s, 9H), 0.04 (s, 6H); ^{13}C NMR (100 MHz, CDCl_3) δ 157.6, 140.1, 139.9, 130.2, 130.2, 128.4, 128.3, 127.6, 127.4, 103.7, 103.4, 102.1, 97.6, 96.4, 26.1, 16.9, -0.3, -0.5. EIMS m/z 414.2 (M^+ , 47), 73.0 ($[\text{C}_3\text{H}_9\text{Si}(\text{TMS})]^+$, 100); HRMS calcd. for $\text{C}_{27}\text{H}_{34}\text{Si}_2$ (M^+) 414.2199, found 414.2191. Anal. calcd. for $\text{C}_{27}\text{H}_{34}\text{Si}_2$: C, 78.28; H, 8.27. Found: C, 77.94; H, 8.27.

1,11-Bis(triethylsilyl)-3,6,9-tri(diphenylmethylidene)-1,4,7,10-undecatriyne (35)



*Monomer **33** (122 mg, 0.295 mmol) was desilylated with 2 equiv. of TBAF and cross-coupled with triflate **31** (274 mg, 0.588 mmol) in degassed THF (20 mL) in the presence of $\text{Pd}(\text{PPh}_3)_4$ (34 mg, 0.029 mmol), *i*-Pr₂NH (2 mL), and CuI (17 mg, 0.088 mmol) for 12 h under reflux, as described in the general procedure. Flash column chromatography (hexanes/ CH_2Cl_2 2:1) afforded **35** (220 mg, 87%) as a yellow solid and **37** (20 mg, 6%) as a deep yellow solid. *Spectral data were consistent with literature values.³

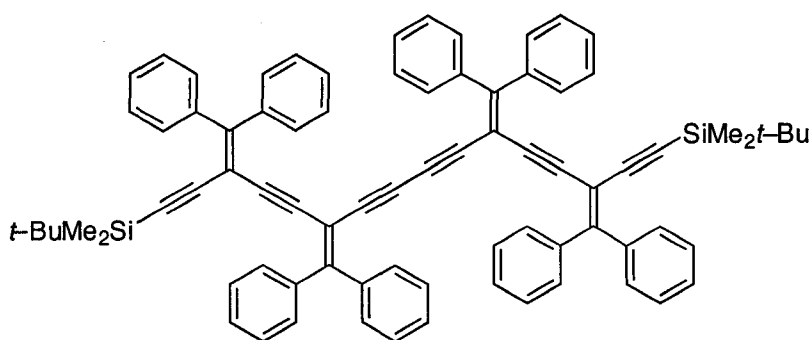
1,11-Bis(tert-butyl dimethylsilyl)-3,6,9-tri(diphenylmethylidene)-1,4,7,10-undecatriyne (36)



Monomer **34** (559 mg, 1.35 mmol) was desilylated with 2 equiv. of TBAF and cross-coupled with triflate **32** (2.8 mg, 1.3 mmol) in degassed THF (20 mL) in the

presence of Pd(PPh₃)₄ (156 mg, 0.135 mmol), *i*-Pr₂NH (3 mL), and CuI (51 mg, 0.27 mmol) for 12 h under refluxing, as described in the general procedure. Flash column chromatography (hexanes/CH₂Cl₂ 2:1) afforded **36** (874 mg, 76%) as a yellow solid. Mp 169–171 °C (Decomp.). *R*_f = 0.4 (hexanes/CH₂Cl₂ 2:1); UV–vis (CHCl₃) λ_{max} (ε) 257 (48300), 324 (25300), 369 (31200) nm; IR (CH₂Cl₂, cast) 3054, 3030, 2953, 2927, 2855, 2143, 1493, 1470, 1442, 1249 cm⁻¹; ¹H NMR (400 MHz, CDCl₃) δ 7.42–7.18 (m, 30H), 0.82 (s, 18H), 0.04 (s, 12H); ¹³C NMR (100 MHz, CDCl₃) δ 156.6, 154.8, 140.4, 140.0, 139.7, 130.3 (2x), 130.2, 128.5, 128.4, 128.2, 127.7, 127.6, 127.5, 103.5, 102.1, 95.9, 90.6, 90.1, 26.2, 16.8, –4.7 (one signal not observed). ESIMS *m/z* (MeOH/toluene 3:1): 883.4 ([M + Na⁺]⁺, 100). Anal. calcd. for C₆₂H₆₀Si₂: C, 86.54; H, 7.03. Found: C, 84.64; H, 6.82.

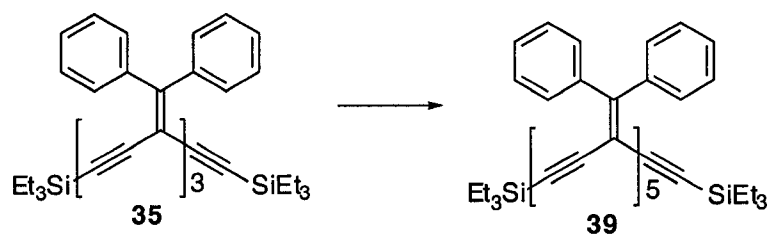
1,16-Bis(tertbutyldimethylsilyl)-3,6,11,14-tetra(diphenylmethylidene)-1,4,7,9,12,15-hexadecahexayne (38)



38

Homocoupled tetramer **38** was isolated from the synthesis of **36** as a deep yellow solid in 5% yield. $R_f = 0.3$ (hexanes/ CH_2Cl_2 2:1). IR (CH_2Cl_2 , cast) 3080, 3054, 3030, 2953, 2927, 2855, 2142, 1492, 1470, 1442, 1249 cm^{-1} ; ^1H NMR (500 MHz, CDCl_3) δ 7.39-7.17 (m, 40H), 0.80 (s, 18H), 0.03 (s, 12H); ^{13}C NMR (100 MHz, CDCl_3) δ 157.6, 157.2, 140.2, 139.8, 139.5 (2x), 130.3 (2x), 130.0, 128.8, 128.7, 128.2, 127.8 (2x), 127.7, 127.5, 103.1, 101.7, 101.2, 96.1, 91.6, 89.6, 81.0, 26.2, 16.8, -4.7 (3 signals not observed). ESIMS m/z (MeOH/toluene 3:1): 1111.5 ($[\text{M} + \text{Na}]^+$, 100).

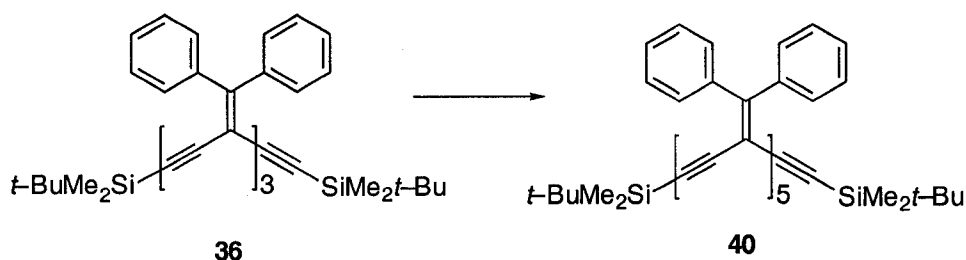
1,17-Bis(triethylsilyl)-3,6,9,12,15-penta(diphenylmethylidene)-1,4,7,10,13,16-heptadecahexayne (39)



*Trimer **35** (174 mg, 0.202 mmol) was desilylated with 2 equiv. of TBAF and cross-coupled with triflate **31** (198 mg, 0.424 mmol) in degassed THF (20 mL) in the presence of $\text{Pd}(\text{PPh}_3)_4$ (24 mg, 0.02 mmol), $i\text{-Pr}_2\text{NH}$ (2 mL), and CuI (7.7 mg, 0.041 mmol) for 12 h under reflux, as described in the general procedure. Flash column chromatography (hexanes/ CH_2Cl_2 2:1) afforded **39** (197 mg, 77%) as a yellow solid.

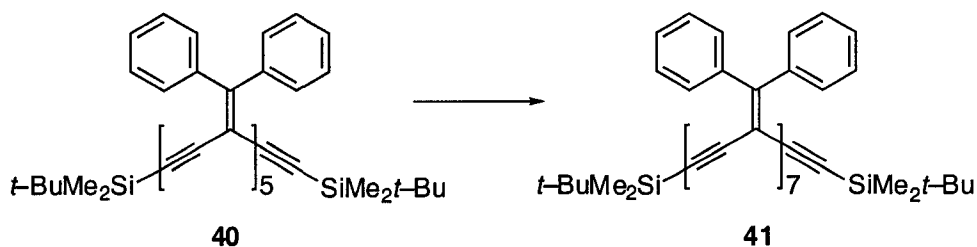
*Spectral data were consistent with literature values.³

1,17-Bis(tert-butyldimethylsilyl)-3,6,9,12,15-penta(diphenylmethylidene)-1,4,7,10,13,16-heptadecahexayne (40)



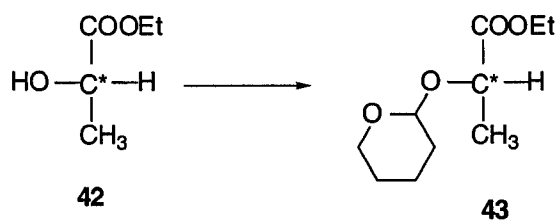
Trimer **36** (135 mg, 0.157 mmol) was desilylated with 2 equiv. of TBAF and cross-coupled with triflate **32** (154 mg, 0.329 mmol) in degassed THF (20 mL) in the presence of Pd(PPh₃)₄ (18 mg, 0.016 mmol), *i*-Pr₂NH (2 mL), and CuI (6 mg, 0.03 mmol) for 12 h under refluxing, as described in the general procedure. Flash column chromatography (hexanes/CH₂Cl₂ 2:1) afforded **40** (131 mg, 66%) as a yellow solid. Mp 119-121 °C. *R*_f = 0.6 (hexanes/CH₂Cl₂ 1:1); UV-vis (CHCl₃) λ_{max} (ε) 259 (81000), 377 (55200) nm; IR (CDCl₃, cast) 3054, 2962, 2927, 2855, 2141, 1492, 1260 cm⁻¹; ¹H NMR (400 MHz, CDCl₃) δ 7.40-7.10 (m, 50H), 0.82 (s, 18H), 0.04 (s, 12H); ¹³C NMR (100 MHz, CDCl₃, APT) δ 157.0, 155.0, 154.9, 140.5, 140.1, 140.0, 139.8, 130.4, 130.3, 130.2, 128.8, 128.6, 128.5, 128.2, 127.8, 127.7, 127.6, 103.5, 102.1, 102.0, 95.9, 90.7, 90.3, 90.2, 90.1, 26.1, 16.7, -4.8 (7 signals not observed). ESIMS *m/z* (MeOH/toluene 3:1): 1288.6 ([M + Na]⁺, 100). Anal. calcd. for C₉₄H₈₀Si₂: C, 89.27; H, 6.38. Found: C, 88.77; H, 6.24.

1,12-Bis(tert-butyldimethylsilyl)-3,6,9,12,115,18,21-hepta(diphenylmethylidene)-1,4,7,10,13,16,19,22-tricosaoctayne (41)



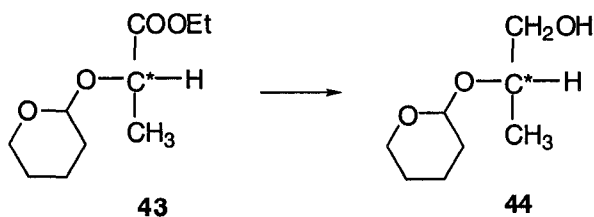
Pentamer **40** (52 mg, 0.041 mmol) was desilylated with 2 equiv. of TBAF and cross-coupled with triflate **32** (40 mg, 0.086 mmol) in degassed THF (10 mL) in the presence of Pd(PPh₃)₄ (5 mg, 0.004 mmol), *i*-Pr₂NH (2 mL), and CuI (2 mg, 0.01 mmol) for 12 h under refluxing, as described in the general procedure. Size-exclusion chromatography (toluene) afforded **41** (34 mg, 50%) as a yellow solid. Mp 116-118 °C. *R_f* = 0.5 (hexanes/CH₂Cl₂ 1:1); UV-vis (CHCl₃) λ_{max} (ε) 260 (104000), 378 (71700) nm; IR (CH₂Cl₂, cast) 3053, 2954, 2926, 2855, 2141, 1492, 1442, 1259 cm⁻¹; ¹H NMR (500 MHz, CDCl₃) δ 7.39-7.12 (m, 70H), 0.82 (s, 18H), 0.03 (s, 12H); ¹³C NMR (125 MHz, CDCl₃, APT) δ 156.9, 155.4, 155.1, 155.0, 140.5, 140.0 (2x), 139.9, 139.7, 130.4, 130.2, 128.7, 128.6, 128.5, 128.4, 128.2, 127.7 (2x), 127.6, 103.5, 102.1, 102.0, 101.9, 95.8, 90.7, 90.4 (2x), 90.2, 90.1, 26.1, 16.7, -4.8 (13 signals not observed). ESIMS (pos) *m/z* (MeOH/toluene 3:1): 1693.6 ([M + Na]⁺, 100). Anal. calcd. for C₁₂₆H₁₀₀Si₂: C, 90.68; H, 6.04. Found: C, 87.64; H, 6.06.

Ethyl (2S)-2-((Tetrahydropyran-2'-yl)oxy)propanoate (43)



*To a solution of ethyl (S)-lactate (10.0 g, 85.0 mmol, $[\alpha]_{\text{D}}^{24} -11.1$ {neat}) **42** and 3,4-dihydro-2H-pyran (11.6 g, 140 mmol) were slowly added 1 drop of concentrated HCl at 0 °C. The solution was stirred for 10 h while it reached room temperature. Na_2CO_3 (0.82 g) was added, and stirring was continued for 10 h. The reaction mixture was then filtered, concentrated to small volume, and distilled to give **43** (16.44 g, 96%) of a colorless oil. Bp 62-65 °C (0.4 mm) (lit. bp 66-68 °C (0.2 mm)); $[\alpha]_{\text{D}}^{22} -56.9$ (c = 0.282, CHCl_3). *Spectral data were consistent with literature values.^{4,5}

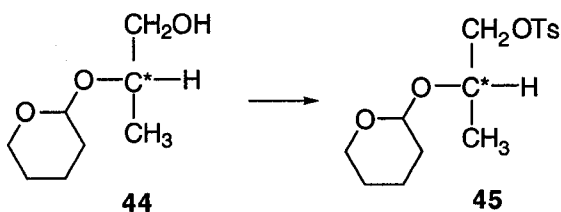
(2S)-2-((Tetrahydropyran-2'-yl)oxy)-1-propanol (44)



*To a suspension of LAH (3.4 g, 90 mmol) in dry diethyl ether (30 mL) was added a solution of **43** (15.09 g, 74.60 mmol) in dry diethyl ether (20 mL) at 0 °C under nitrogen atmosphere over 8 h. After 12 h at room temperature, the reaction mixture was refluxed for 5 h. Methyl acetate (1.5 mL), 10% NaOH (7.0 mL), and H₂O (23 mL) were then added respectively to the mixture cooled at room temperature. The precipitate was filtered off, the solution was concentrated, dried over K₂CO₃, and finally distilled to give **44** (11.69 g, 97%) of a colorless oil. Bp 63-66 °C (0.4 mm) (lit bp 64–66 °C (1 mm)); $[\alpha]_D^{22} = +15.6$ ($c = 0.3$, CHCl₃). *Spectral data were consistent with literature values.^{4,5}

(2S)-1-((p-Tolylsulfonyl)oxy)-2-((tetrahydropyran-2'-yl)oxy)propane

(45)

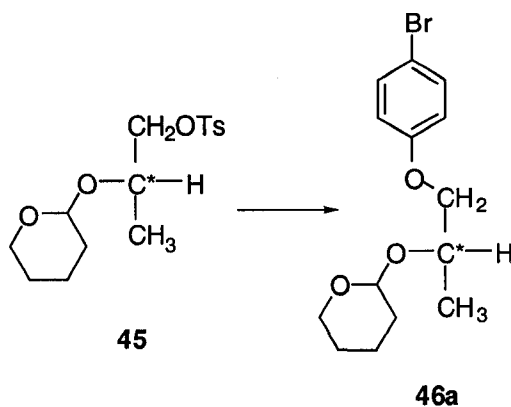


*A solution of **44** (6.51 g, 40.4 mmol) in dry pyridine (15 mL) was cooled in a water-ice bath under nitrogen atmosphere. p-Toluenesulfonyl chloride (8.63 g, 44.4 mmol) was added in small portions over 5 min. After being stirred at room temperature for 18 h, the mixture was filtered and the precipitate was washed with benzene (6 x 3 mL). The filtrate and washings were concentrated and shaken twice with iced water. The aqueous phase was slowly acidified with cold 3 N HCl to pH = 4–5 and extracted with benzene (3 x 5 mL). The organic fractions were washed with (5 mL) cold 3 N HCl and

H₂O and then dried over MgSO₄. After evaporation of the solvent, a clear oily **45** (10.66 g, 84%) was obtained that was used without further purification. $[\alpha]_D^{22} = -3.32$ ($c = 0.3$, CHCl₃). *Spectral data were consistent with literature values.^{4,5}

(2S)-1-((p-Bromophenyl)oxy)-2-((tetrahydropyran-2'-yl)oxy)propane

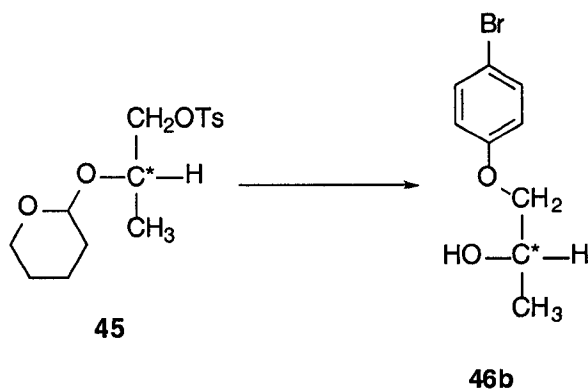
(46a)



A mixture of 4-bromophenol (0.73 g, 4.2 mmol) and pulverized KOH (0.24 g, 4.2 mmol) in purified DMF (25 mL) was stirred for 10 min. **45** (1.11 g, 3.52 mmol) was then added and stirred until tosylate reacted completely as judged by TLC analysis. The mixture was poured into iced water, extracted with Et₂O, washed with saturated aqueous NaCl, and dried with MgSO₄. Solvent removal and purification by column chromatography (silica gel, hexanes/CH₂Cl₂ 2:1) afforded **46a** (0.83 g, 75%) as a colorless oil as approximately 5:1 mixture of diastereomers. $R_f = 0.64$ (hexanes/CH₂Cl₂ 2:1). $[\delta]_D^{22} = -30.4$ ($c = 0.5$, CHCl₃); IR (CH₂Cl₂, cast) 3052, 2927, 2853, 1590,

1489, 1456, 1265 cm^{-1} . Major isomer: ^1H NMR (500 MHz, CDCl_3) δ 7.32 (d, $^3J_{\text{H,H}} = 8.8$ Hz, 2H), 6.74 (d, $^3J_{\text{H,H}} = 8.8$ Hz, 2H), 4.80 (t, $^3J_{\text{H,H}} = 5.2$ Hz, 1H), 4.12 (m, 1H), 3.85 (m, 3H), 3.48 (m, 1H), 1.80 (m, 1H), 1.67 (m, 1H), 1.52 (m, 4H), 1.29 (d, $^3J_{\text{H,H}} = 6.5$ Hz, 3H); ^{13}C NMR (125 MHz, CDCl_3 , APT) δ 158.1, 132.2, 116.4, 112.8, 96.8, 72.1, 71.2, 62.7, 30.9, 25.5, 19.7, 18.6. Minor isomer: ^1H NMR (500 MHz, CDCl_3) δ 7.34 (d, $^3J_{\text{H,H}} = 8.8$ Hz, 2H), 6.78 (d, $^3J_{\text{H,H}} = 8.8$ Hz, 2H), 4.74 (dd, $^3J_{\text{H,H}} = 5.2$ Hz, 1H), 4.02 (m, 1H), 1.22 (d, $^3J_{\text{H,H}} = 6.5$ Hz, 3H); ^{13}C NMR (125 MHz, CDCl_3 , APT) δ 96.6, 71.9, 70.2, 62.2, 19.5, 16.8. EIMS m/z 314.1 (M^+ , 3.9), 171.9 ($[\text{M} - \text{C}_8\text{H}_{15}\text{O}_2]^+$, 100); HRMS calcd. for $\text{C}_{14}\text{H}_{19}\text{O}_3^{79}\text{Br}$ (M^+) 314.0517, found 314.0528. Anal. calcd. for $\text{C}_{14}\text{H}_{19}\text{O}_3^{79}\text{Br}$: C, 53.53; H, 6.10. Found: C, 53.46; H, 6.20.

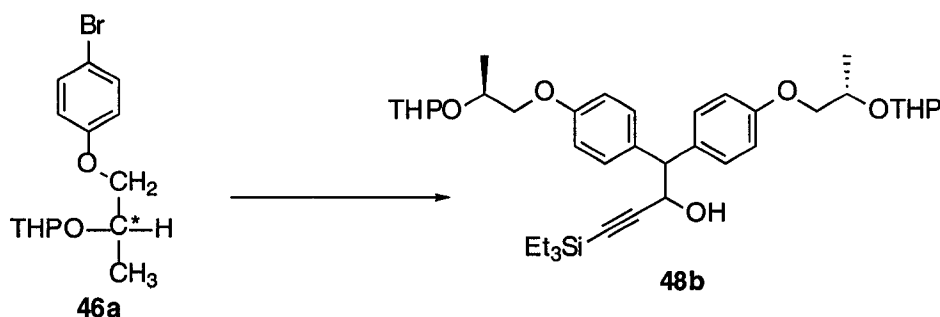
Attempted Synthesis of 46a: (2S)-1-((p-Bromophenyl)oxy)-propan-2-ol (46b)



*A mixture of 4-Bromophenol (287 mg, 1.66 mmol) and CsF (760 mg, 4.98 mmol) in purified DMF (25 mL) was stirred for 1 h. Compound **45** (522 mg, 1.66 mmol) was then added and stirred at rt until tosylate reacted completely as judged by TLC analysis. The mixture was poured into water, extracted with Et_2O , washed with saturated aqueous

NaCl, and dried with MgSO₄. Solvent removal and purification by column chromatography (silica gel, hexanes/CH₂Cl₂ 2:1) afforded **46b** (286 mg, 75%), **46a** (52 mg, 10%) and **46c** (43 mg, 10%) as a colorless oil. *Spectral data for **46b**, **46c** were consistent with literature values.^{6,7}

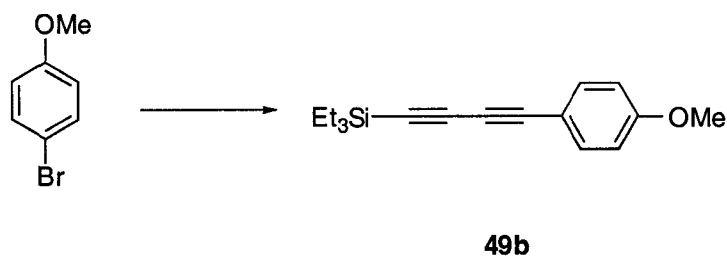
Attempted Synthesis of **48a** using Negishi Cross-Coupling Conditions



Compound **46a** (357 mg, 1.14 mmol) was dissolved in dry THF (5 mL) and cooled to -78 °C. To this was added butyllithium (2.5 M solution in hexanes, 0.460 mL, 1.14 mmol). The solution was stirred at -78 °C for 10 min and zinc chloride (0.5 M solution in THF, 2.28 mL, 1.14 mmol) was added. The mixture was stirred for 10 min at the initial temperature, then warmed to rt for 35 min. Compound **47** (87 mg, 0.23 mmol) and Pd(PPh₃)₄ (26 mg, 0.023 mmol) were sequentially added and the mixture stirred under reflux until TLC analysis no longer showed the presence of the starting material. Ether and saturated aqueous NH₄Cl were added, the organic phase separated, washed with saturated aqueous NaCl, and dried with MgSO₄. Solvent removal and purification by column chromatography (silica gel, hexanes/CH₂Cl₂ 2:1) afforded **48b** as a colorless oil. IR (CH₂Cl₂, cast) 3364, 2940, 2872, 1602, 1511, 1233 cm⁻¹. ¹H NMR (300 MHz, CDCl₃) δ 7.75 (m, 2H), 7.4 (m, 2H), 6.76 (m, 4H), 4.88 (t, 2H), 4.18 (m, 2H), 3.90

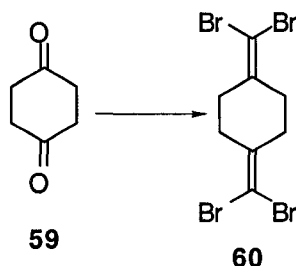
(m, 6H), 3.56 (m, 2H), 1.82 (m, 2H), 1.70 (m, 2H), 1.56 (m, 8H), 1.32 (d, $^3J_{\text{H,H}} = 5.8$ Hz, 6H), 0.92 (t, $^3J_{\text{H,H}} = 8.1$ Hz, 9H), 0.51 (q, $^3J_{\text{H,H}} = 8.1$ Hz, 6H); ^{13}C NMR (125 MHz, CDCl_3 , APT) δ 166.1, 153.2, 149.6, 134.8, 128.0, 116.4, 116.0, 113.8, 99.5, 96.5, 73.0, 71.2, 62.7, 30.9, 25.5, 19.7, 18.6, 7.8, 4.3. Attempts for MS analyses were unsuccessful.

Attempted Synthesis of 49a using Negishi Cross-Coupling Conditions



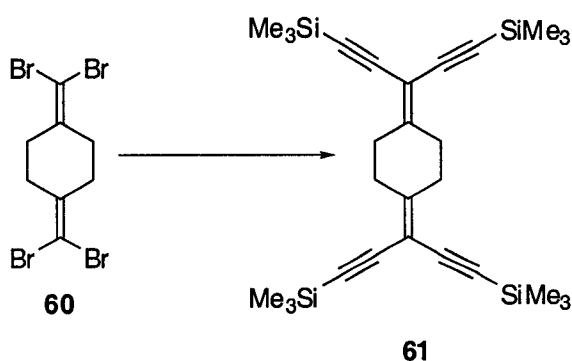
*Diyne **49b** was isolated in 30% yield following the above procedure using *p*-bromoanisole (400 mg, 2.14 mmol), *n*-BuLi (0.86 mL, 2.14 mmol), ZnCl_2 (4.28 mL, 2.14 mmol), compound **47** (164 mg, 0.428 mmol) and $\text{Pd}(\text{PPh}_3)_4$ (99 mg, 0.086 mmol). *Spectral data were consistent with literature values.⁸

1,4-Bis(dibromomethylene)cyclohexane (**60**)



*To a solution of PPh_3 (13.64 g, 51.94 mmol) in anhydrous benzene (100 mL) was added CBr_4 (8.62 g, 26.0 mmol). After stirring at rt for 30 min, cyclohexane-1,4-dione (1.12 g, 9.99 mmol) **59** was added and the mixture was subsequently stirred for 15 h at rt. The green precipitate was removed from the solution by filtration, the filtrate was evaporated under reduced pressure and the residue absorbed on Celite. Column chromatography (silica gel, hexanes/ CH_2Cl_2 10:1) yielded **60** (3.94 g, 93%) as a colorless solid. *Spectral data were consistent with literature values.^{9,10}

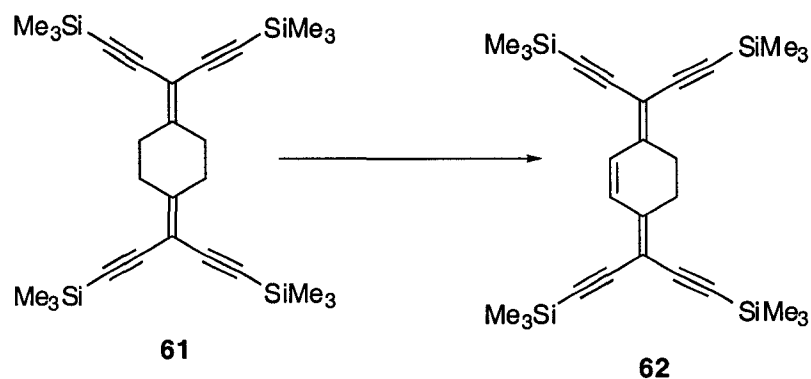
1,4-Bis[1,5-bis(trimethylsilyl)penta-1,4-diyne-3-ylidene]cyclohexane (61)



*To a solution of $i\text{-Pr}_2\text{NH}$ (3 mL), **60** (400 mg, 0.944 mmol), and trimethylsilylacetylene (1.03 mL, 714 mg, 7.27 mmol) in anhydrous benzene (30 mL) was added $\text{PdCl}_2(\text{PPh}_3)_2$ (133 mg, 0.189 mmol) and CuI (72 mg, 0.38 mmol). The mixture was stirred at rt for 48 h, concentrated *in vacuo*, and the residue was absorbed on Celite. Column chromatography (silica gel, hexanes) gave a yellow zone. Evaporation of the solvent *in vacuo* and recrystallization from Et_2O /hexanes, yielded **61**

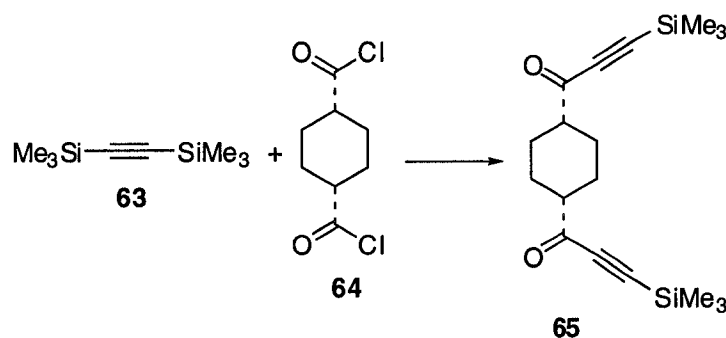
(370 mg, 80%) as a bright yellow crystals. *Spectral data were consistent with literature values.^{9,10}

1,4-Bis[1,5-bis(trimethylsilyl)penta-1,4-diyn-3-ylidenyl]cyclohex-2-ene (62)



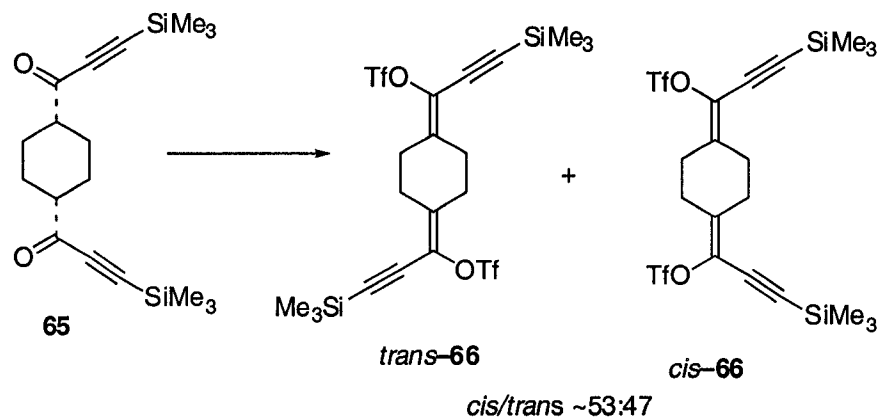
*DDQ (819 mg, 3.61 mmol) was added to a solution of **61** (444 mg, 0.901 mmol) in anhydrous benzene (25 mL). The mixture was heated to reflux for 4 h, filtered after cooling, the solvent was evaporated *in vacuo* and the residue absorbed on Celite. Column chromatography (silica gel, hexanes) gave a yellow zone. Evaporation of the solvent *in vacuo* and recrystallization from Et₂O/hexanes, yielded **62** (221 mg, 50%) as orange needles. *Spectral data were consistent with literature values.^{9,10}

1,4-Bis(1-oxo-3-trimethylsilylprop-2-ynyl)cyclohexane (65)



Bis(trimethylsilyl)acetylene (6.77 g, 40.0 mmol) was added under stirring to a solution of cyclohexane-1,4-dicarbonyl dichloride **64** (4.15 g, 20.0 mmol) in CH_2Cl_2 (100 mL) at 0°C under nitrogen. Aluminium chloride (5.29 g, 40.0 mmol) was slowly added in portions, while the solution was stirred at 0°C . The solution was kept stirring at 0°C for 3 h, then poured into a mixture of 10% HCl solution (100 mL) and ice (100 g). The aqueous layer was extracted with diethyl ether (3 x 50 mL) and the combined organic phases were subsequently washed with saturated aqueous NaHCO_3 and saturated aqueous NaCl, and then dried with MgSO_4 . Solvent removal and purification by column chromatography (silica gel, hexanes/ CH_2Cl_2 2:1) afforded **65** (4.32 g, 65%) as a colorless solid as approximately 5.2:4.8 mixture of diastereomers. This compound was characterized as a mixture. $R_f = 0.37$ (hexanes/ CH_2Cl_2 2:1). IR (CHCl_3 , cast) 2993, 2860, 2151, 1671, 1251, 1120 cm^{-1} ; ^1H NMR (300 MHz, CDCl_3) δ 2.38 (m, 2H), 2.18 (m, 3H), 1.98 (m, 1H), 1.78 (m, 1H), 1.42 (m, 3H), 0.42 (s, 18H); ^{13}C NMR (75.5 MHz, CDCl_3) δ 190.2, 101.2, 99.3, 51.3, 27.2, -0.7. EIMS m/z 332.2 (M^+ , 3), 73.0 (Me_3Si^+ , 100); HRMS calcd. for $\text{C}_{18}\text{H}_{28}\text{O}_2\text{Si}_2$ (M^+) 332.1628, found 332.1626. Anal. calcd. for $\text{C}_{18}\text{H}_{28}\text{O}_2\text{Si}_2$: C, 65.08; H, 8.49. Found: C, 64.70; H, 8.45.

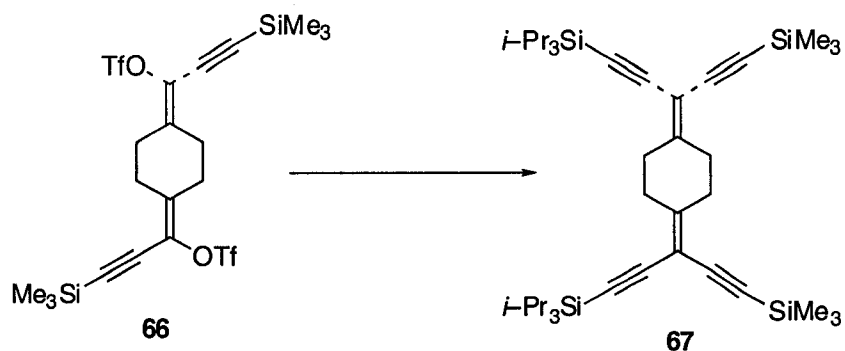
1,4-Bis(1-trifluoromethanesulfonyloxy-3-trimethylsilylprop-2-yn-1-ylidene)cyclohexane (66)



Reaction of **65** (0.89 g, 2.7 mmol) with trifluoromethane-sulfonic anhydride (1.35 mL, 2.26 g, 8.0 mmol) and 2,6-di-*t*-butyl-4-methyl pyridine (1.37 g, 6.7 mmol) in CH₂Cl₂ (50 mL) was conducted under nitrogen atmosphere for 3 days. The CH₂Cl₂ was removed *in vacuo* and the residue extracted with hexanes. The organic solution was washed with 10% HCl, saturated aqueous NaHCO₃, saturated aqueous NaCl, and dried with MgSO₄. Solvent removal and purification by column chromatography (silica gel, hexanes/CH₂Cl₂ 2:1) afforded **66** (0.95 g, 60%) as a colorless solid (mixture of isomers). Characterized as a pure diastereomer, *trans*-**66**: Mp 131-132 °C. *R_f* = 0.6 (hexanes/CH₂Cl₂ 2:1). IR (CH₂Cl₂, cast) 2968, 2154, 1417, 1220, 1139 cm⁻¹; ¹H NMR (400 MHz, CDCl₃) δ 2.56 (s, 8H), 0.21 (s, 18H); ¹³C NMR (100 MHz, CDCl₃) δ 140.4, 125.1, 118.2 (q, ¹J_{C,F} = 320 Hz), 104.6, 93.4, 29.7, 27.5, -0.6. EIMS *m/z* 596.1 (M⁺, 21); HRMS calcd. for C₂₀H₂₆O₆F₆Si₂S₂ (M⁺) 596.0613, found 596.0606. Anal. calcd. for C₂₀H₂₆O₆Si₂S₂F₆: C, 40.29; H, 4.39. Found: C, 40.25; H, 4.30. Characterized as ~ 1:1 mixture by comparison to *trans*-**66**, of *cis*-**66**: ¹H NMR (400

MHz, CDCl₃) δ 2.60 (s, 4H), 2.51 (s, 4H), 0.20 (s, 18H); ¹³C NMR (100 MHz, CDCl₃) δ 140.5, 125.0, 118.2 (q, ¹J_{C,F} = 320 Hz), 104.5, 93.5, 29.9, 27.1, -0.5.

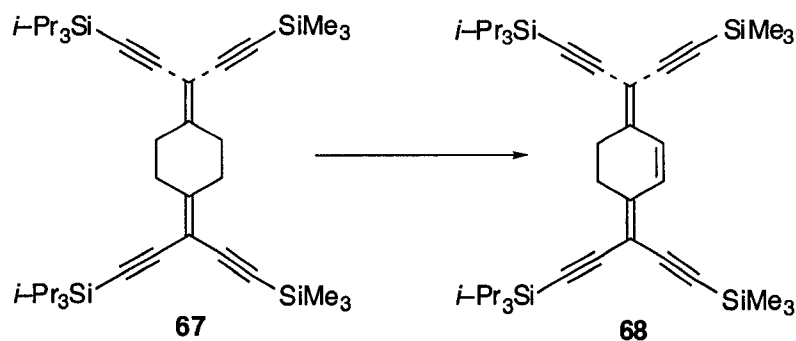
1,4-Bis[1-triisopropylsilyl-5-trimethylsilylpenta-1,4-diyne-3-ylidene]cyclohexane (67)



Triflate **66** (200 mg, 0.336 mmol) was cross-coupled with triisopropylsilylacetylene (0.185 mL, 147 mg, 0.806 mmol) in degassed THF (20 mL) in the presence of Pd(PPh₃)₄ (39 mg, 0.034 mmol), *i*-Pr₂NH (3 mL), CuI (19 mg, 0.11 mmol) for 2 h at rt as described in the general procedure. Flash column chromatography (hexanes/CH₂Cl₂ 5:1) afforded **67** (201 mg, 91%) as a light yellow solid as approximately 5.3:4.7 mixture of diastereomers. This compound was characterized as a mixture. Mp 104-106 °C. *R*_f = 0.3 (hexanes/CH₂Cl₂ 10:1). IR (CHCl₃, cast) 2943, 2865, 2150, 1598, 1463, 1249 cm⁻¹; ¹H NMR (400 MHz, CDCl₃) δ 2.64 (s, 8H), 1.09 (s, 21H), 1.08 (s, 21H), 0.19 (s, 9H), 0.18 (s, 9H); ¹³C NMR (100 MHz, CDCl₃, APT) δ 158.7, 158.5, 102.9, 102.8, 101.1, 101.0, 100.8, 100.7, 97.2, 97.1, 94.0 (2x), 31.6, 31.5 (2x), 31.4, 18.7 (2x), 11.4, 0.0. EIMS *m/z* 660.4 (M⁺, 70), 73.0

(TMS⁺, 100); HRMS calcd. for C₄₀H₆₈Si₄ (M⁺) 660.4398, found 660.4390. Anal. calcd. for C₄₀H₆₈Si₄: C, 72.73; H, 10.37. Found: C, 69.02; H, 10.17.

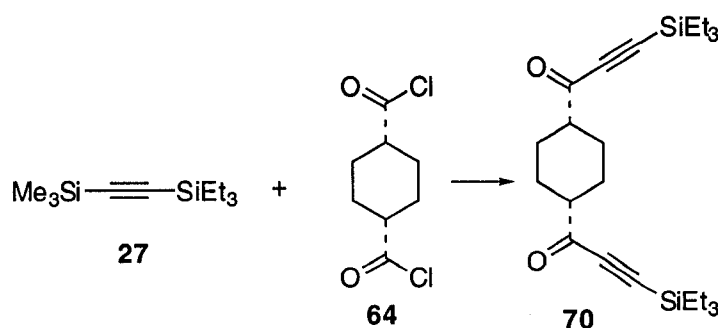
1,4-Bis[1-triisopropylsilyl-5-trimethylsilylpenta-1,4-diyne-3-ylidene]cyclohex-2-ene (68)



DDQ (1.63 g, 7.20 mmol) was added to a solution of **67** (1.19 g, 1.80 mmol) in anhydrous benzene (40 mL). The mixture was heated to reflux for 4 h and filtered after cooling. The solvent was evaporated *in vacuo* and the residue absorbed on Celite. Column chromatography (silica gel, hexanes) gave a yellow zone, evaporation of the solvent *in vacuo* yielded **68** (0.59 g, 50%) as a bright yellow solid as approximately 2.4:1.4:6.2 mixture of diastereomers. This compound was characterized as a mixture. Mp 98–100 °C. $R_f = 0.6$ (hexanes/CH₂Cl₂ 5:1). IR (CHCl₃, cast) 2960, 2865, 2149, 2063, 1651, 1462, 1260 cm⁻¹; ¹H NMR (400 MHz, CDCl₃) δ 6.96 (m, 2H), 2.72 (m, 4H), 1.09 (s, 21H), 1.08 (s, 21H), 0.22 (s, 9H), 0.21 (s, 9H); ¹³C NMR (100 MHz, CDCl₃, APT) δ 150.6, 150.5, 150.4, 130.5, 104.3, 104.2, 103.1, 103.0, 102.9, 102.5, 102.2, 102.1, 101.2, 100.1, 100.0, 99.5, 99.4, 97.2, 97.1, 29.9, 27.1, 27.0, 18.9 (3x), 11.6 (2x), 1.3, 0.1. EIMS m/z 658.4 (M⁺, 100); HRMS calcd. for C₄₀H₆₆Si₄

(M⁺) 658.4242, found 658.4225. Anal. calcd. for C₄₀H₆₆Si₄: C, 72.96; H, 10.10. Found: C, 72.74; H, 10.69.

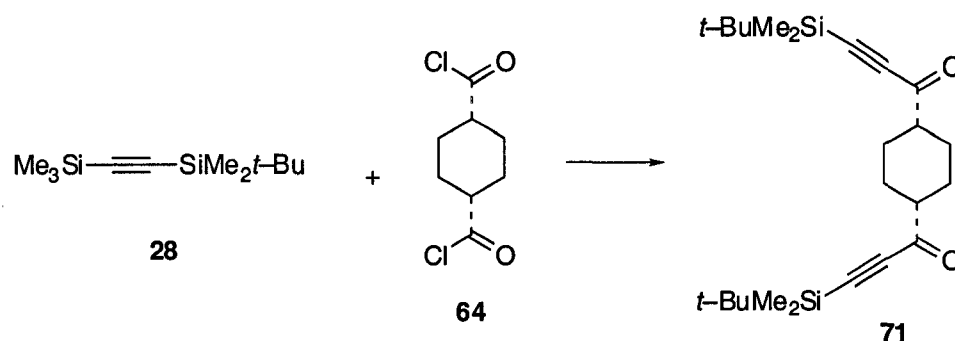
1,4-Bis(1-oxo-3-triethylsilylprop-2-yn)cyclohexane (70)



1-Triethylsilyl-2-trimethylsilylacetylene **27** (5.10 g, 24.0 mmol) was added under stirring to a solution of cyclohexane-1,4-dicarbonyl dichloride **64** (2.50 g, 12.0 mmol) in CH_2Cl_2 (100 mL) at 0 °C under nitrogen. Aluminium chloride (3.21 g, 24.0 mmol) was slowly added in portions, while the solution was stirred at 0 °C. The solution was kept stirring at 0 °C for 3 h, then poured into a mixture of 10% HCl solution (100 mL) and ice (100 g). The aqueous layer was extracted with diethyl ether (3 x 50 mL) and the combined organic phases were subsequently washed with saturated aqueous NaHCO_3 and saturated aqueous NaCl , and then dried with MgSO_4 . Solvent removal and purification by column chromatography (silica gel, hexanes/ CH_2Cl_2 2:1) afforded **70** (3.20 g, 64%) as a yellow oily solid as approximately 6:4 mixture of diastereomers. This compound was characterized as a mixture. $R_f = 0.3:0.4$ (hexanes/ CH_2Cl_2 2:1). IR (CH_2Cl_2 , cast) 2956, 2913, 2876, 2146, 1672, 1236, 1003 cm^{-1} ; ^1H NMR (500 MHz, CDCl_3) δ 2.46 (m, 1H), 2.35 (m, 1H), 2.15 (m, 2H), 1.98 (m, 2H), 1.74 (m, 2H), 1.44 (m, 2H), 0.99 (t, $^3J_{\text{H,H}} = 8.1$ Hz, 18H), 0.65 (q, $^3J_{\text{H,H}} = 8.1$ Hz, 12H); ^{13}C NMR

(125 MHz, CDCl₃) δ 189.9, 102.4, 102.3, 97.6, 97.2, 51.4, 49.2, 27.2, 25.1, 25.0, 7.3, 3.8. EIMS m/z 416.3 (M⁺, 0.74), 387.2 ([M - Et]⁺, 100); HRMS calcd. for C₂₄H₄₀O₂Si₂ (M⁺) 416.2567, found 416.2590. Anal. calcd. for C₂₄H₄₀O₂Si₂: C, 69.25; H, 9.68. Found: C, 65.79; H, 8.55.

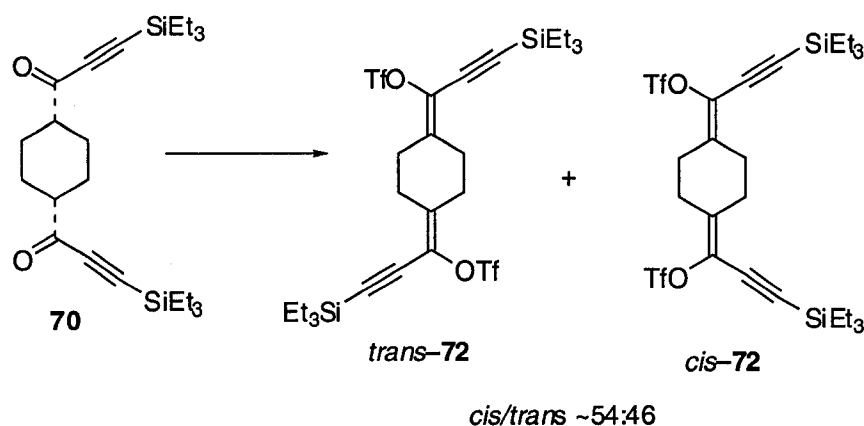
1,4-Bis(1-oxo-3-*tert*-butyldimethylsilylprop-2-ynyl)cyclohexane (71)



1-*Tert*-butyldimethylsilyl-2-trimethylsilylacetylene **28** (5.10 g, 24.0 mmol) was added under stirring to a solution of cyclohexane-1,4-dicarbonyl dichloride **64** (2.50 g, 12.0 mmol) in CH₂Cl₂ (100 mL) at 0 °C under nitrogen. Aluminium chloride (3.21 g, 24.0 mmol) was slowly added in portions, while the solution was stirred at 0 °C. The solution was kept stirring at 0 °C for 3 h, then poured into a mixture of 10% HCl solution (100 mL) and ice (100 g). The aqueous layer was extracted with diethyl ether (3 x 50 mL) and the combined organic phases were subsequently washed with saturated aqueous NaHCO₃ and saturated aqueous NaCl, and then dried with MgSO₄. Solvent removal and purification by column chromatography (silica gel, hexanes/CH₂Cl₂ 2:1) afforded **71** (3.10 g, 62%) as a colorless solid as approximately 8:2 mixture of diastereomers. This compound was characterized as a mixture. Mp 126–128 °C. R_f = 0.5:0.6 (hexanes/CH₂Cl₂ 2:1). IR (CHCl₃, cast) 2929, 2857, 2146, 1668, 1253, 1114

cm⁻¹; ¹H NMR (400 MHz, CDCl₃) δ 2.35 (m, 2H), 2.14 (m, 3H), 1.97 (m, 1H), 1.75 (m, 1H), 1.42 (m, 3H), 0.95 (s, 18H), 0.15 (s, 12H); ¹³C NMR (100 MHz, CDCl₃) δ 188.8, 101.6, 97.6, 51.7, 27.4, 25.9, 24.4, 16.8. EIMS *m/z* 359.2 ([M - *t*-Bu], 50)⁺; HRMS calcd. for C₂₀H₃₁O₂Si₂ ([M⁺ - *t*-Bu]) 359.1863, found 359.1861. Anal. calcd. for C₂₄H₄₀O₂Si₂: C, 69.25; H, 9.68. Found: C, 69.97; H, 9.00.

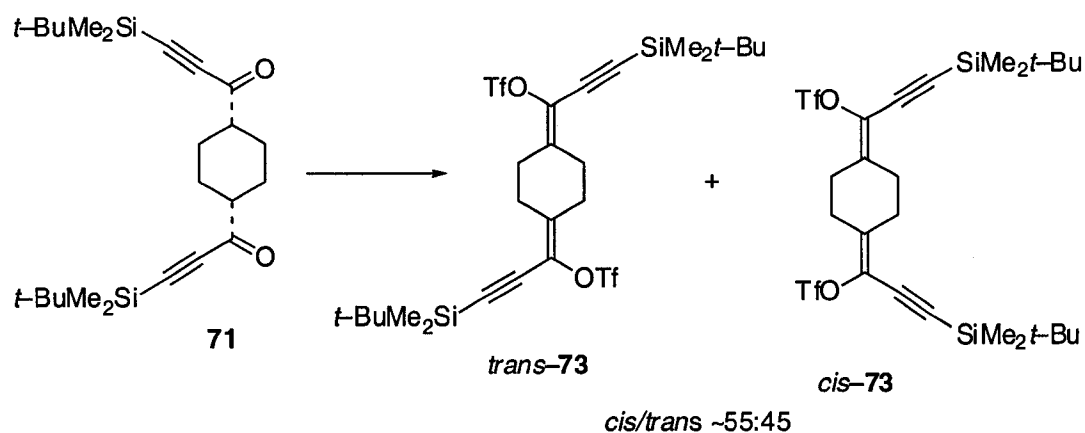
1,4-Bis(1-trifluoromethanesulfonyloxy-3-triethylsilylprop-2-yn-1-ylidene)cyclohexane (72)



Reaction of **70** (2.85 g, 6.82 mmol) with trifluoromethane-sulfonic anhydride (3.50 mL, 5.78 g, 20.5 mmol) and 2,6-di-*t*-butyl-4-methyl pyridine (4.21 g, 20.5 mmol) in CH₂Cl₂ (100 mL) was conducted under nitrogen for 3 days. The CH₂Cl₂ was removed *in vacuo* and the residue extracted with hexanes. The organic solution was washed with 10% HCl, saturated aqueous NaHCO₃, saturated aqueous NaCl, and dried with MgSO₄. Solvent removal and purification by column chromatography (silica gel, hexanes/CH₂Cl₂ 2:1) afforded **72** (3.33 g, 72%) as a colorless solid (mixture of

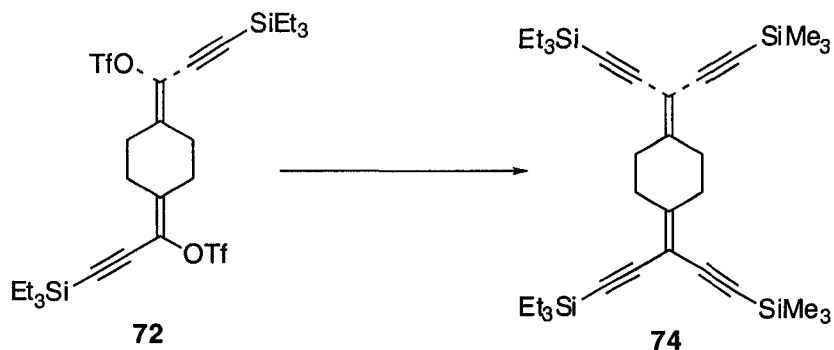
isomers). Characterized as a pure diastereomer, *trans*-72: Mp 94–96 °C. $R_f = 0.5$ (hexanes/ CH_2Cl_2 4:1). IR (CH_2Cl_2 , cast) 2959, 2914, 2878, 2150, 1651, 1419, 1205, 1138 cm^{-1} ; ^1H NMR (500 MHz, CDCl_3) δ 2.60 (s, 8H), 1.01 (t, $^3J_{\text{H,H}} = 8.2$ Hz, 18H), 0.68 (q, $^3J_{\text{H,H}} = 8.2$ Hz, 12H); ^{13}C NMR (125 MHz, CDCl_3) δ 140.4, 125.2, 118.3 (q, $^1J_{\text{C,F}} = 321.2$ Hz), 102.7, 94.5, 29.6, 27.4, 7.2, 3.9. EIMS m/z 680.2 (M^+ , 14); HRMS calcd. for $\text{C}_{26}\text{H}_{38}\text{O}_6\text{F}_6\text{Si}_2\text{S}_2$ (M^+) 680.1553, found 680.1561. Anal. calcd. for $\text{C}_{26}\text{H}_{38}\text{O}_6\text{F}_6\text{Si}_2\text{S}_2$: C, 45.90; H, 5.63. Found: C, 45.62; H, 5.75. Characterized as ~ 1:1 mixture by comparison to *trans*-72, (^1H and ^{13}C NMR) of *cis*-72: ^1H NMR (500 MHz, CDCl_3) δ 2.64 (s, 4H), 2.55 (s, 4H), 1.01 (t, $J = 8.1$ Hz, 18H), 0.68 (q, $J = 8.1$ Hz, 12H); ^{13}C NMR (125 MHz, CDCl_3) δ 140.3, 125.1, 118.3 (q, $J = 321.2$ Hz), 102.6, 94.6, 29.8, 26.9, 7.2, 3.7.

1,4-Bis(1-trifluoromethanesulfonyloxy-3-*tert*-butyldimethylsilylprop-2-yn-1-ylidenyl)cyclohexane (73)



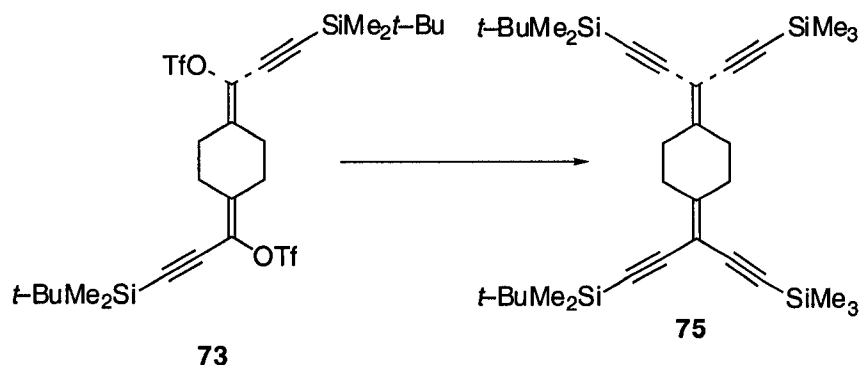
Reaction of **71** (2.86 g, 6.88 mmol) with trifluoromethane–sulfonic anhydride (3.50 mL, 5.82 g, 20.6 mmol) and 2,6–di-*t*-butyl-4-methyl pyridine (4.23 g, 20.6 mmol) in CH₂Cl₂ (100 mL) was conducted under nitrogen for 3 days. The CH₂Cl₂ was removed *in vacuo* and the residue extracted with hexanes. The organic solution was washed with 10% HCl, saturated aqueous NaHCO₃, saturated aqueous NaCl, and dried with MgSO₄. Solvent removal and purification by column chromatography (silica gel, hexanes/CH₂Cl₂ 2:1) afforded **73** (3.09 g, 66%) as a colorless solid (mixture of isomers). Characterized as a pure diastereomer, *cis*-**73**: Mp 93–94 °C. *R_f* = 0.3 (hexanes/CH₂Cl₂ 4:1). IR (CH₂Cl₂, cast) 2931, 2858, 2150, 1650, 1422, 1213, 1138 cm⁻¹; ¹H NMR (400 MHz, CDCl₃) δ 2.61 (s, 4H), 2.52 (s, 4H), 0.95 (s, 18H), 0.15 (s, 12H); ¹³C NMR (100 MHz, CDCl₃) δ 140.4, 125.0, 119.2 (q, ¹*J*_{C,F} = 332.2 Hz), 103.6, 94.2, 29.8, 26.9, 25.9, 16.5. EIMS *m/z* 115.1 (*t*-BuMe₂Si⁺, 2); HRMS calcd. for C₆H₁₅Si (*t*-BuMe₂Si⁺) 115.0943, found 115.0948. ESIMS (pos) *m/z* (MeOH/toluene 3:1): 703.1 ([M + Na⁺]⁺, 100). Anal. calcd. for C₂₆H₃₈O₆F₆Si₂S₂: C, 45.90; H, 5.63. Found: C, 45.46; H, 5.59. Characterized as ~ 1:1 mixture by comparison to *cis*-**73**, of *trans*-**73**: ¹H NMR (400 MHz, CDCl₃) δ 2.58 (s, 8H), 0.96 (s, 18H), 0.16 (s, 12H); ¹³C NMR (100 MHz, CDCl₃) δ 140.5, 125.1, 119.2 (q, ¹*J*_{C,F} = 332.2 Hz), 103.2, 94.3, 29.9, 27.0, 26.0, 16.6.

**1,4-Bis[1-triethylsilyl-5-trimethylsilylpenta-1,4-diyne-3-ylidenyl]-
cyclohexane (74)**



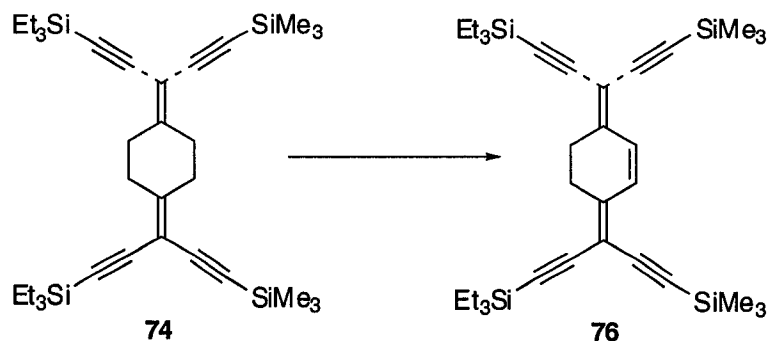
Triflate **72** (2.77 g, 4.07 mmol) was cross-coupled with trimethylsilylacetylene (2.30 mL, 1.59 g, 16.3 mmol) in degassed THF (30 mL) in the presence of Pd(PPh₃)₄ (0.47 g, 0.41 mmol), *i*-Pr₂NH (5 mL), CuI (0.23 g, 1.2 mmol) for 2 h at rt as described in the general procedure. Flash column chromatography (hexanes/CH₂Cl₂ 2:1) afforded **74** (2.16 g, 92%) as a light yellow solid (mixture of isomers). This compound was characterized as a mixture. Mp 106-108 °C. *R_f* = 0.7 (hexanes/CH₂Cl₂ 4:1). IR (CH₂Cl₂, cast) 2957, 2911, 2876, 2149, 1591, 1458, 1249 cm⁻¹; ¹H NMR (400 MHz, CDCl₃) δ 2.63 (s, 8H), 0.99 (t, ³*J*_{H,H} = 8.0 Hz, 18H), 0.62 (q, ³*J*_{H,H} = 8.0 Hz, 12H), 0.18 (s, 18H); ¹³C NMR (100 MHz, CDCl₃, APT) δ 159.1, 159.0, 101.9, 100.9, 100.8, 100.5, 97.2, 97.1, 94.9, 31.4, 31.3, 31.2, 7.4 (2x), 4.4, -0.1. EIMS *m/z* 576.3 (M⁺, 64), 73.0 (TMS⁺, 100); HRMS calcd. for C₃₄H₅₆Si₄ (M⁺) 576.3459, found 576.3444. Anal. calcd. for C₃₄H₅₆Si₄: C, 70.84; H, 9.79. Found: C, 70.52; H, 10.02.

1,4-Bis[1-*tert*-butyldimethylsilyl-5-trimethylsilylpenta-1,4-diyne-3-ylidenyl]cyclohexane (75)



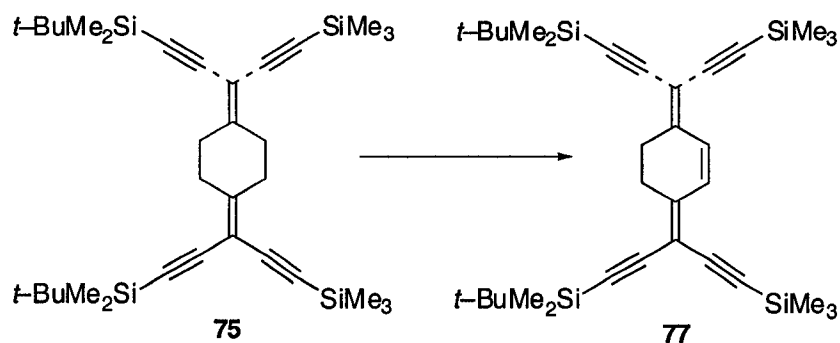
Triflate **73** (806 mg, 1.19 mmol) was cross-coupled with trimethylsilylacetylene (0.680 mL, 466 mg, 4.74 mmol) in degassed THF (20 mL) in the presence of Pd(PPh₃)₄ (137 mg, 0.119 mmol), *i*-Pr₂NH (5 mL), CuI (45 mg, 0.22 mmol) for 2 h at rt as described in the general procedure. Flash column chromatography (hexanes/CH₂Cl₂ 3:1) afforded **75** (622 mg, 91%) as a light yellow solid as approximately 5.3:4.7 mixture of diastereomers. This compound was characterized as a mixture. Mp 146-148 °C. *R_f* = 0.6 (hexanes/CH₂Cl₂ 3:1). IR (CHCl₃, cast) 2955, 2856, 2149, 1588, 1471, 1250 cm⁻¹; ¹H NMR (400 MHz, CDCl₃) δ 2.62 (s, 8H), 0.96 (s, 9H), 0.93 (s, 9H), 0.19 (s, 9H), 0.18 (s, 9H), 0.13 (s, 6H), 0.11 (s, 6H); ¹³C NMR (100 MHz, CDCl₃, APT) δ 159.1, 159.0, 101.3, 100.7, 100.6, 100.4, 97.2, 95.7, 31.4, 31.3 (2x), 31.2, 26.1, 16.8, -0.1, -0.5. EIMS *m/z* 576.3 (M⁺, 41), 73.0 (TMS⁺, 100); HRMS calcd. for C₃₄H₅₆Si₄ (M⁺) 576.3459, found 576.3460. Anal. calcd. for C₃₄H₅₆Si₄: C, 70.84; H, 9.79. Found: C, 70.38; H, 10.00.

**1,4-Bis[1-triethylsilyl-5-trimethylsilylpenta-1,4-diyne-3-ylidenyl]-
cyclohex-2-ene (76)**



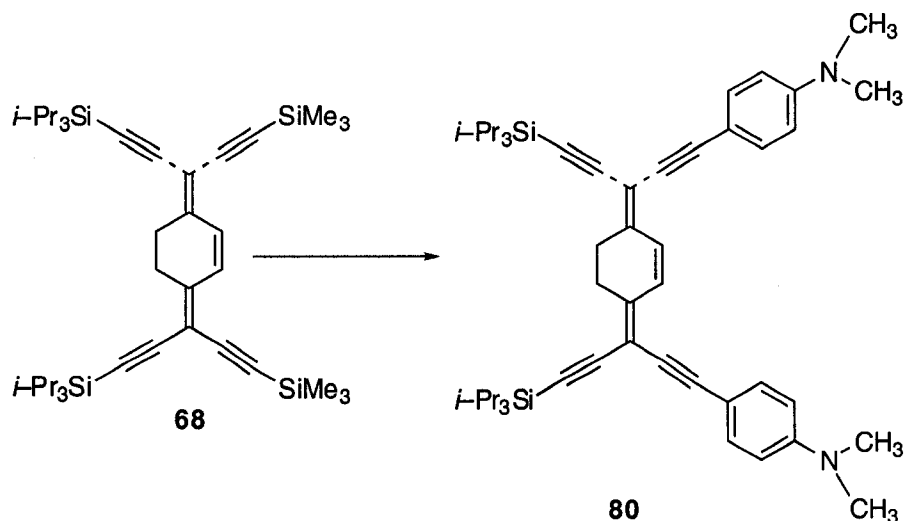
DDQ (1.65 g, 7.29 mmol) was added to a solution of **74** (1.05 g, 1.82 mmol) in anhydrous benzene (50 mL). The mixture was heated to reflux for 4 h and filtered after cooling. The solvent was evaporated *in vacuo* and the residue absorbed on Celite. Column chromatography (silica gel, hexanes) gave a yellow zone, evaporation of the solvent *in vacuo* yielded **76** (287 mg, 28%) as a bright yellow solid as approximately 5.1:4.9 mixture of diastereomers. This compound was characterized as a mixture. $R_f = 0.58$ (hexanes/ CH_2Cl_2 5:1). IR (CH_2Cl_2 , cast) 2956, 2875, 2145, 2126, 1652, 1456, 1212 cm^{-1} ; ^1H NMR (400 MHz, CDCl_3) δ 6.92 (m, 2H), 2.70 (2 x s, 4H), 1.01 (2 x t, $^3J_{\text{H,H}} = 8.0$ Hz, 18H), 0.64 (2 x q, $^3J_{\text{H,H}} = 8.0$ Hz, 12H), 0.20 (2 x s, 18H); ^{13}C NMR (100 MHz, CDCl_3 , APT) δ 150.8, 150.7, 130.3, 103.2, 102.7, 102.1, 101.9, 100.8, 99.9, 99.8, 97.7, 29.7, 26.8, 7.4 (2x), 4.4 (2x), -0.1. EIMS m/z 574.3 (M^+ , 92); HRMS calcd. for $\text{C}_{34}\text{H}_{54}\text{Si}_4$ (M^+) 574.3303, found 574.3323.

1,4-Bis[1-*tert*-butyldimethylsilyl-5-trimethylsilylpenta-1,4-diyne-3-ylidenyl]cyclohex-2-ene (77)



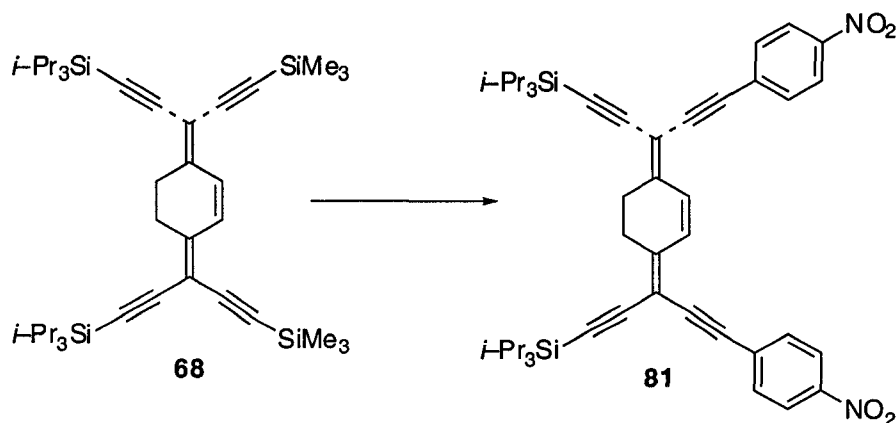
DDQ (306 mg, 1.35 mmol) was added to a solution of **75** (190 mg, 0.337 mmol) in anhydrous benzene (25 mL). The mixture was heated to reflux for 4 h and filtered after cooling; the solvent was evaporated in *vacuo* and the residue absorbed on Celite. Column chromatography (silica gel, hexanes) gave a yellow zone, evaporation of the solvent in *vacuo* yielded **77** (101 mg, 52%) as a bright yellow solid as approximately 4.9:1.6:3.5 mixture of diastereomers. This compound was characterized as a mixture. Mp 122–124 °C. $R_f = 0.5$ (hexanes/ CH_2Cl_2 5:1). IR (CH_2Cl_2 , cast) 2927, 2855, 2142, 2124, 1462, 1249 cm^{-1} ; ^1H NMR (500 MHz, CDCl_3) δ 6.92 (m, 2H), 2.70 (m, 4H), 0.96 (s, 9H), 0.95 (s, 9H), 0.22 (s, 9H), 0.21 (s, 9H), 0.16 (s, 6H), 0.15 (s, 6H); ^{13}C NMR (125 MHz, CDCl_3 , APT) δ 150.7, 150.6, 130.3, 102.6, 102.5, 102.0, 101.9, 101.2, 100.8, 100.7, 100.6, 100.0, 99.9, 98.6, 98.5, 29.8, 26.9 (2x), 26.2 (3x), 16.9, 1.1, 0.0, -4.5. EIMS m/z 574.3 (M^+ , 100); HRMS calcd. for $\text{C}_{34}\text{H}_{54}\text{Si}_4$ (M^+) 574.3302, found 574.3298. Anal. calcd. for $\text{C}_{34}\text{H}_{54}\text{Si}_4$: C, 71.09; H, 9.48. Found: C, 68.03; H, 9.81.

1,4-Bis[1-{4-(dimethylamino)phenyl}-5-triisopropylsilylpenta-1,4-diyne-3-ylidene]cyclohex-2-ene (80)



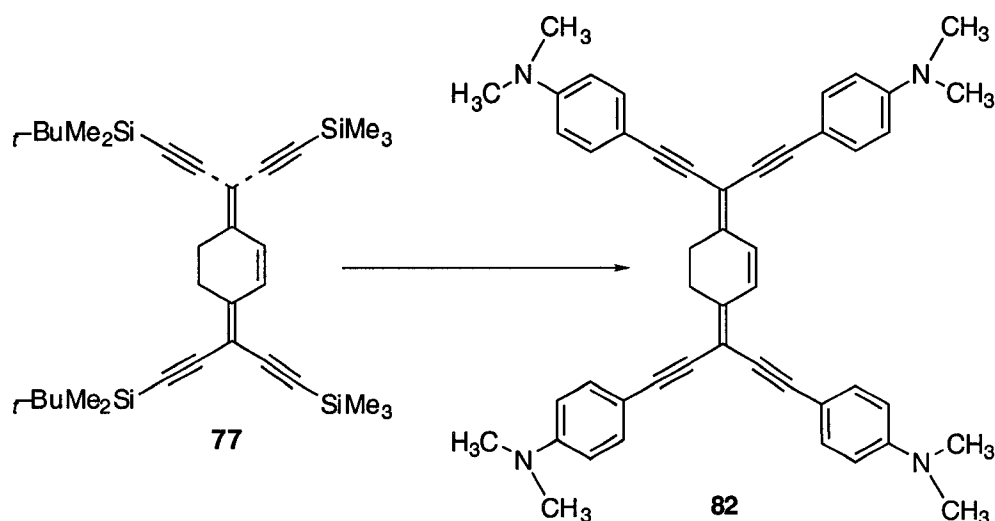
Compound **68** (30 mg, 0.046 mmol) was selectively desilylated with K_2CO_3 (3 mg, 0.02 mmol) and cross-coupled with *p*-iodo-*N,N*-dimethylaniline (23 mg, 0.092 mmol) in degassed Et_3N (10 mL) in the presence of $\text{PdCl}_2(\text{PPh}_3)_2$ (4 mg, 0.005 mmol), and CuI (3 mg, 0.01 mmol) for 24 h at rt as described in the general procedure. The Et_3N was removed *in vacuo* and the residue was passed through a plug (silica gel, CH_2Cl_2). Solvent removal and purification by column chromatography (silica gel, hexanes/ CH_2Cl_2 2:1) afforded **80** (7 mg, 20%) as deep red needles as approximately 3.1:3.3:3.6 mixture of diastereomers. This compound was characterized as a mixture. $R_f = 0.4$ (hexanes/ CH_2Cl_2 1:1). IR (μscope) 2961, 2925, 2865, 2185, 2136, 1608, 1547, 1520, 1462, 1261 cm^{-1} . $^1\text{H NMR}$ (500 MHz, CDCl_3) δ 7.34 (m, 4H), 7.02 (m, 2H), 6.65 (m, 4H), 2.98 (2 x s, 12H), 2.81 (m, 4H), 1.12 (3 x s, 42H). ESIMS m/z (MeOH/toluene 3:1): 751 ($[\text{M} + \text{H}]^+$, 38).

1,4-Bis[1-(4-nitrophenyl)-5-triisopropylsilylpenta-1,4-diyne-3-ylidene]cyclohex-2-ene (81)



Compound **68** (54 mg, 0.083 mmol) was cross-coupled with *p*-iodonitrobenzene (34 mg, 0.14 mmol) in the presence of TBAF (0.2 mL), Pd(PPh₃)₄ (10 mg, 0.0081 mmol), CuI (2 mg, 0.02 mmol), and DMF (10 mL) for 24 h, at rt. Solvent removal and purification by column chromatography (silica gel, hexanes/CH₂Cl₂ 2:1) afforded **81** (16 mg, 25%) as a deep red solid as approximately 28:28:44 mixture of diastereomers. This compound was characterized as a mixture. Mp 174–176 °C (Decomp.). *R_f* = 0.4 (hexanes/CH₂Cl₂ 1:1). IR (CH₂Cl₂, cast) 3195, 2922, 2852, 2194, 2138, 1654, 1593, 1517, 1466, 1340 cm⁻¹. ¹H NMR (500 MHz, CDCl₃) δ 8.21 (m, 4H), 7.60 (m, 4H), 7.09 (m, 2H), 2.87 (s, 4H), 1.13 (3 x s, 42H); ¹³C NMR (125 MHz, CDCl₃, APT) δ 150.8, 147.0, 133.2, 132.1, 132.0 (2x), 130.9, 130.6, 129.8, 123.6 (3x), 102.7, 101.8, 98.2, 94.3, 92.5, 91.2, 27.2, 18.8 (2x), 11.4. ESIMS (pos) *m/z* (MeOH/toluene 3:1): 756.4 (M⁺, 100). HRMS calcd. for C₄₆H₅₆N₂O₄Si₂ (M⁺) 756.3773 found 756.3774

1,4-Bis{1,5-bis-[4-(dimethylamino)phenyl]penta-1,4-diyne-3-ylidenyl}cyclohex-2-ene (82)



Compound **77** (138 mg, 0.241 mmol) was desilylated with TBAF (1.93 mL, 0.482 mmol) and cross-coupled with *p*-iodo-*N,N*-dimethylaniline (238 mg, 0.964 mmol) in degassed THF (20 mL) in the presence of Et₃N (5 mL), Pd(PPh₃)₄ (56 mg, 0.048 mmol), and CuI (18 mg, 0.096 mmol) for 24 h, under reflux as described in the general procedure. The Et₃N was removed *in vacuo* and the residue was passed through a plug (silica gel, CH₂Cl₂). Solvent removal and purification by column chromatography (silica gel, hexanes/CH₂Cl₂ 2:1) afforded **82** (8 mg, 5%) as deep red needles. *R*_f = 0.1 (hexanes/CH₂Cl₂ 2:1). IR (CH₂Cl₂, cast) 2955, 2924, 2854, 2175, 1604, 1520, 1436 cm⁻¹. ¹H NMR (300 MHz, CDCl₃) δ 7.41 (m, 8H), 7.08 (s, 2H), 6.66 (m, 8H), 2.98 (2 x s, 24H), 2.89 (s, 4H). ESIMS (pos) *m/z* (MeOH/toluene 3:1): 679.4 ([M + H]⁺, 100). HRMS calcd. for C₄₈H₄₇N₄ ([M + H]⁺)⁺ 679.3795, found 679.3804.

References

- (1) Dawson, D. J.; Frazier, J. D.; Brock, P. J.; Twieg, R. J. *Polymers for High Technology*; ACS: Washington, D.C., **1987**; Vol. 346, page 445.
- (2) Brandsma, L. *Preparative Acetylene Chemistry*; 2nd ed.; Elsevier Science: Amsterdam, 1998.
- (3) Zhao, Y. Cross-conjugated Enyne Oligomers: Synthesis, Properties, and Nonlinear Optical Investigations. Ph.D. Thesis, University of Alberta, Edmonton, AB, June 2002.
- (4) Perkins, M. V.; Kitching, W.; Konig, W. A.; Drew, R. A. I. *J. Chem. Soc., Perkin Trans. 1* **1990**, 2501-2506.
- (5) Chiellini, E.; Galli, G.; Carrozzino, S.; Gallot, B. *Macromolecules* **1990**, *23*, 2106-2112.
- (6) Alekperov, R. K.; Gasanov, V. S.; Guseinov, II *Zhur. Org. Khim.* **1977**, *13*, 2311-2316.
- (7) Karimi, B.; Maleki, W. *Tetrahedron Lett.* **2002**, *43*, 5353-5355.
- (8) Eastmond, R.; Walton, D. R. M. *Tetrahedron* **1972**, *28*, 4591-4599.
- (9) Neidlein, R.; Winter, M. *Synthesis* **1998**, 1362-1366.
- (10) Hopf, H.; Kampen, J.; Bubenitschek, P.; Jones, P. G. *Eur. J. Org. Chem.* **2002**, 1708-1721.

Appendix

1. Crystal Structure Data for Triflate 66a

For details of the X-ray structure contact Dr. Robert McDonald, X-ray crystallography laboratory, University of Alberta.

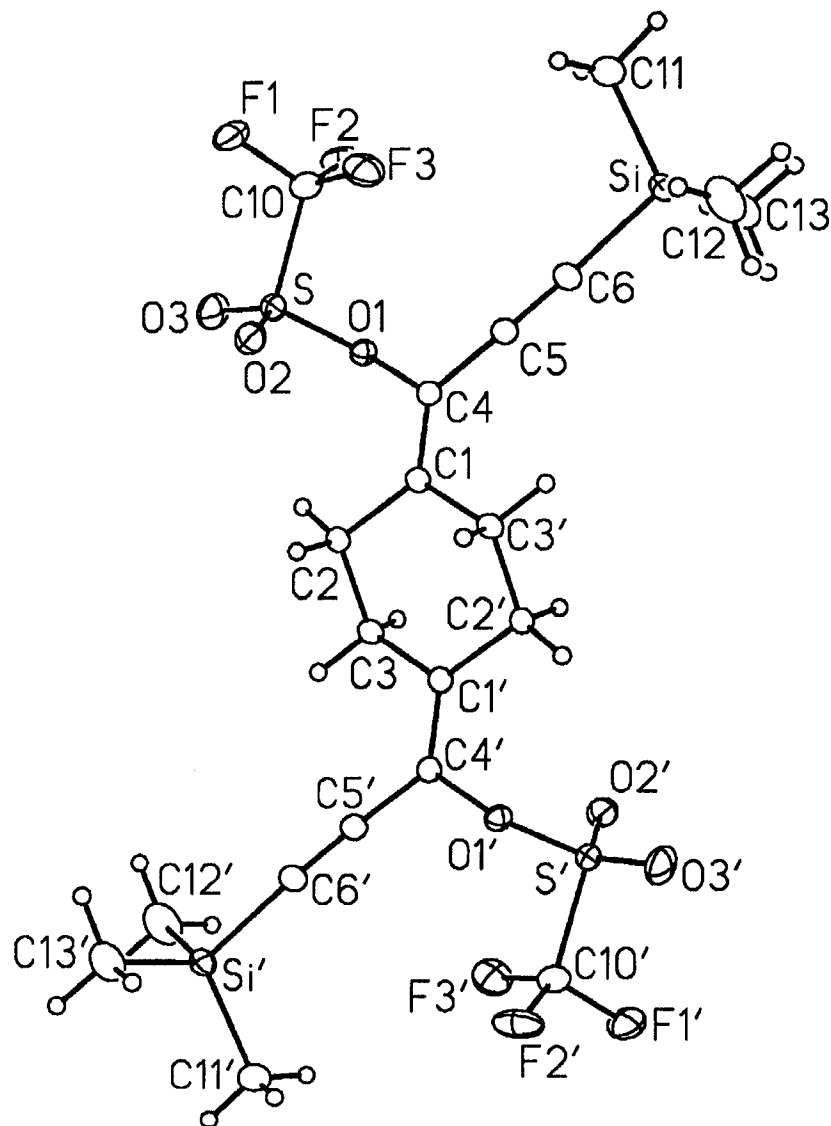


Fig. A.1 Perspective view of the Triflate **66a** molecule showing the atom labelling scheme. Non-hydrogen atoms are represented by Gaussian ellipsoids at the 20%

probability level. Hydrogen atoms are shown with arbitrarily small thermal parameters. Primed atoms are related to unprimed ones via the crystallographic inversion center (0, 0, 0) at the center of the cyclohexane ring.

Table 1. Crystallographic Experimental Details

A. Crystal Data

formula	$C_{20}H_{22}F_6O_6S_2Si_2$
formula weight	596.71
crystal dimensions (mm)	$0.90 \times 0.19 \times 0.11$
crystal system	monoclinic
space group 14])	$P2_1/n$ (an alternate setting of $P2_1/c$ [No. 14])
unit cell parameters ^a	
a (Å)	14.182 (2)
b (Å)	6.3369 (9)
c (Å)	15.707 (2)
β (deg)	93.439 (3)
V (Å ³)	1409.0 (3)
Z	2
ρ_{calcd} (g cm ⁻³)	1.406
μ (mm ⁻¹)	0.346

B. Data Collection and Refinement Conditions

diffractometer	Bruker PLATFORM/SMART 1000 CCD ^b
radiation (λ [Å])	graphite-monochromated Mo K α (0.71073)
temperature (°C)	-80
scan type	ω scans (0.2°) (25 s exposures)
data collection 2θ limit (deg)	52.84

total data collected	7300 ($-10 \leq h \leq 17, -7 \leq k \leq 7, -19 \leq l \leq 19$)
independent reflections	2866 ($R_{\text{int}} = 0.0213$)
number of observed reflections (<i>NO</i>)	2505 [$F_o^2 \geq 2\sigma(F_o^2)$]
structure solution method	direct methods (<i>SHELXS-86</i> ^c)
refinement method	full-matrix least-squares on F^2 (<i>SHELXL-93</i> ^d)
absorption correction method	empirical (<i>SADABS</i>)
range of transmission factors	0.9630–0.7462
data/restraints/parameters	2866 [$F_o^2 \geq -3\sigma(F_o^2)$] / 0 / 163
goodness-of-fit (<i>S</i>) ^e	1.052 [$F_o^2 \geq -3\sigma(F_o^2)$]
final <i>R</i> indices ^f	
R_1 [$F_o^2 \geq 2\sigma(F_o^2)$]	0.0359
wR_2 [$F_o^2 \geq -3\sigma(F_o^2)$]	0.1010
largest difference peak and hole	0.364 and $-0.333 \text{ e } \text{\AA}^{-3}$

^aObtained from least-squares refinement of 4875 reflections with $5.20^\circ < 2\theta < 52.84^\circ$.

^bPrograms for diffractometer operation, data collection, data reduction and absorption correction were those supplied by Bruker.

^cSheldrick, G. M. *Acta Crystallogr.* **1990**, *A46*, 467–473.

^dSheldrick, G. M. *SHELXL-93*. Program for crystal structure determination. University of Göttingen, Germany, 1993. Refinement on F_o^2 for all reflections (all of these having $F_o^2 \geq -3\sigma(F_o^2)$). Weighted *R*-factors wR_2 and all goodnesses of fit *S* are based on F_o^2 ; conventional *R*-factors R_1 are based on F_o , with F_o set to zero for negative F_o^2 . The observed criterion of $F_o^2 > 2\sigma(F_o^2)$ is used only for calculating R_1 , and is not relevant to the choice of reflections for refinement. *R*-factors based on F_o^2 are statistically about twice as large as those based on F_o , and *R*-factors based on ALL data will be even larger.

^e $S = [\sum w(F_o^2 - F_c^2)^2 / (n - p)]^{1/2}$ (n = number of data; p = number of parameters varied; $w = [\sigma^2(F_o^2) + (0.0518P)^2 + 0.5626P]^{-1}$ where $P = [\text{Max}(F_o^2, 0) + 2F_c^2]/3$).

^f $R_1 = \sum ||F_o| - |F_c|| / \sum |F_o|$; $wR_2 = [\sum w(F_o^2 - F_c^2)^2 / \sum w(F_o^4)]^{1/2}$.

Table 2. Atomic Coordinates and Equivalent Isotropic Displacement Parameters

Atom	<i>x</i>	<i>y</i>	<i>z</i>	$U_{\text{eq}}, \text{\AA}^2$
S	0.22845(3)	0.47863(7)	-0.06654(3)	0.03731(14)*
Si	-0.08730(4)	0.61988(8)	-0.32599(3)	0.03940(16)*
F1	0.32817(9)	0.6906(3)	-0.16760(11)	0.0782(5)*
F2	0.19714(12)	0.8377(2)	-0.14191(10)	0.0766(5)*
F3	0.19907(11)	0.5781(3)	-0.22653(7)	0.0716(4)*
O1	0.11990(8)	0.49260(17)	-0.05060(7)	0.0332(3)*
O2	0.25337(10)	0.2774(2)	-0.09479(10)	0.0527(4)*
O3	0.27545(12)	0.5790(3)	0.00364(10)	0.0665(5)*
C1	0.04290(12)	0.1561(3)	-0.05265(10)	0.0304(3)*
C2	0.09483(12)	0.0852(3)	0.02864(10)	0.0337(4)*
C3	0.02598(13)	0.0011(3)	0.09252(10)	0.0339(4)*
C4	0.05488(11)	0.3416(3)	-0.08973(10)	0.0303(3)*
C5	0.00678(12)	0.4212(3)	-0.16538(10)	0.0348(4)*
C6	-0.03157(14)	0.4956(3)	-0.22878(11)	0.0400(4)*
C10	0.23867(14)	0.6595(3)	-0.15653(13)	0.0449(4)*
C11	-0.00241(18)	0.8122(5)	-0.36476(17)	0.0729(7)*
C12	-0.1172(2)	0.4120(5)	-0.40391(16)	0.0781(8)*
C13	-0.19374(18)	0.7613(5)	-0.29268(16)	0.0694(7)*

Anisotropically-refined atoms are marked with an asterisk (*). The form of the anisotropic displacement parameter is: $\exp[-2\pi^2(h^2a^{*2}U_{11} + k^2b^{*2}U_{22} + l^2c^{*2}U_{33} + 2klb^{*c^{*}}U_{23} + 2hla^{*c^{*}}U_{13} + 2hka^{*b^{*}}U_{12})]$.

Table 3. Selected Interatomic Distances (Å)

Atom1	Atom2	Distance
S	O1	1.5769(13)
S	O2	1.4023(15)
S	O3	1.4057(15)
S	C10	1.832(2)
Si	C6	1.8525(18)
Si	C11	1.842(2)
Si	C12	1.831(3)
Si	C13	1.858(2)
F1	C10	1.306(2)
F2	C10	1.301(2)
F3	C10	1.310(2)
O1	C4	1.4409(19)
C1	C2	1.504(2)
C1	C3'	1.505(2)
C1	C4	1.327(2)
C2	C3	1.537(2)
C4	C5	1.426(2)
C5	C6	1.202(2)

Table 4. Selected Interatomic Angles (deg)

Atom1	Atom2	Atom3	Angle
O1	S	O2	111.61(7)
O1	S	O3	105.76(9)
O1	S	C10	102.16(8)
O2	S	O3	122.89(11)
O2	S	C10	106.95(9)
O3	S	C10	105.43(10)
C6	Si	C11	107.39(10)
C6	Si	C12	108.38(10)
C6	Si	C13	106.67(10)
C11	Si	C12	112.64(15)
C11	Si	C13	109.40(14)
C12	Si	C13	112.08(14)
S	O1	C4	120.06(10)
C2	C1	C3'	115.35(14)
C2	C1	C4	124.62(15)
C3'	C1	C4	120.03(14)
C1	C2	C3	111.10(14)
C1'	C3	C2	112.32(13)
O1	C4	C1	119.77(14)
O1	C4	C5	112.47(14)
C1	C4	C5	127.69(15)
C4	C5	C6	177.34(19)
Si	C6	C5	177.60(17)
S	C10	F1	108.65(14)
S	C10	F2	110.44(13)
S	C10	F3	110.58(14)
F1	C10	F2	110.25(18)
F1	C10	F3	108.60(17)
F2	C10	F3	108.31(18)

Primed atoms are related to unprimed ones via the crystallographic inversion center (0, 0, 0).

Table 5. Torsional Angles (deg)

Atom1	Atom2	Atom3	Atom4	Angle
O2	S	O1	C4	-19.95(14)
O3	S	O1	C4	-155.89(13)
C10	S	O1	C4	94.01(13)
O1	S	C10	F1	169.52(14)
O1	S	C10	F2	48.49(17)
O1	S	C10	F3	-71.39(15)
O2	S	C10	F1	-73.13(17)
O2	S	C10	F2	165.84(15)
O2	S	C10	F3	45.96(16)
O3	S	C10	F1	59.18(17)
O3	S	C10	F2	-61.86(18)
O3	S	C10	F3	178.27(15)
C11	Si	C6	C5	21(4)
C12	Si	C6	C5	143(4)
C13	Si	C6	C5	-96(4)
S	O1	C4	C1	84.13(17)
S	O1	C4	C5	-98.55(15)
C3'	C1	C2	C3	-50.7(2)
C4	C1	C2	C3	129.88(17)
C2	C1	C3'	C2'	51.3(2)
C4	C1	C3'	C2'	-129.25(17)
C2	C1	C4	O1	-1.5(2)
C2	C1	C4	C5	-178.39(16)
C3'	C1	C4	O1	179.09(14)
C3'	C1	C4	C5	2.2(3)
C1	C2	C3	C1'	49.1(2)
O1	C4	C5	C6	4(4)
C1	C4	C5	C6	-179(100)
C4	C5	C6	Si	3(8)

Primed atoms are related to unprimed ones via the crystallographic inversion center (0, 0, 0).

Table 6. Least-Squares Planes

Plane	Coefficients ^a			Defining Atoms with Deviations (Å) ^b				
1	10.691(6)	-2.383(5)	-9.158(4)	0.578(2)				
					Si	-0.0033(9)	O1	-0.0069(5)
					C1	-0.0095(7)	C4	0.0162(14)
					C5	0.0050(16)	C6	0.0016(15)
2	10.749(11)	-2.431(15)	-8.99(2)	0.555(2)				
					C1		C2	C3'
3	-5.663(18)	5.791(4)	1.52(2)	0.0				
					C2		C3	C2'
								C3'
Dihedral angle between planes 1 and 2:				0.81(19)°				
Dihedral angle between planes 1 and 3:				46.84(10)°				
Dihedral angle between planes 2 and 3:				46.23(18)°				

^aCoefficients are for the form $ax+by+cz = d$ where x , y and z are crystallographic coordinates.

^bPrimed atoms are related to unprimed ones via the crystallographic inversion center (0, 0, 0).

2. NMR Spectra

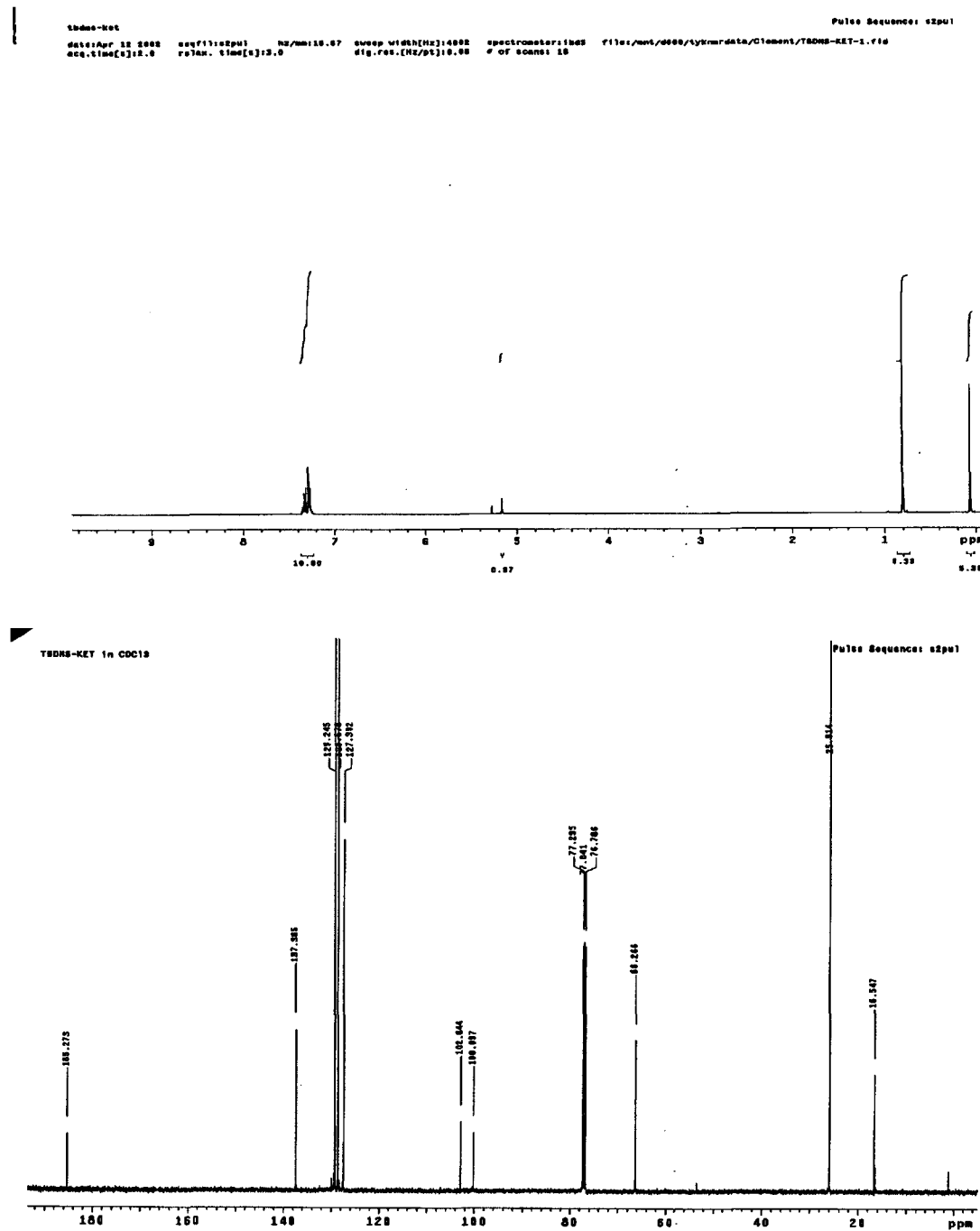


Fig. A.2 ^1H and ^{13}C NMR spectra of compound 30

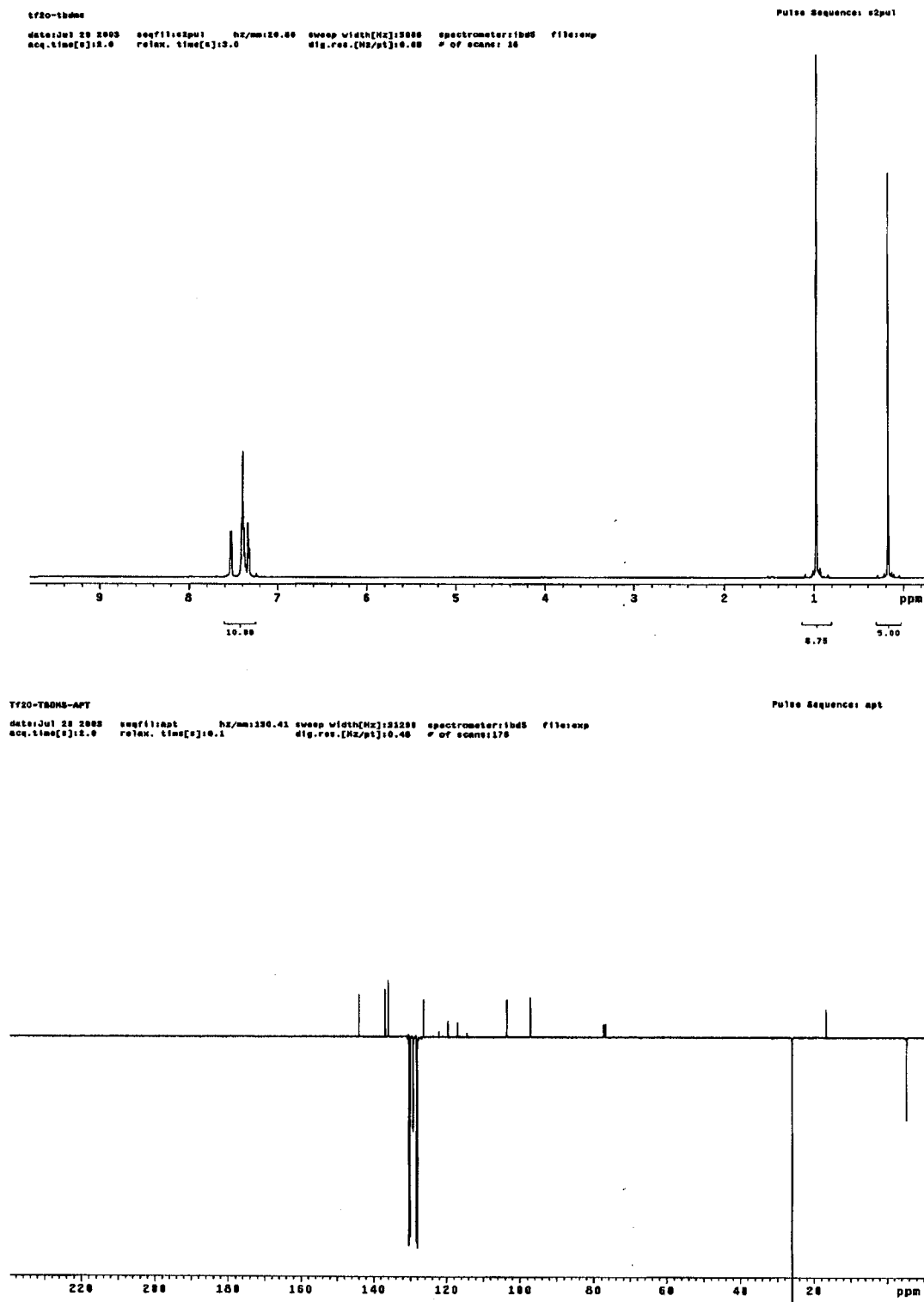


Fig. A.3 ^1H and ^{13}C NMR spectra of compound 32

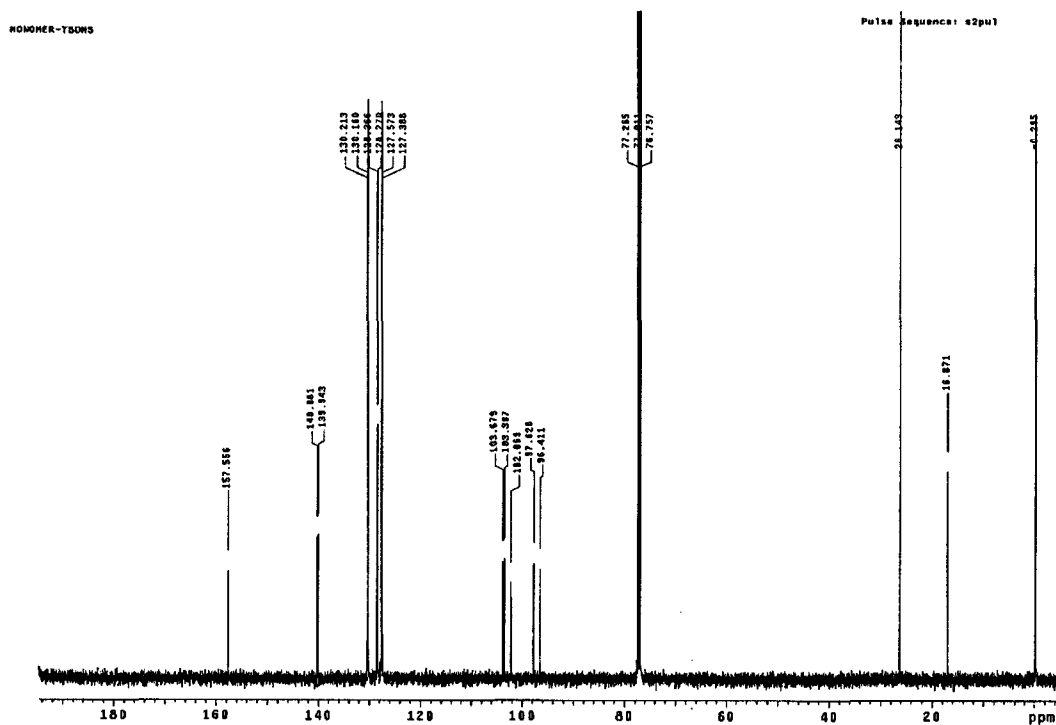
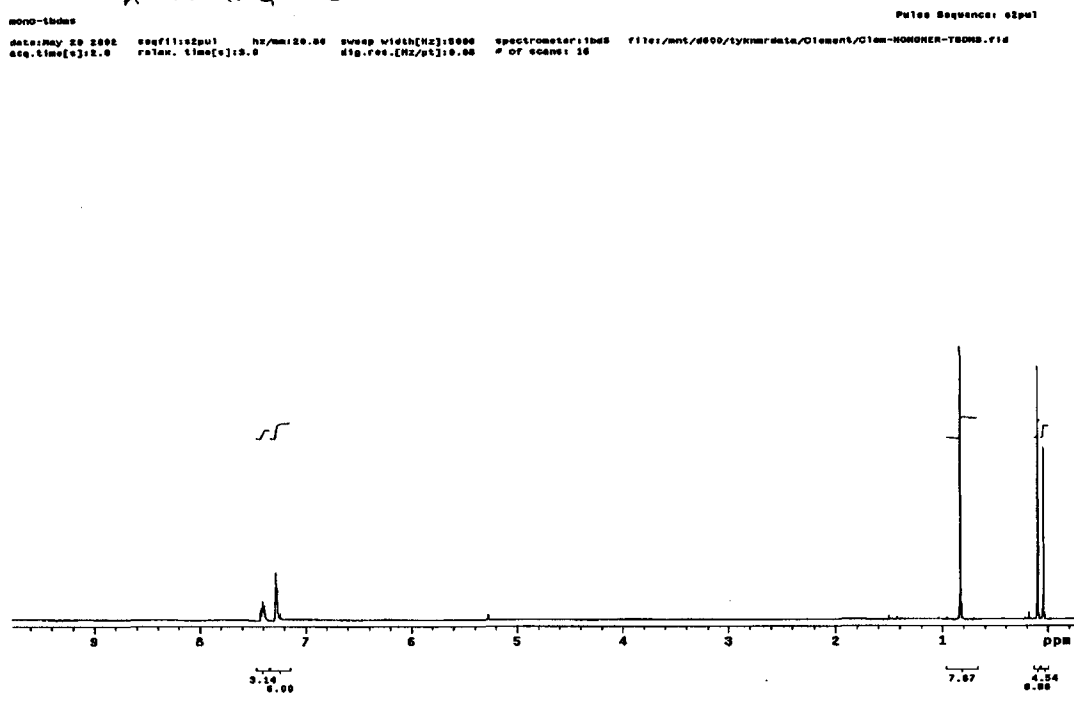


Fig. A.4 ^1H and ^{13}C NMR spectra of compound 34

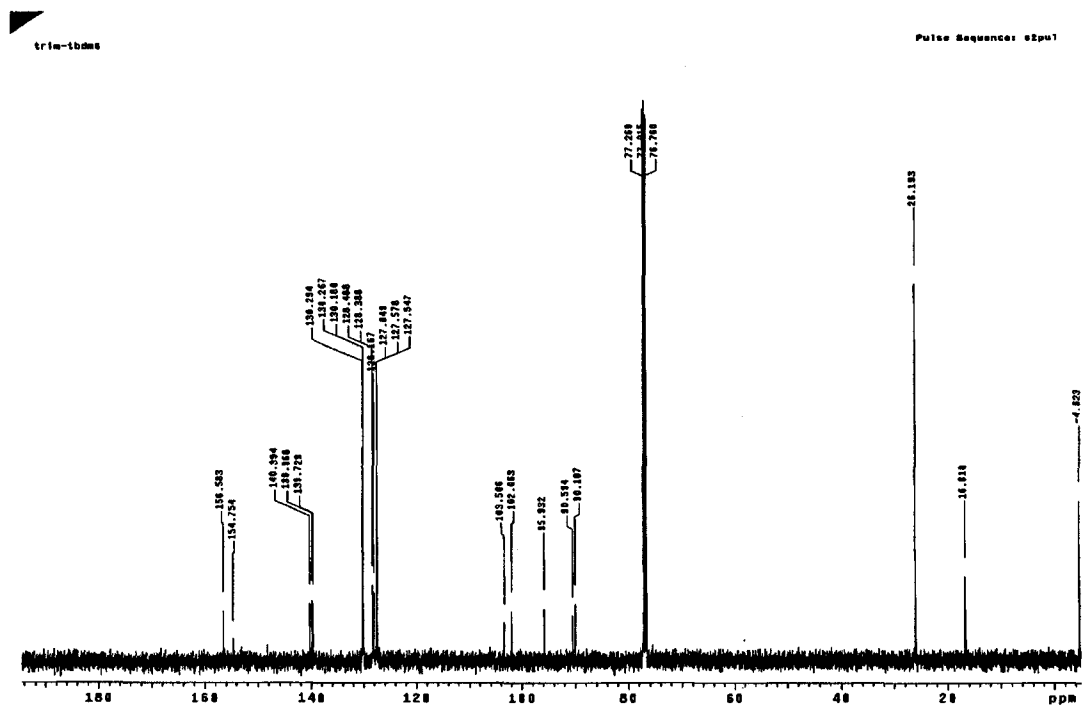
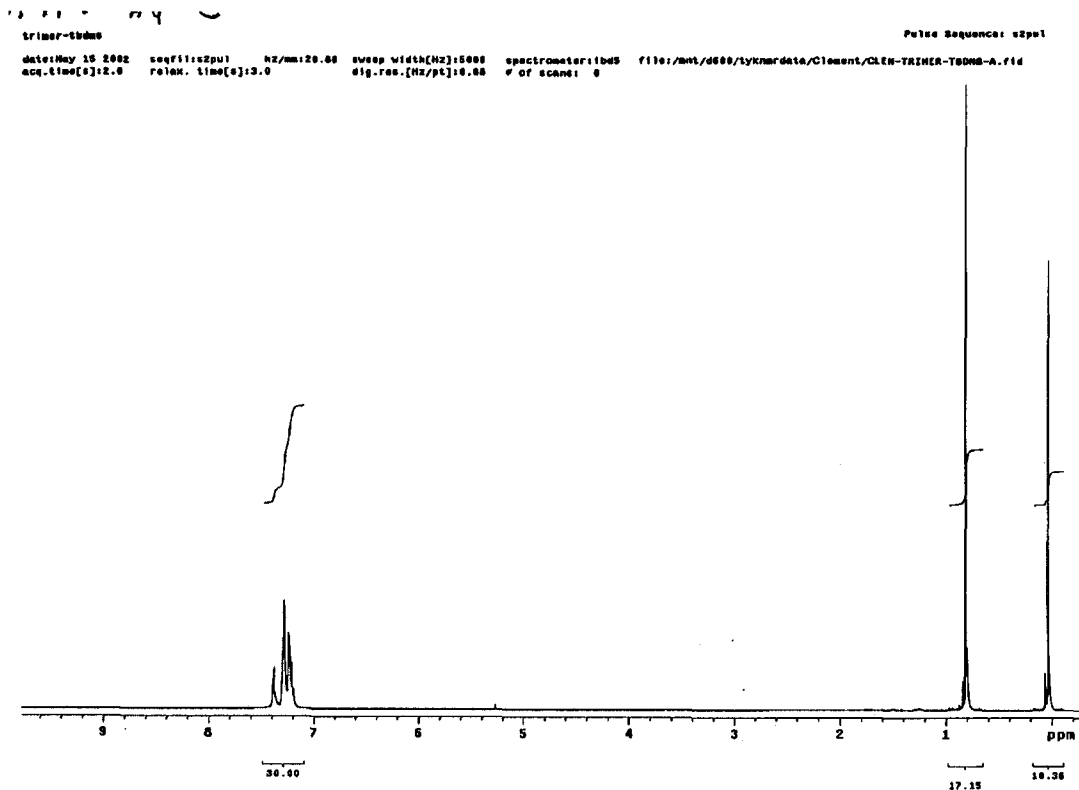


Fig. A.5 ^1H and ^{13}C NMR spectra of compound 36

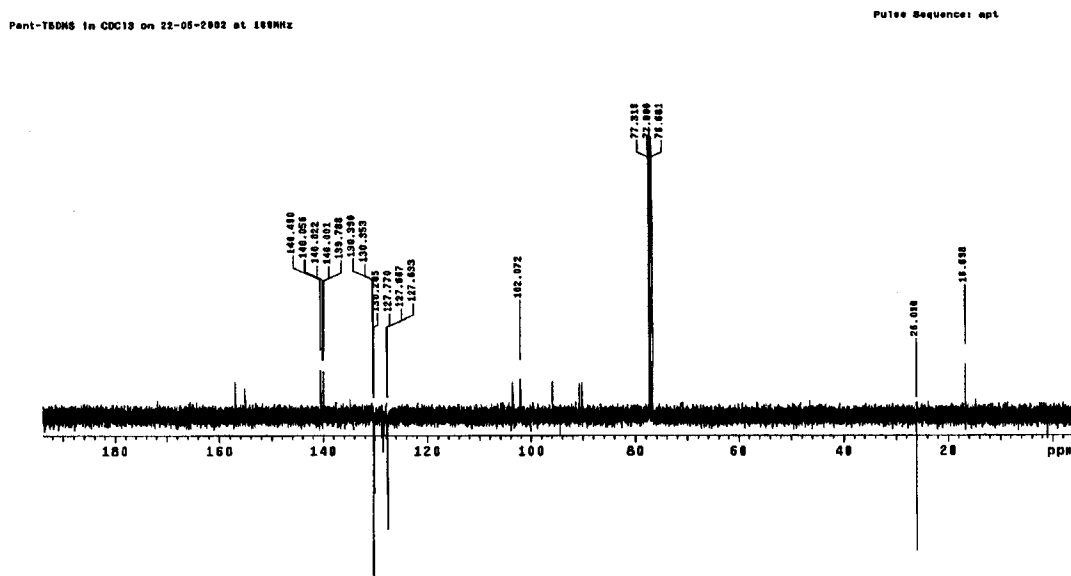
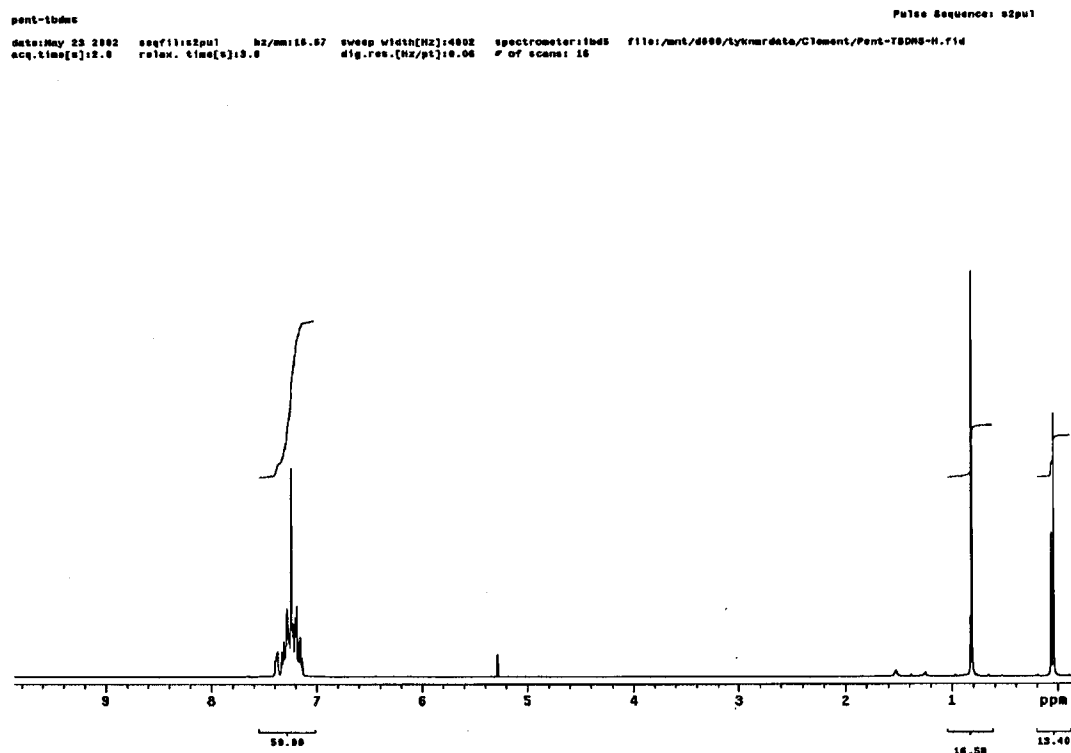


Fig. A.6 ^1H and ^{13}C NMR spectra of compound 40

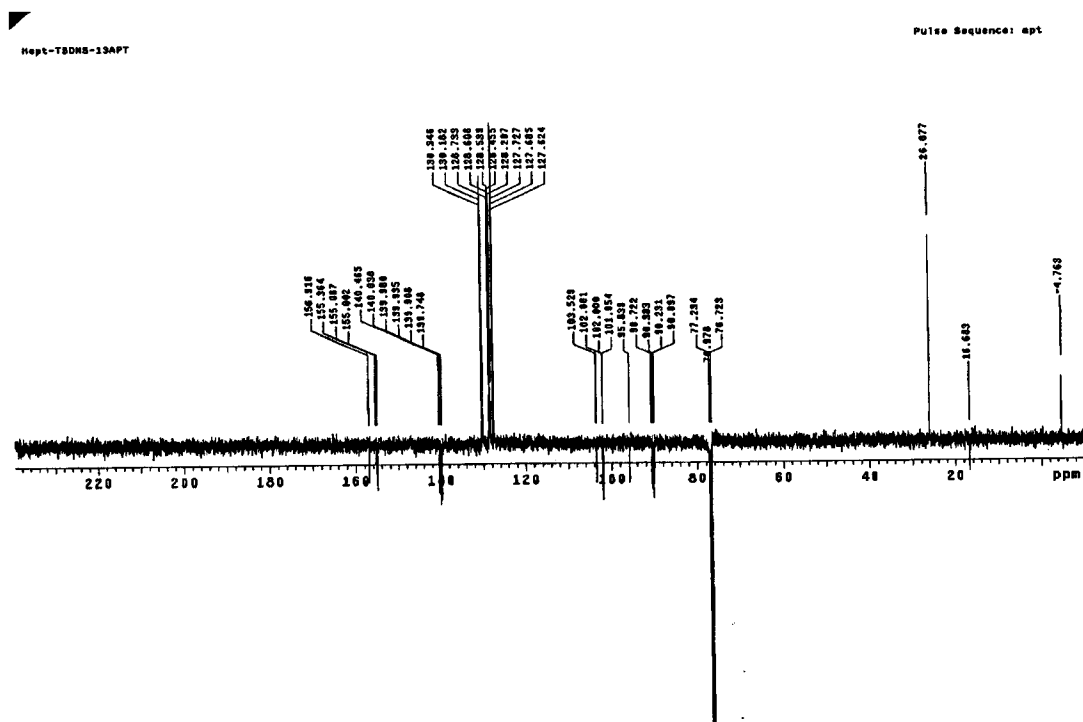
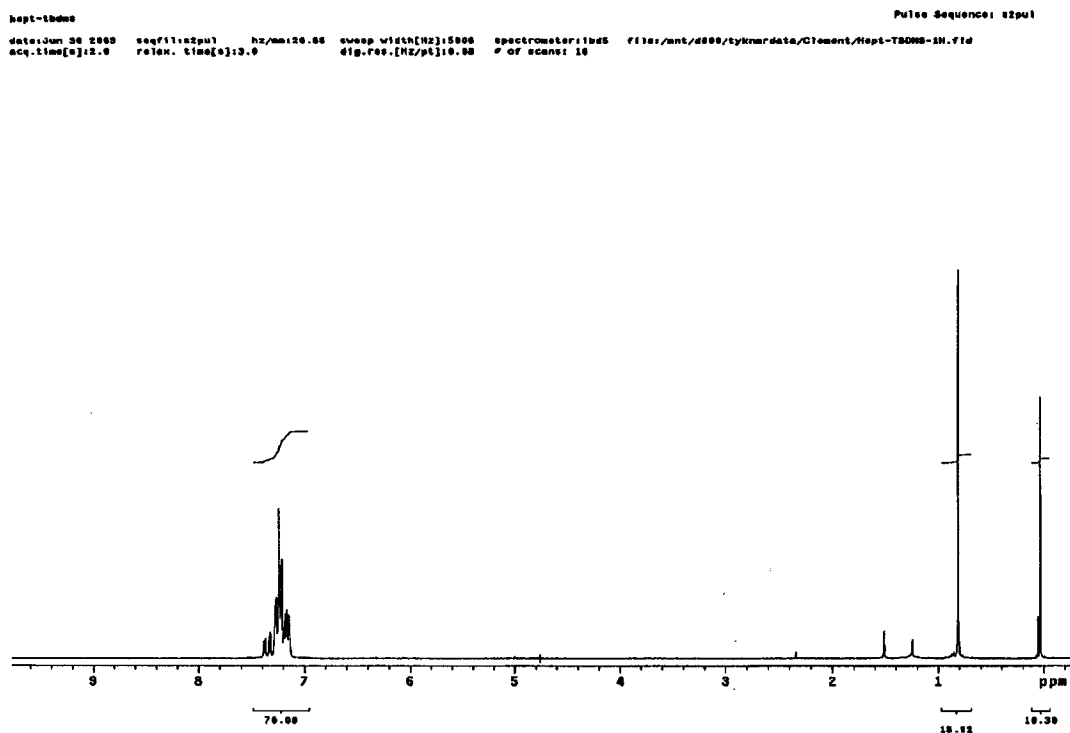


Fig. A.7 ^1H and ^{13}C NMR spectra of compound 41

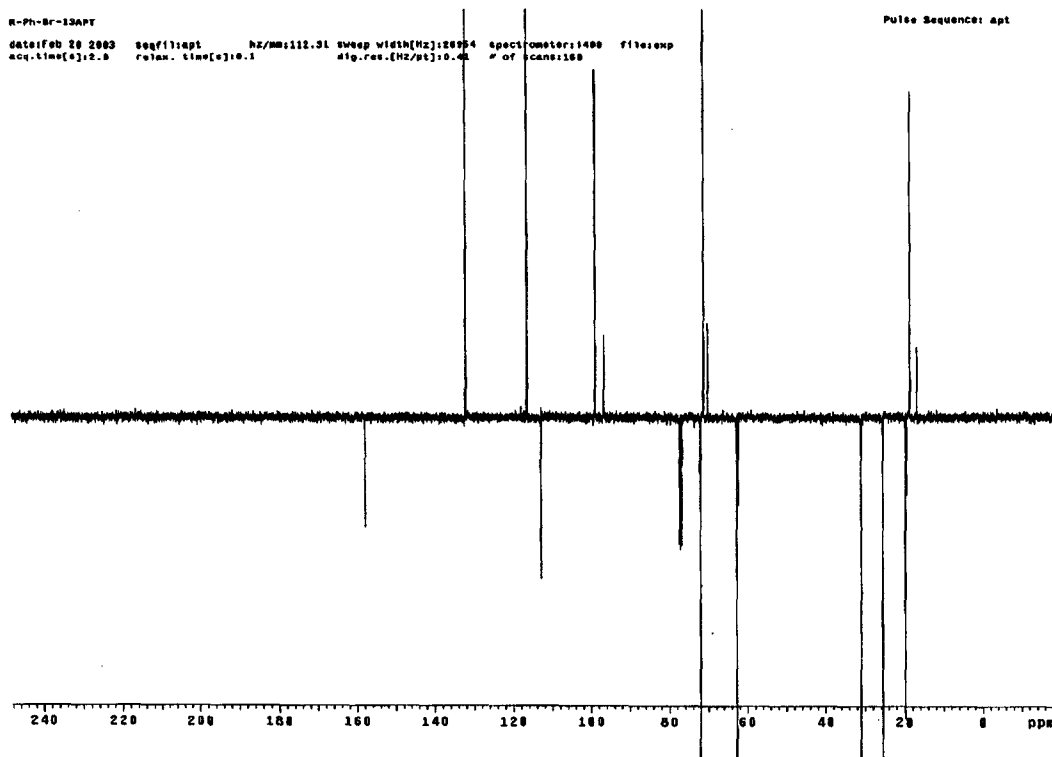
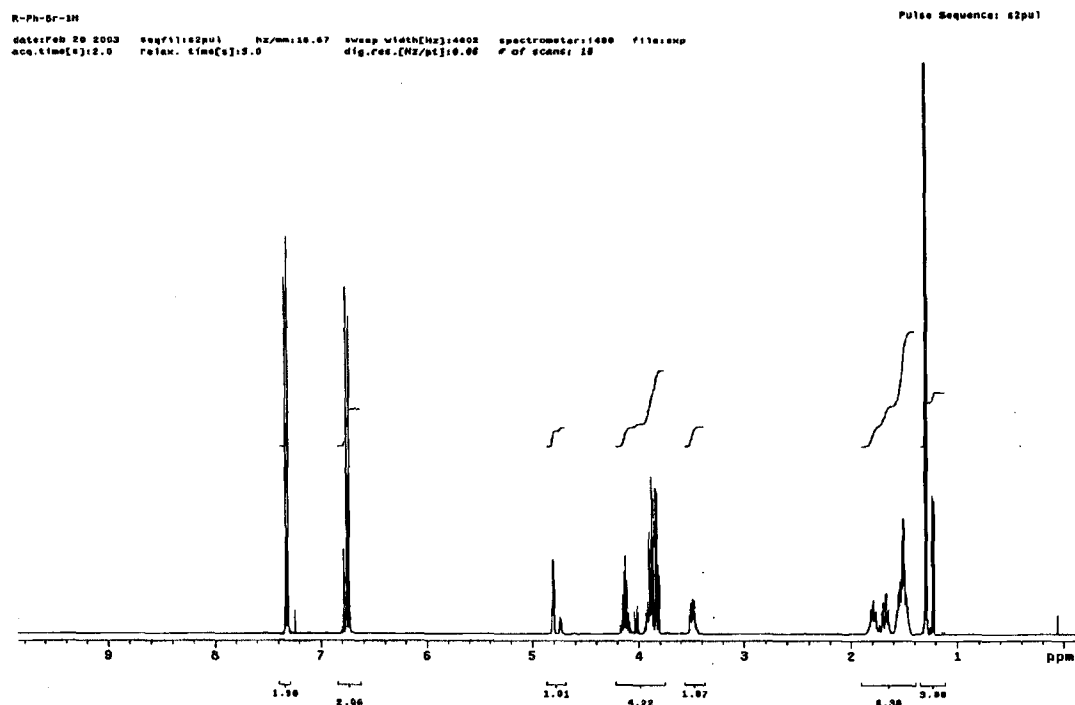


Fig. A.8 ^1H and ^{13}C NMR spectra of compound **46a**

4-184
date: Aug 5 2003 seq: f11e2pu1 hz/mm: 20.00 sweep width(Hz): 8000 spectrometer: lbed5 file: exp
acq. time(s): 18.0 relax. time(s): 0.0 sig. res. (Hz/pt): 0.00 # of scans: 18
Pulse Sequence: s2pu1

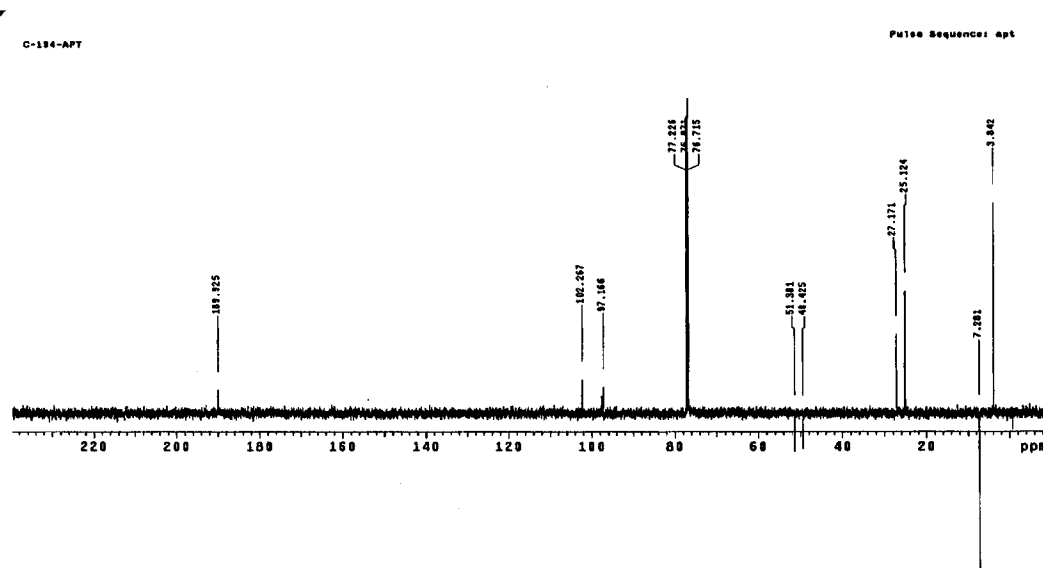
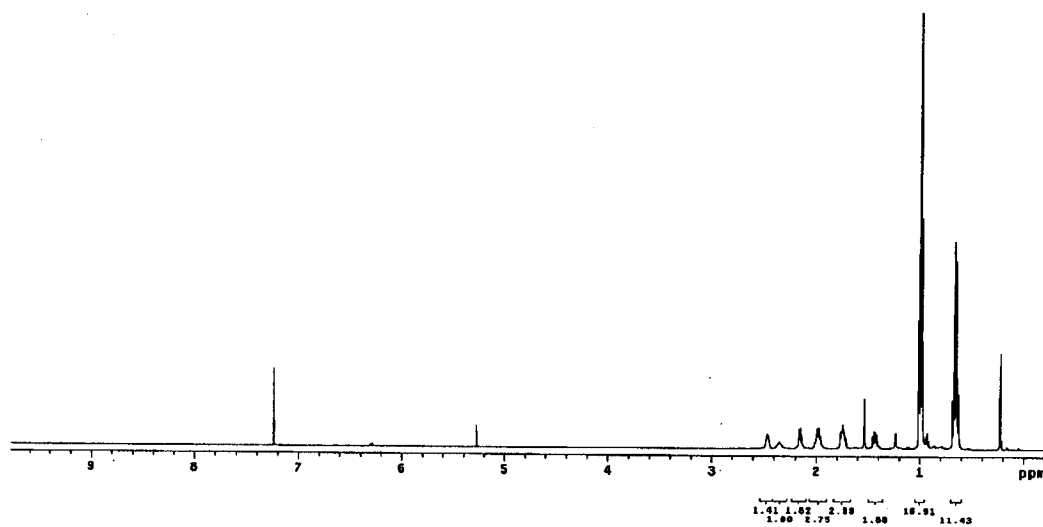


Fig. A.10 ^1H and ^{13}C NMR spectra of compound 70

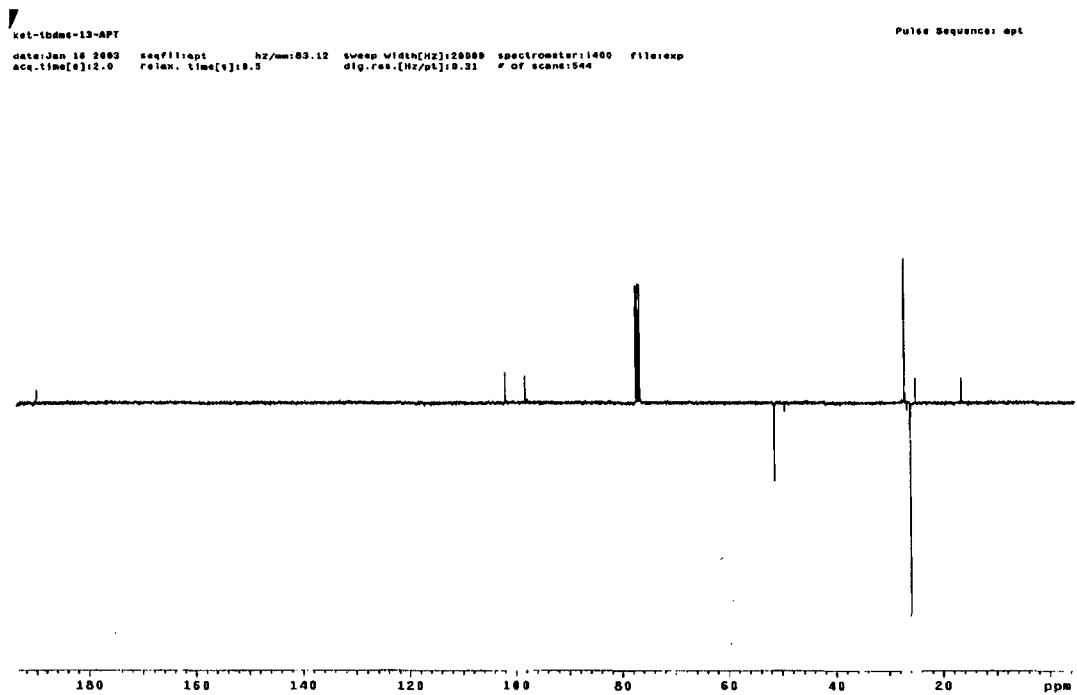
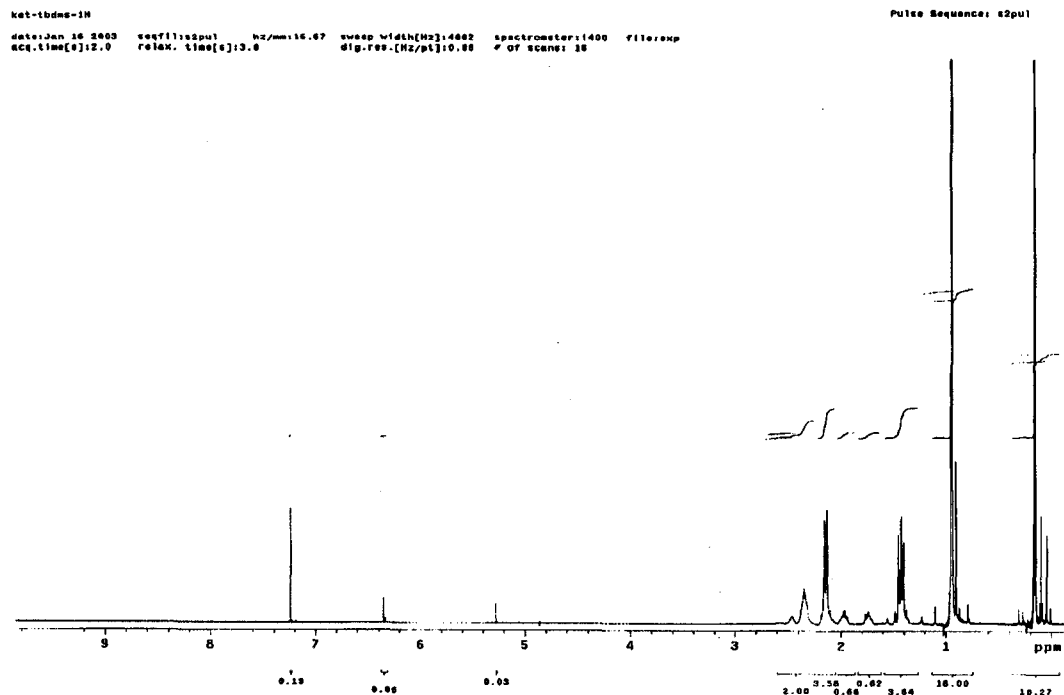


Fig. A.11 ^1H and ^{13}C NMR spectra of compound 71

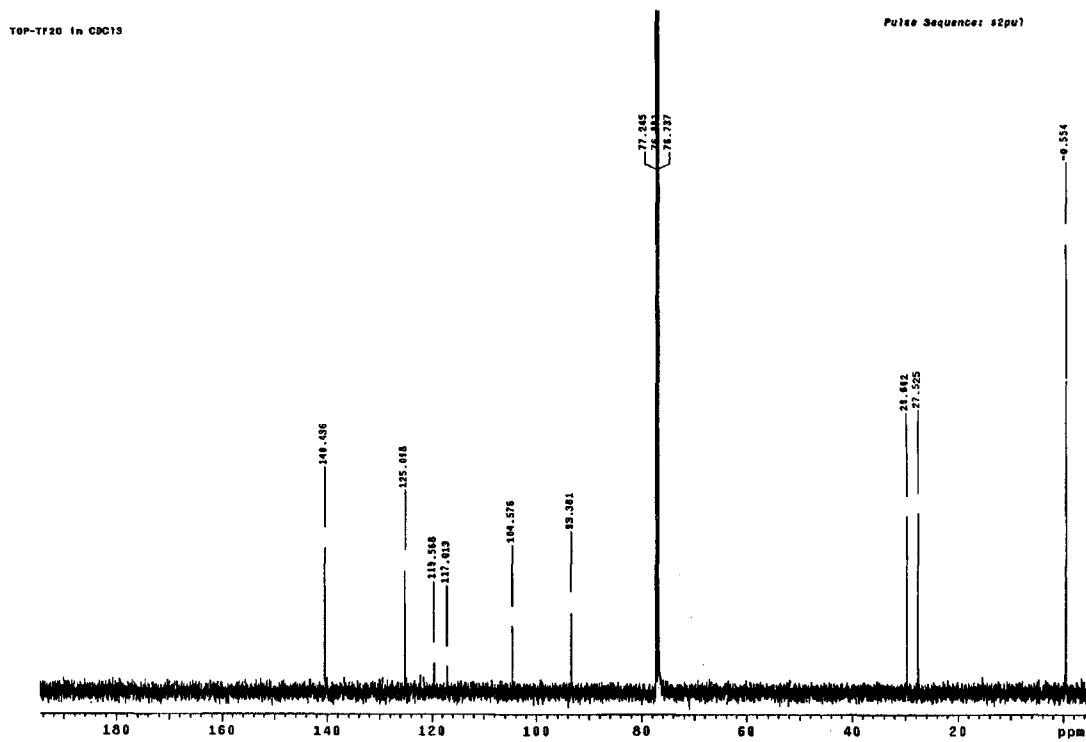
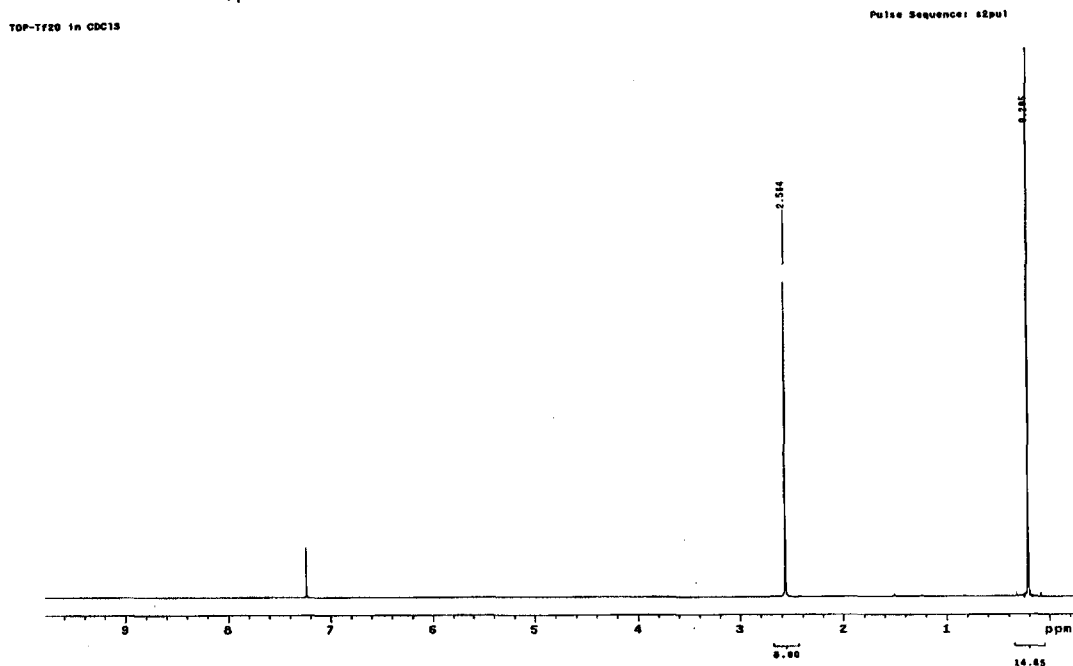


Fig. A.13 ^1H and ^{13}C NMR spectra of compound *trans*-66

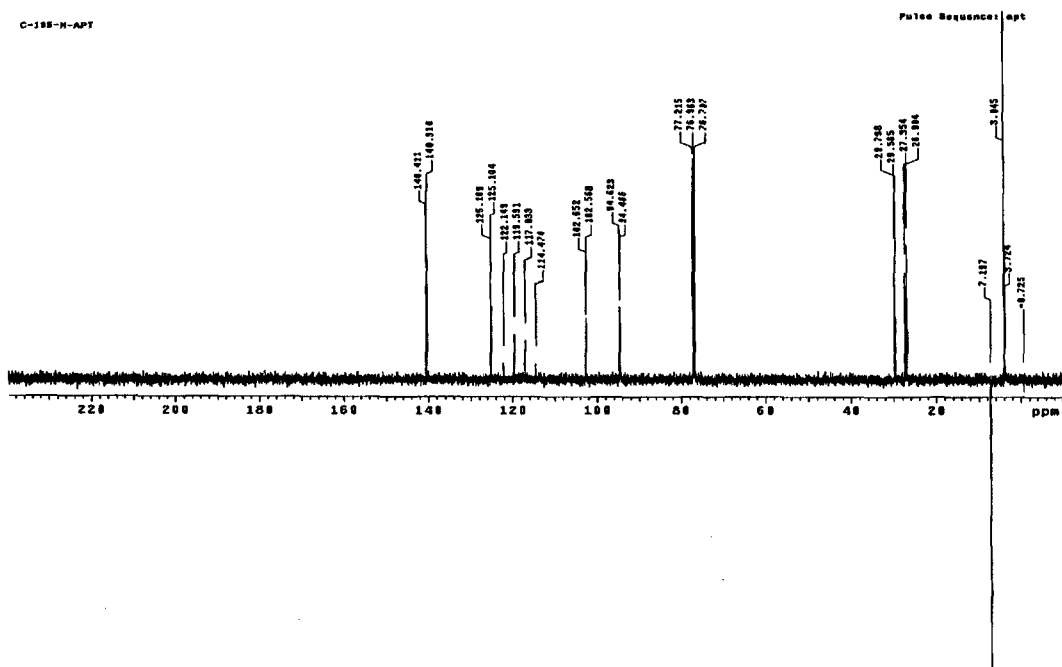
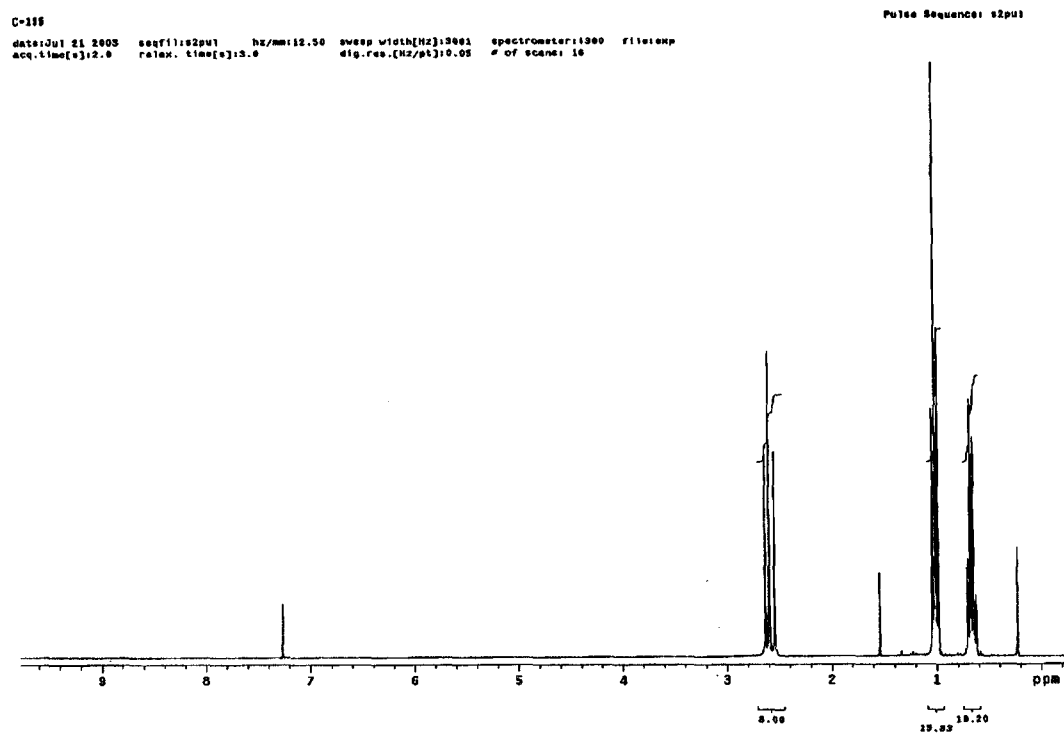


Fig. A.14 ^1H and ^{13}C NMR spectra of compound 72

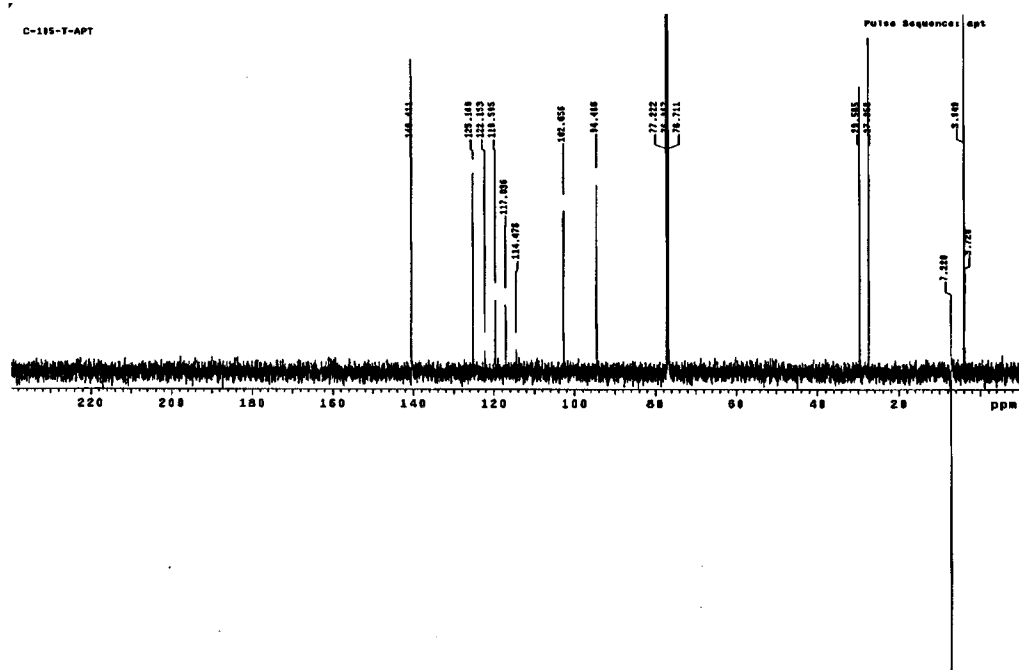
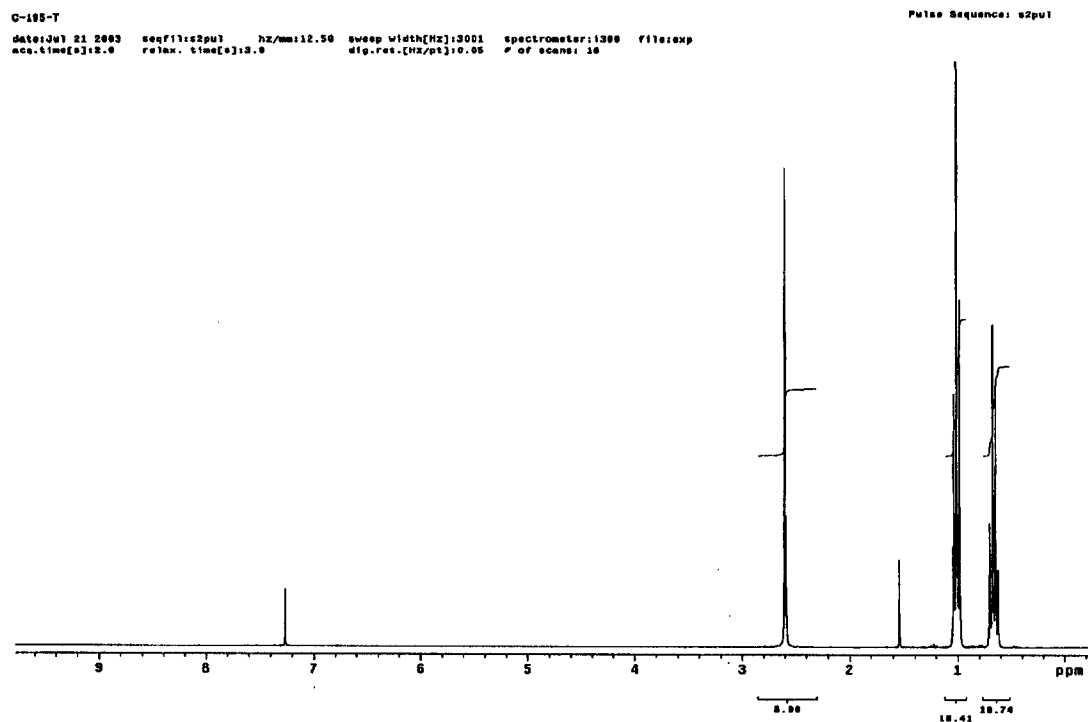


Fig. A.15 ^1H and ^{13}C NMR spectra of compound *trans*-72

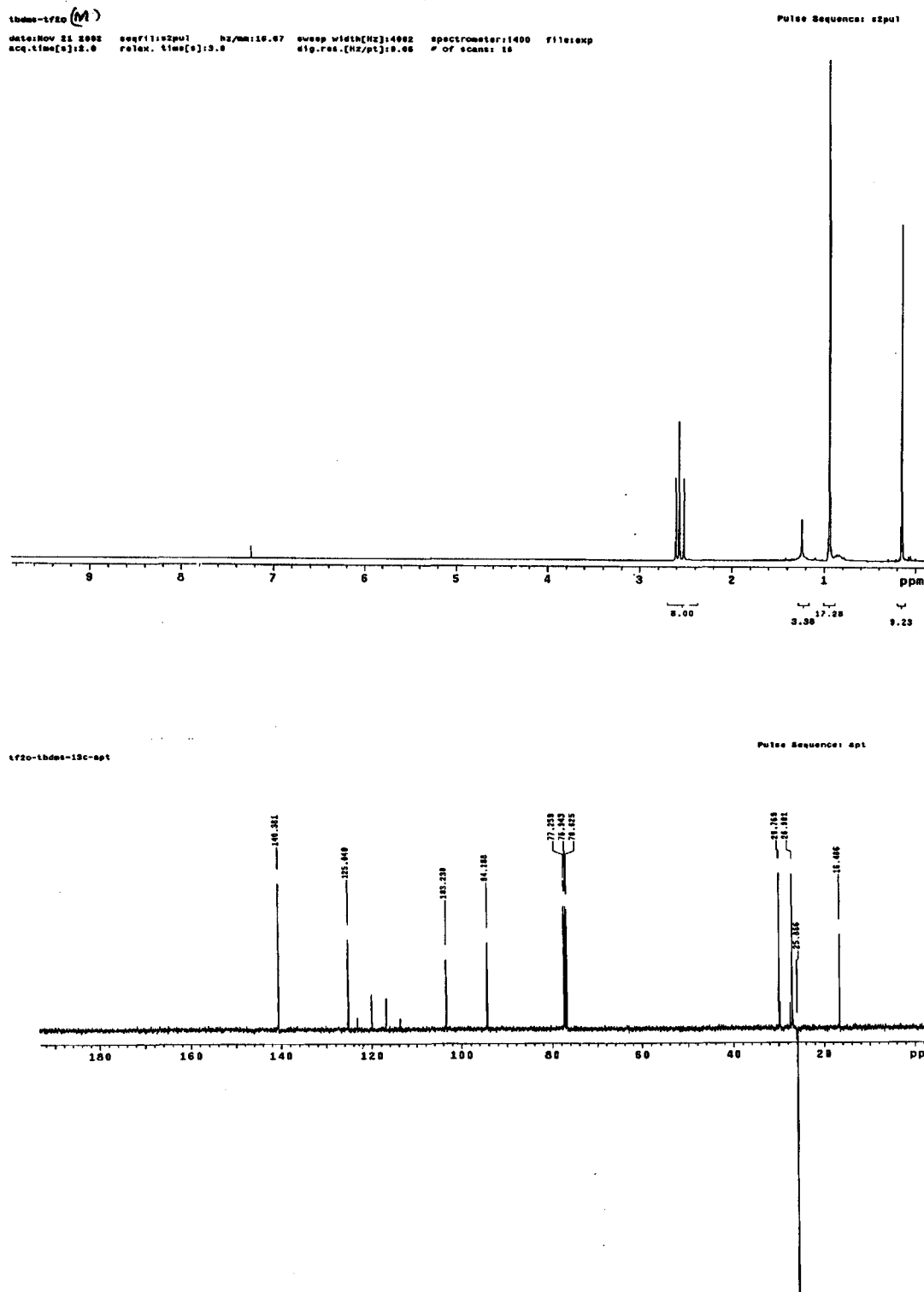


Fig. A.16 ^1H and ^{13}C NMR spectra of compound **73**

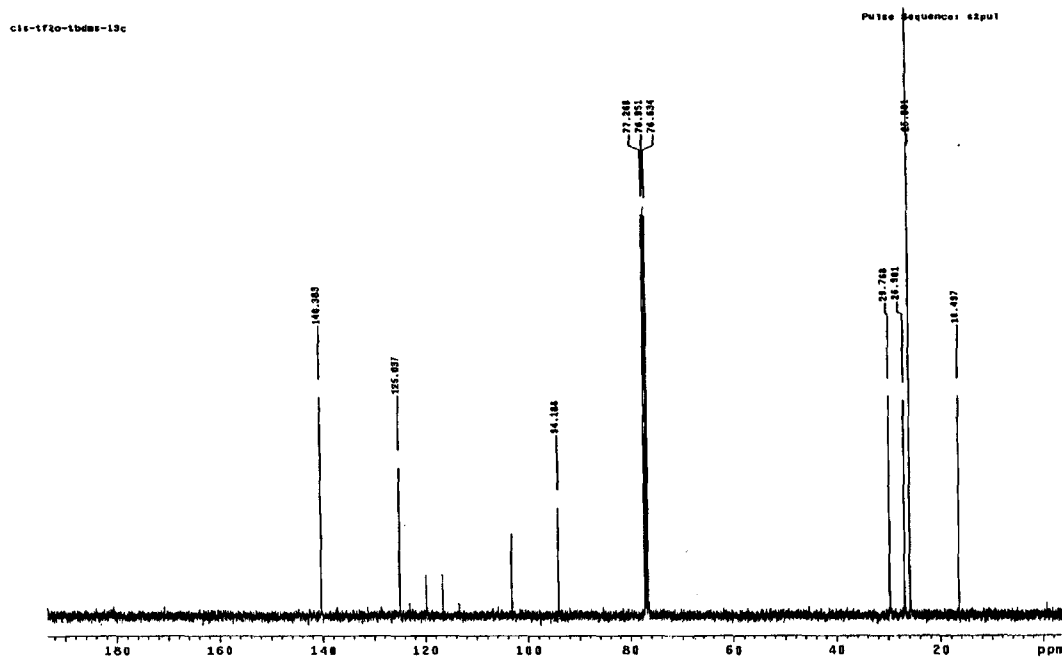
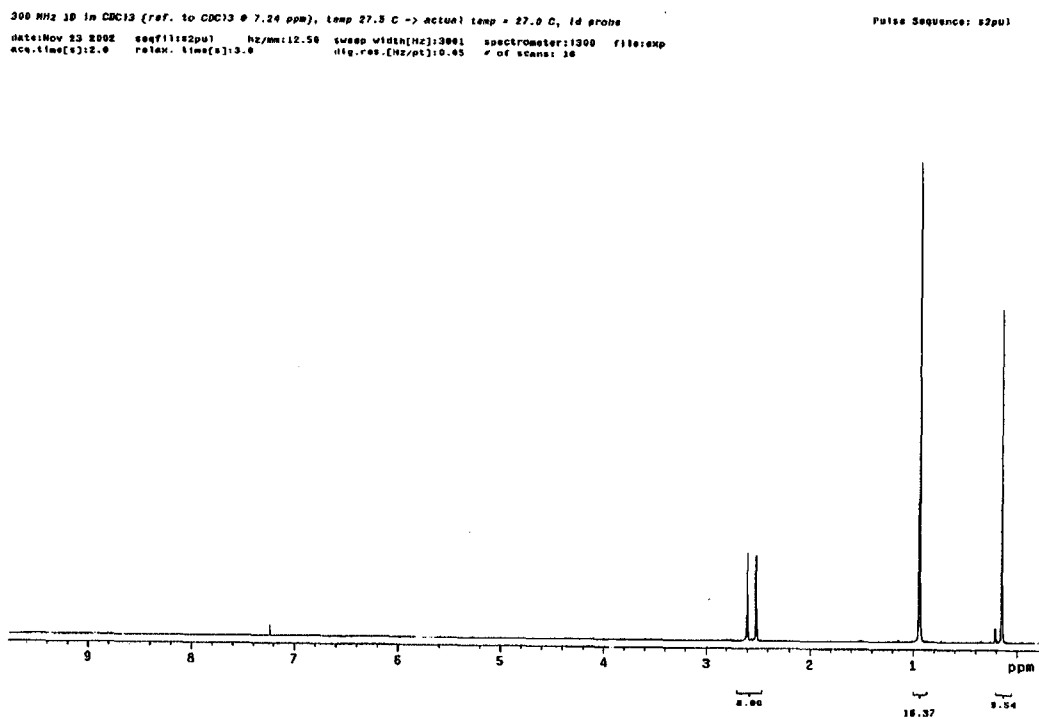


Fig. A.17 ¹H and ¹³C NMR spectra of compound *cis-73*

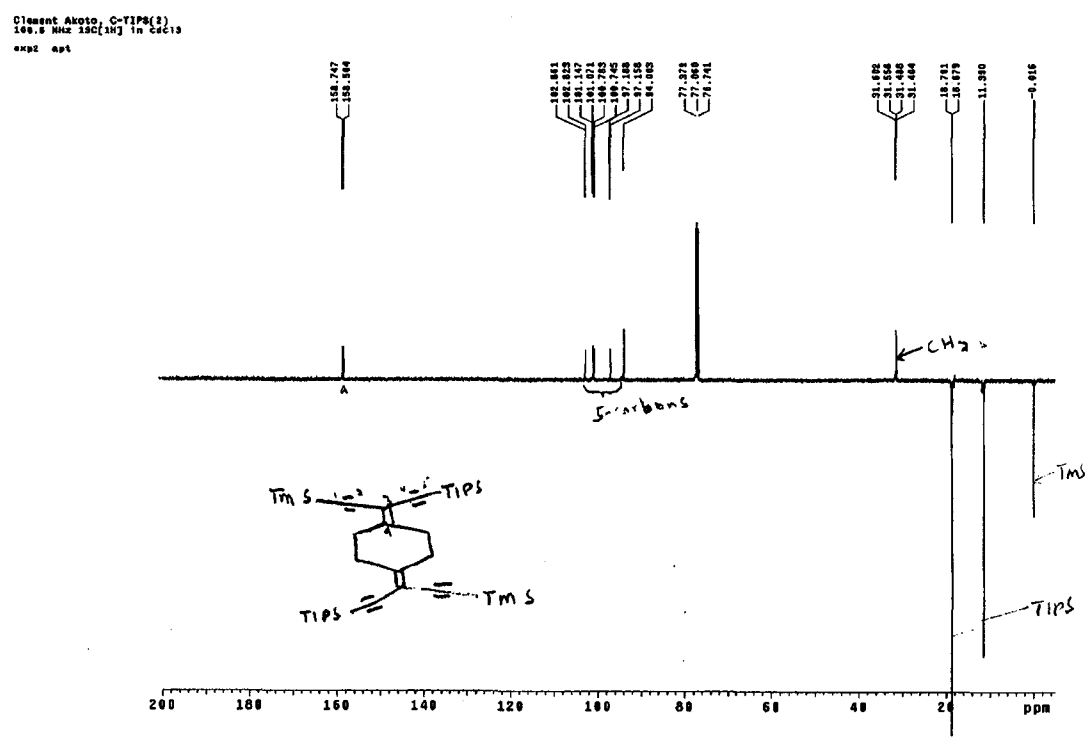
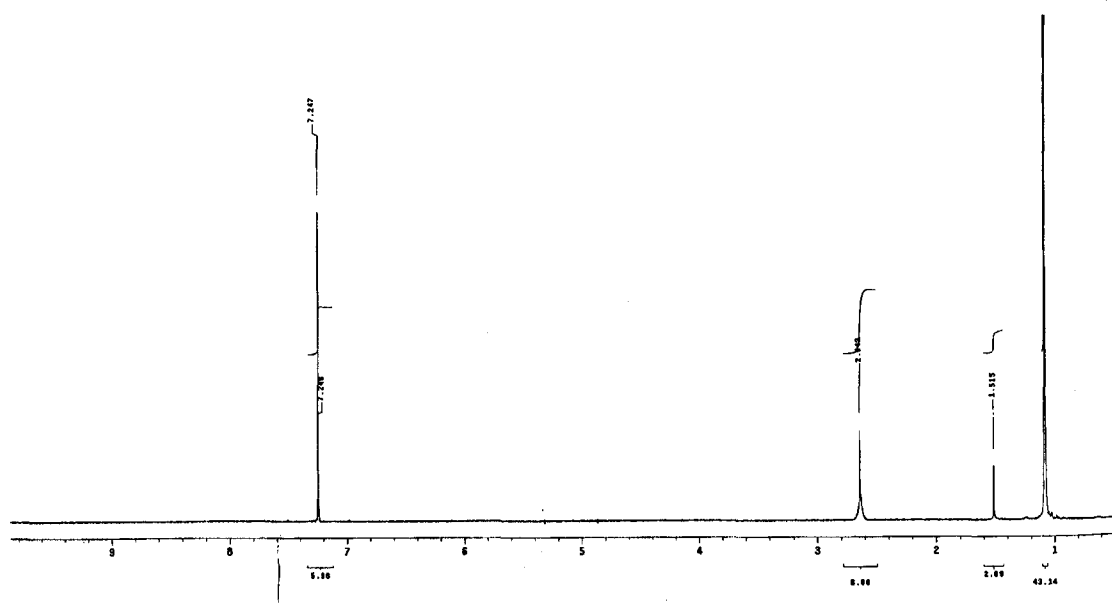


Fig. A.18 ^1H and ^{13}C NMR spectra of compound 67

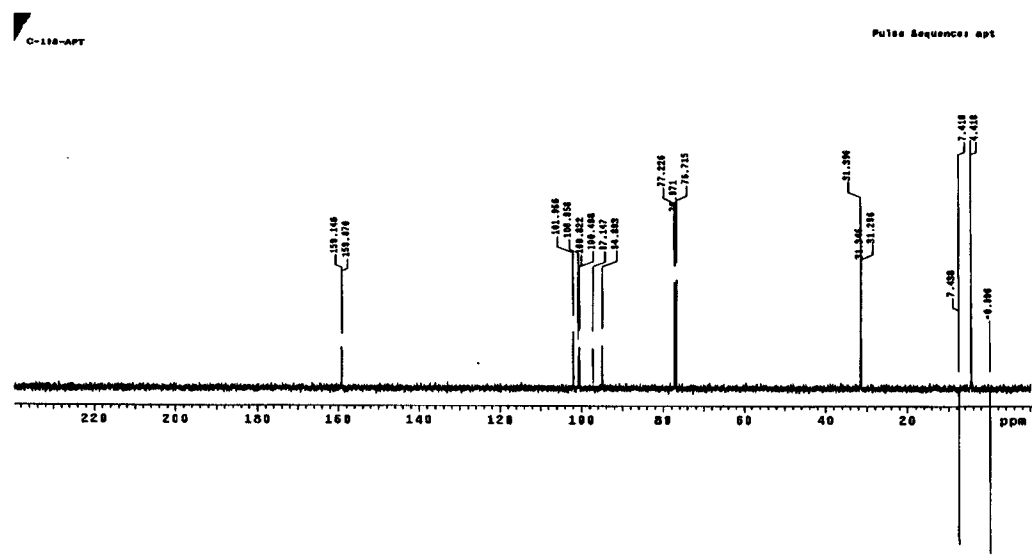
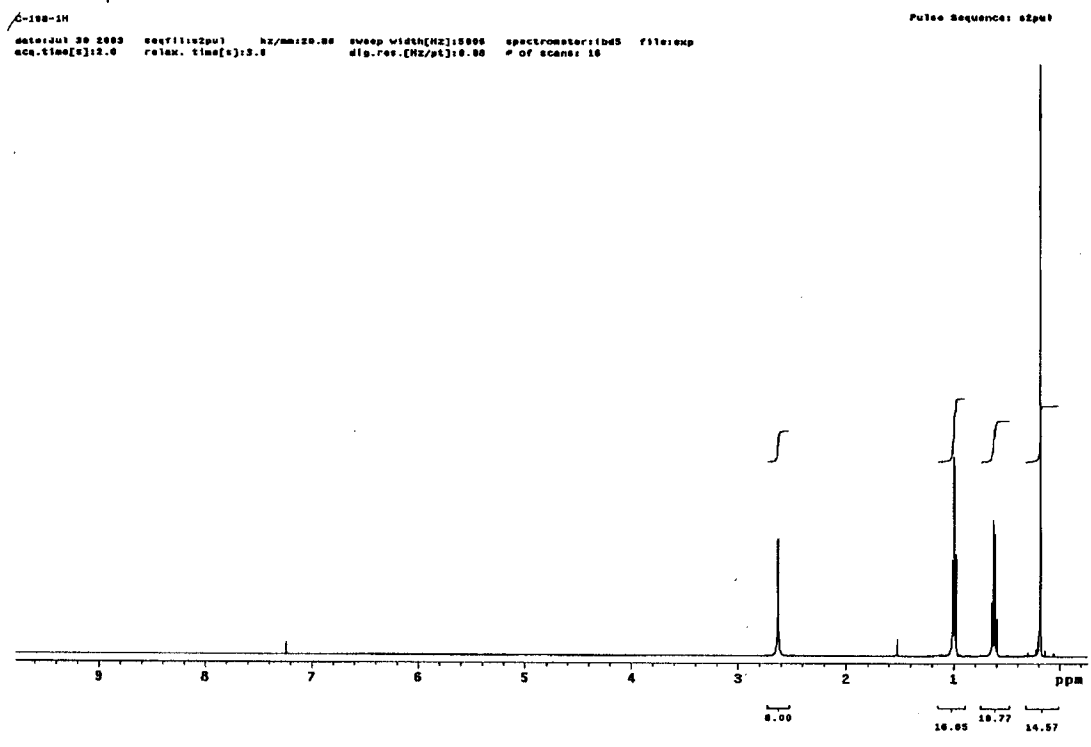


Fig. A.19 ¹H and ¹³C NMR spectra of compound 74

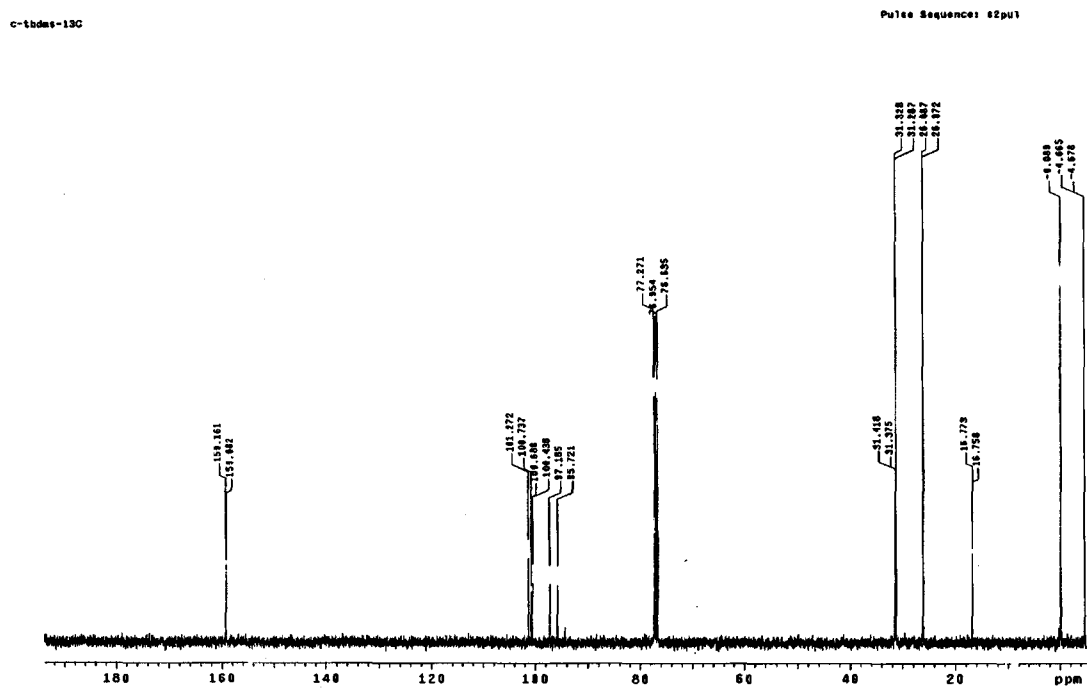
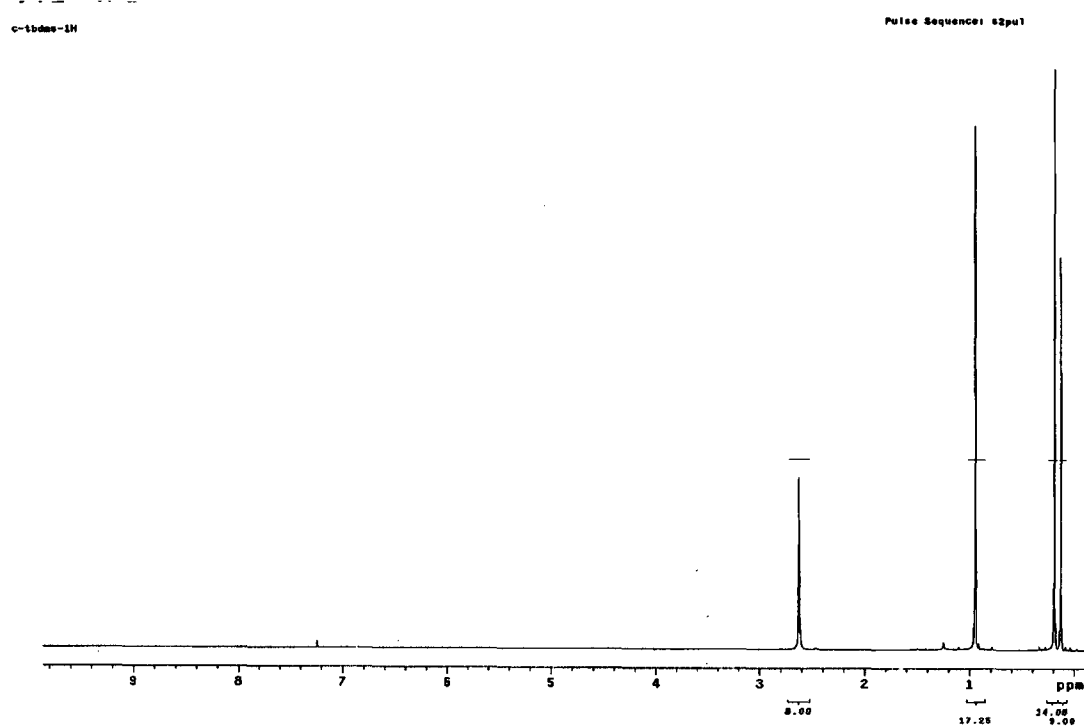


Fig. A.20 ^1H and ^{13}C NMR spectra of compound 75

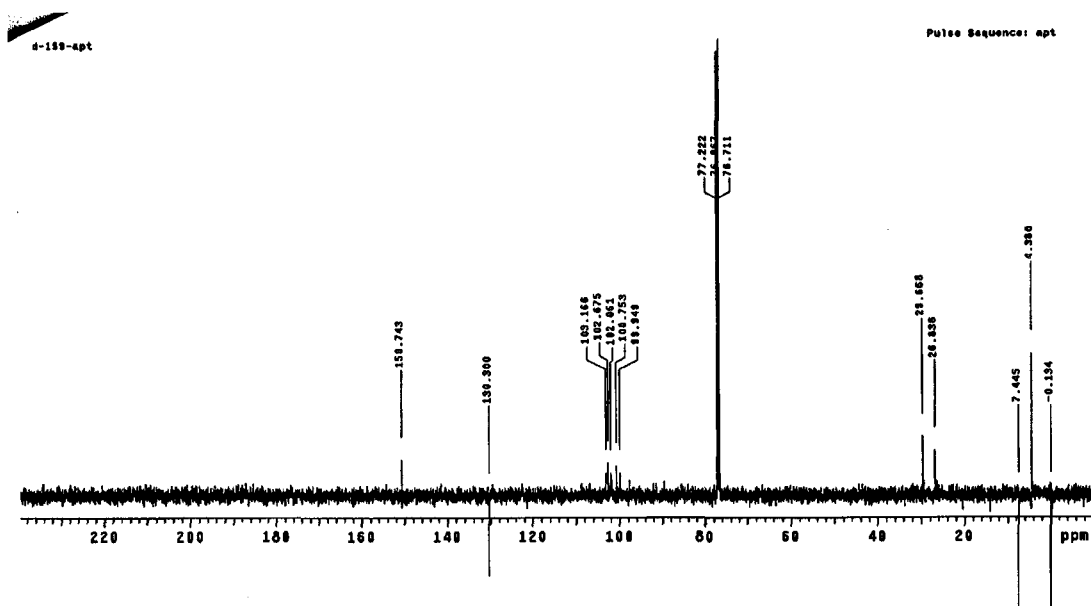
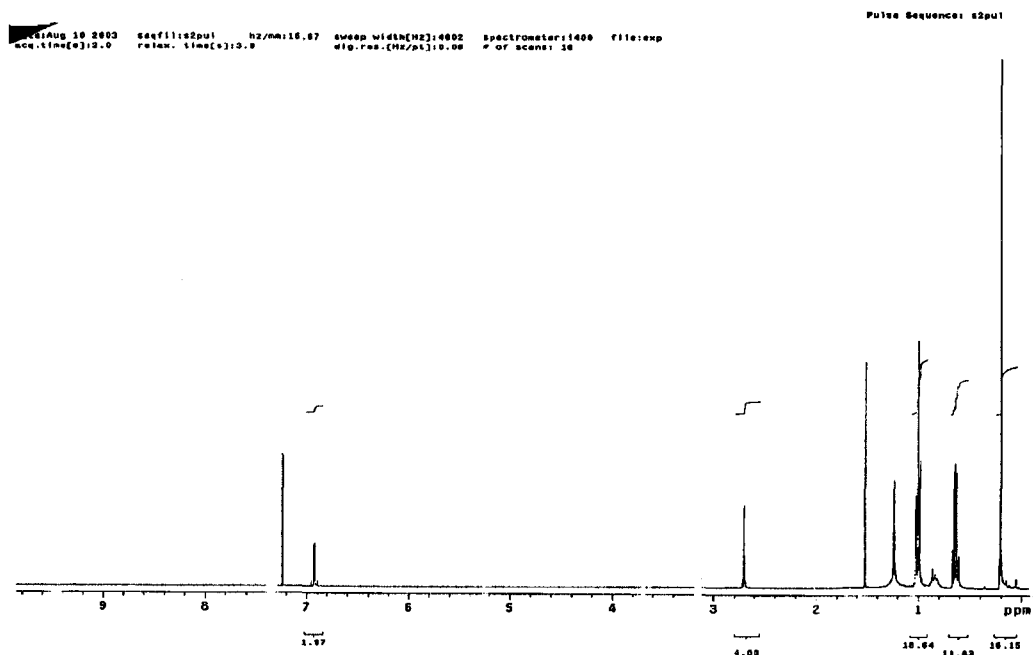


Fig. A.22 ^1H and ^{13}C NMR spectra of compound 76

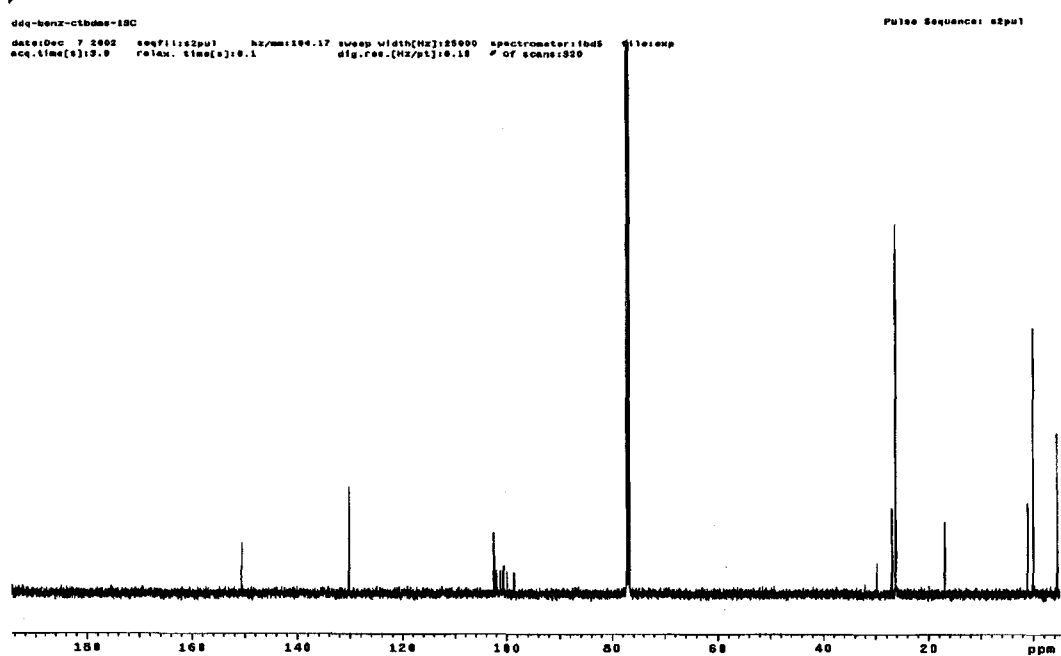
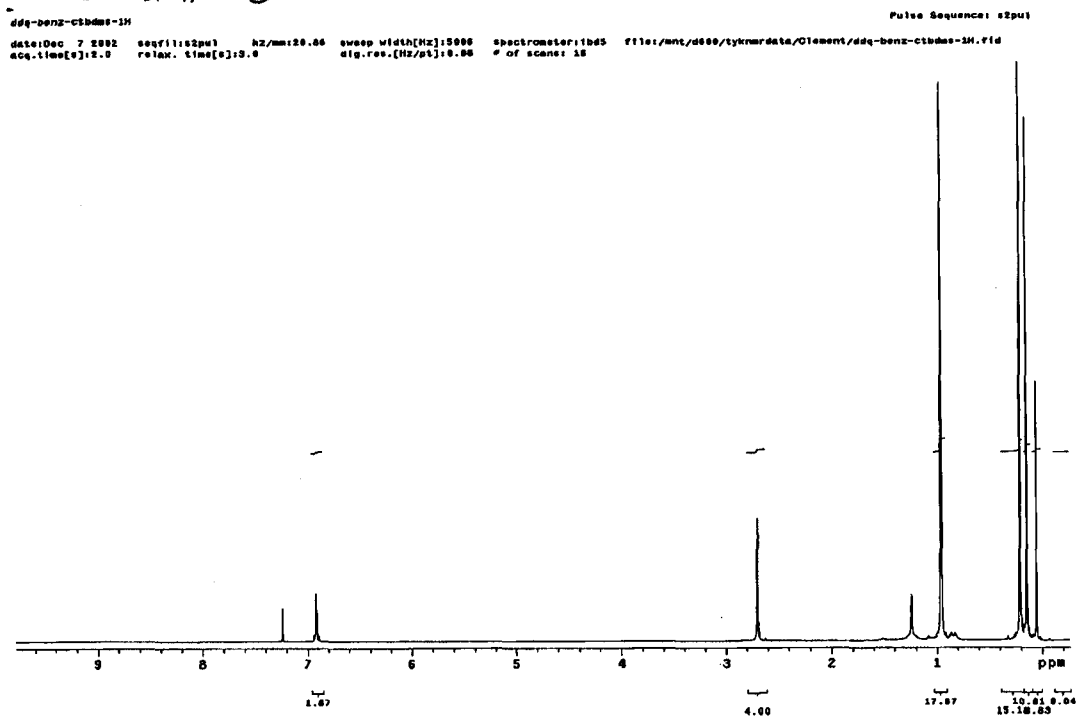


Fig. A.23 ^1H and ^{13}C NMR spectra of compound 77

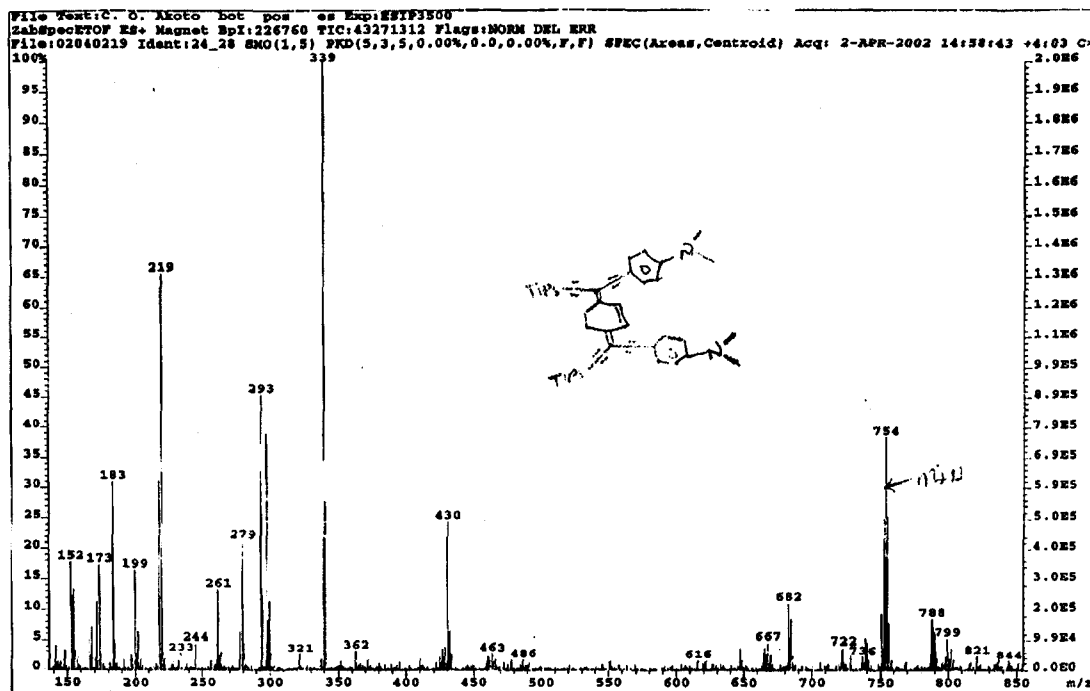
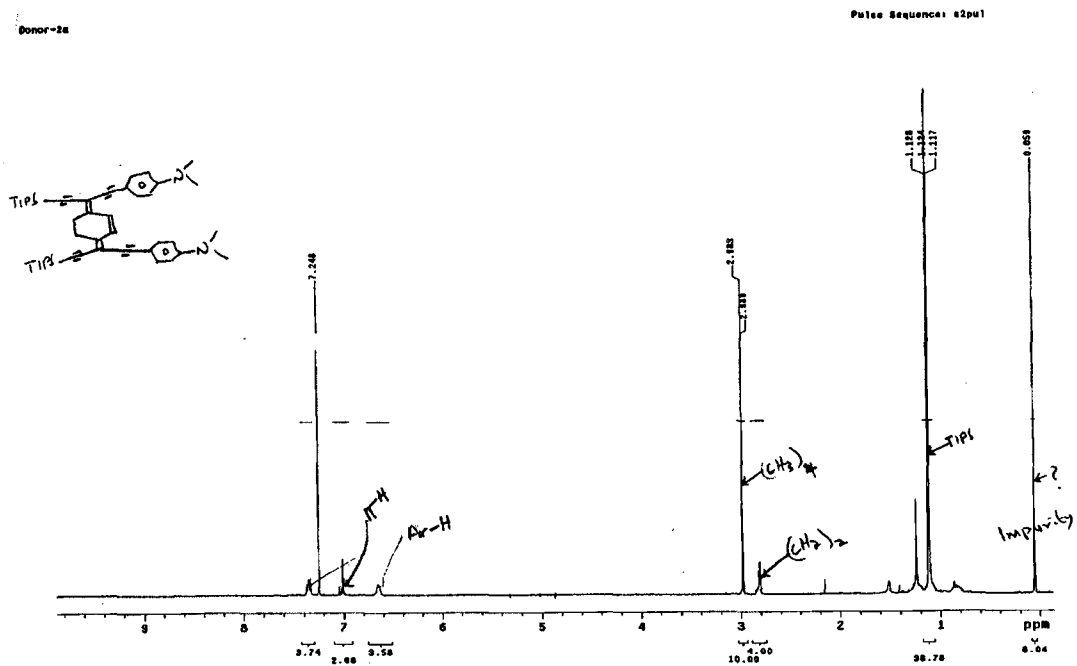


Fig. A.24 ^1H NMR and MS spectra of compound 80

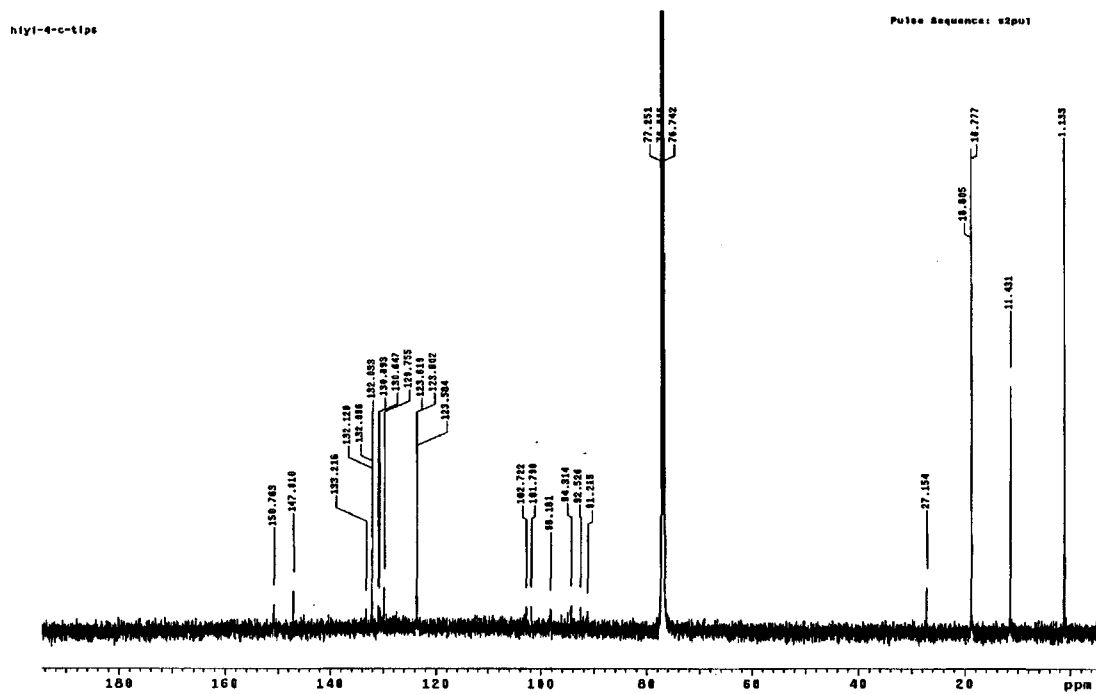
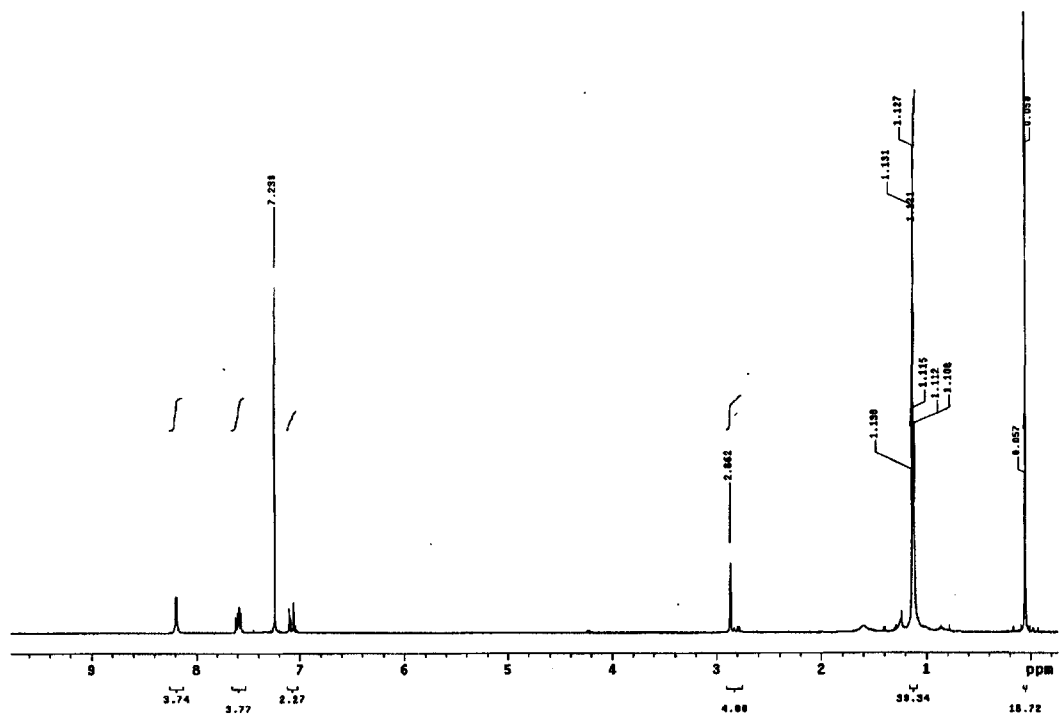


Fig. A.25 ¹H and ¹³C NMR spectra of compound 81

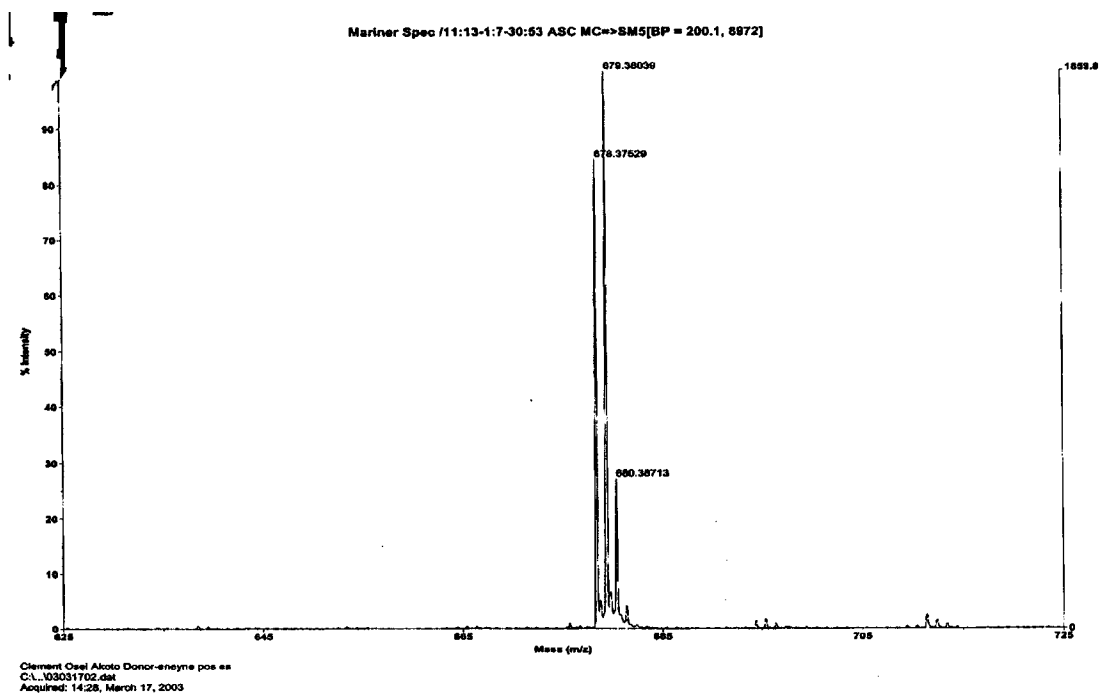
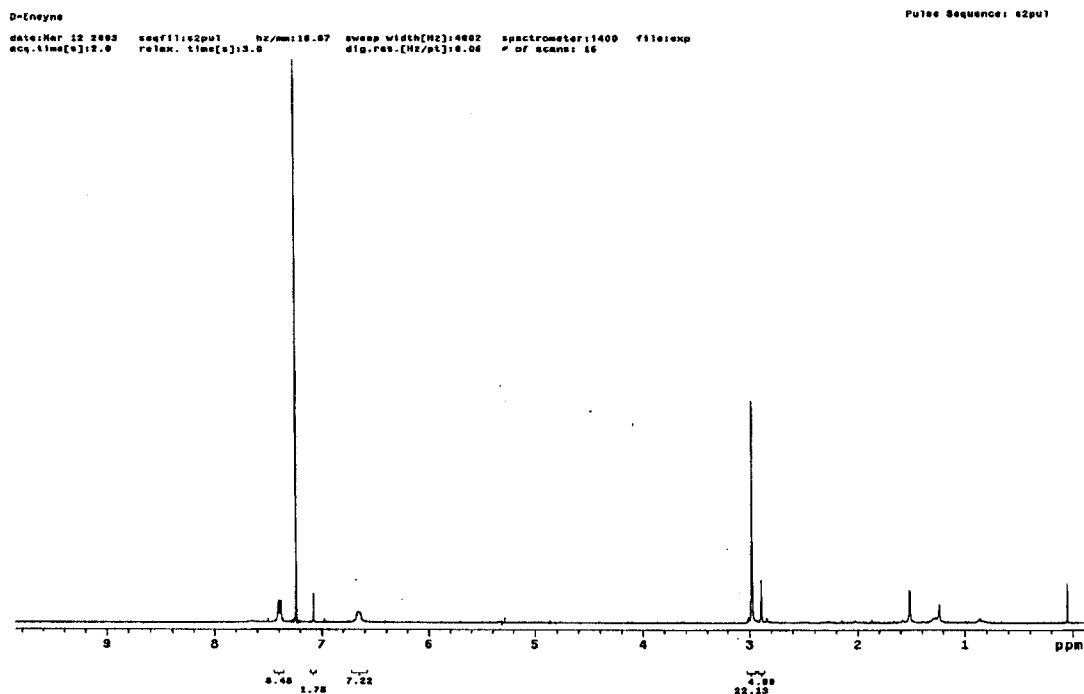


Fig. A.26 ^1H NMR and MS spectra of compound **82**